UNIVERSIDADE ESTADUAL DE CAMPINAS
Faculdade de Engenharia Elétrica e de Computação

Marina Gabriela Sadith Pérez Paredes

Study of Electric Vehicle Modeling and Strategy of Torque Control for Regenerative and Anti-lock Braking Systems

Estudo de Modelagem de Veículos Elétricos e Estratégia de Controle de Torque para Sistemas de Frenagens Regenerativa e Antitravamento

CAMPINAS

2018

Marina Gabriela Sadith Pérez Paredes

Study of Electric Vehicle Modeling and Strategy of Torque Control for Regenerative and Anti-lock Braking Systems

Estudo de Modelagem de Veículos Elétricos e Estratégia de Controle de Torque para Sistemas de Frenagens Regenerativa e Antitravamento

Thesis presented to the School of Electrical and Computer Engineering of the University of Campinas in partial fulfillment of the requirements for the degree of Doctor in Electrical Engineering, in the area of Electrical Energy.

Tese apresentada à Faculdade de Engenharia Elétrica e de Computação da Universidade Estadual de Campinas como parte dos requisitos exigidos para a obtenção do título de Doutora em Engenharia Elétrica, na Área de Energia Elétrica.

Supervisor: Prof. Dr. José Antenor Pomilio

Este exemplar corresponde à versão final da tese defendida pela aluna Marina Gabriela Sadith Pérez Paredes, e orientada pelo Prof. Dr. José Antenor Pomilio

CAMPINAS

2018

Agência(s) de fomento e nº(s) de processo(s): CNPq, 149810/2013-0; CAPES

Ficha catalográfica
Universidade Estadual de Campinas
Biblioteca da Área de Engenharia e Arquitetura
Rose Meire da Silva - CRB 8/5974

P415s

Pérez Paredes, Marina Gabriela Sadith, 1981-
Study of electric vehicle modeling and strategy of torque control for regenerative and anti-lock braking systems / Marina Gabriela Sadith Pérez Paredes. – Campinas, SP : [s.n.], 2018.

Orientador: José Antenor Pomilio.
Tese (doutorado) – Universidade Estadual de Campinas, Faculdade de Engenharia Elétrica e de Computação.

1. Veículos elétricos. 2. Frenagem regenerativa. 3. Sistemas de frenagem antitravamento. I. Pomilio, José Antenor, 1960-. II. Universidade Estadual de Campinas. Faculdade de Engenharia Elétrica e de Computação. III. Título.

Informações para Biblioteca Digital

Título em outro idioma: Estudo de modelagem de veículos elétricos e estratégia de controle de torque para sistemas de frenagens regenerativa e antitravamento
Palavras-chave em inglês:
Electric vehicles
Regenerative braking
Anti-lock braking systems
Área de concentração: Energia Elétrica
Titulação: Doutora em Engenharia Elétrica
Banca examinadora:
José Antenor Pomilio [Orientador]
Auteliano Antunes dos Santos Junior
Fernando Pinhabel Marafão
Niederauer Mastelari
Marcos Ferretti
Data de defesa: 29-10-2018
Programa de Pós-Graduação: Engenharia Elétrica

COMISSÃO JULGADORA – TESE DE DOUTORADO

Candidata: Marina Gabriela Sadith Pérez Paredes RA: 109349

Data da Defesa: 29 de outubro de 2018

Título da Tese: "Estudo de Modelagem de Veículos Elétricos e Estratégia de Controle de Torque para Sistemas de Frenagens Regenerativa e Antitravamento".

Prof. Dr. José Antenor Pomilio
Prof. Dr. Auteliano Antunes dos Santos Junior
Prof. Dr. Fernando Pinhabel Marafão
Prof. Dr. Niederauer Mastelari
Dr. Marcos Ferretti

A ata de defesa, com as respectivas assinaturas dos membros da Comissão Julgadora, encontra-se no SIGA (Sistema de Fluxo de Dissertação/Tese) e na Secretaria de PósGraduação da Faculdade de Engenharia Elétrica e de Computação.

To my parents, Sadith Paredes Lomas and Marino Pérez Gomez
and my siblings, Esther, Elizabeth, Leonardo, Alexandro and Jefferson.

Acknowledgements

(In Portuguese)

Agradeço a Deus, por me fortalecer e estar sempre presente nos momentos de desânimo e de realizações. Porque os deveres são nossos e os resultados são de Deus.

Aos meus pais, meus primeiros mestres, Marino e Sadith por ter me dado amor, educação e valores, assim como a confiança e as asas para voar por mim mesma.

Aos meus queridos irmãos: Esther, Elizabeth, Leonardo, Alexandro e Jefferson, pelo amor, apoio moral e espiritual, apesar da distância, estão sempre presentes.

Ao meu orientador o Professor Pomilio, pela orientação, paciência, sugestões, críticas e correções que tornaram possível mais está conquista na minha formação profissional.

Aos meus amigos de diversos paises com quem tive a oportunidade de conviver neste período e aprender novas culturas, me tornando uma pessoa abençoada.

A todos os professores, funcionários, concursados e todas as pessoas que, de alguma forma, contribuíram para que este trabalho fosse realizado.

À UNICAMP, à CNPq e à CAPES pela oportunidade e pelo suporte financeiro. Ao povo do Brasil, que contribui para o crescimento do país e financia trabalhos acadêmicos.

“When the goal seems difficult to you, do not change your goal; look for a new way how to get there.”

“Quando o objetivo parecer difícil para você, não mude seu objetivo; procure uma nova maneira de chegar até lá.”

“Cuando el objetivo te parezca difícil, no cambies de objetivo; busca un nuevo camino para llegar a él.”

Abstract

The interest in electric vehicles has grown worldwide due to their efficiency for reducing environmental pollution, by using energy elements such as batteries and supercapacitors to drive the electric machine, instead of an internal combustion engine. Contrarily, the low vehicle autonomy remains a barrier to their commercial success. Therefore, automotive institutions together with academics face the challenge through various solutions to increase the available energy. The regenerative braking is one of the implementations that helps a better use of the stored energy.

Regenerative braking is a process in which energy is recovered from a vehicle during decelerations. This research focuses on braking for various road surface conditions. Furthermore, it considers the regenerative braking and the anti-lock braking systems regarding energy recovery performance for friction coefficient changes.

In this work, we will review and analyze the basic aspects of the modeling of a vehicle with or without ABS, as well as the dynamic behavior of wheels. We will also present a contribution to the study of torque control and control strategies for the torque distribution regarding combination and co-operation between electric and mechanical torque. This process is done despite changes in ground surfaces and operating methods such as downhill, leading to better performance in the flexibility of vehicle stability and in the recovery of power.

Keywords: Regenerative Braking System (RBS), Anti-lock Braking System (ABS), Distributed Torque Strategies.

Resumo

Os veículos elétricos têm despertado crescente interesse devido à sua capacidade para reduzir a poluição no meio ambiente, usando elementos de energia elétrica acumulado em baterias e supercapacitores para o acionamento da máquina elétrica no lugar de um motor de combustão interna. Por outro lado, a baixa autonomia do veículo elétrico continua sendo uma barreira para seu sucesso comercial. Instituções automobilísticas junto com a Academia enfrentam esse desafio com diversas soluções para aumentar a energia disponível. Entre as possibilidades está a frenagem regenerativa.

A frenagem regenerativa é um processo no qual recupera-se energia de um veículo durante as desacelerações. Esta pesquisa se concentra nas frenagens para diversas condições com mudanças da superficie da estrada, considerando o sistema de frenagem regenerativo e o sistema de antibloqueio.

Analisamos e revisamos os aspectos básicos da modelagem de um veículo com/sem ABS, assim como o comportamento dinâmico das rodas e mostramos uma contribuição para o estudo do controle de torque na máquina e estratégias de controle para o torque distribuído na combinação e cooperação entre o torque elétrico e o mecânico, mesmo com mudanças do solo e de métodos de operação, como descidas, obtendo estabilidade do veículo e recuperação de energia.

Palavras-chaves: Sistema de Frenagem Regenerativa, Sistema de Frenagem Antitravamento, Estratégias de Torque Distribuidos.

List of Figures

List of Tables

List of Abbreviations

AD	*Analog Digital.*
ABS	*Anti-lock Braking System.*
ACC	*Adaptive Cruise Control.*
BMS	*Battery Monitoring System.*
BT	*Battery.*
CAGR	*Compound Annual Growth Rate.*
DSP	*Digital Signal Processor.*
DTC	*Direct Torque Control.*
EMS	*Energy Management System.*
ESP	*Electronic Stability Program.*
EV	*Electric Vehicle.*
FFC	*Fixed Friction Coefficients.*
HEV	*Hybrid Electric Vehicle.*
ICE	*Internal Combustion Engine.*
IM	*Induction Machine.*
IGBT	*Insulated Gate Bipolar Transistor.*
LPF	*Low Pass Filter.*
RBS	*Regenerative Braking System.*
SC	*Supercapacitor.*
SVM	*Space Vector Modulation.*
TCS	*Traction Control System.*
VFC	*Variable Friction Coefficients.*
VSC	*Vehicle Stability Control.*

Contents

1 Introduction

One of the biggest bets of today's technology is the electric car. It is an alternative with almost zero emission of pollutants, which is capable of reducing the demand for fossil fuels. In these times of awareness, governments are opting incentives for plug-in electric vehicles, by which the increase of electric vehicles in the world market is taking place. Such incentives are reducing the environmental pollution due to the better use of energy resources. For this reason, the electric vehicle (EV) has become a transportation that worldwide people choose to invest due to the reason that it is a clean, efficient, quiet, economical and low maintenance technology.

The company "Accenture" in partnership with "FGV Energia" has published a study to evaluate the opportunities and challenges of implementing electric vehicles in Brazil. According to the survey, Brazilian market has the potential to sell about 150,000 electric car units per year, which would be about 7% of total car sales in 2016. Brazilian entities, such as the Brazilian Electric Vehicle Association (ABVE), operate with the government and business entities related to the automotive sector, to encourage the development and use of electric vehicles, as well as stimulate researches with the academic sector. In 2017, 3296 hybrids and electric vehicles were sold in Brazil, which is still an insignificant figure when compared to the 2,239 million ICE vehicles, according to the National Association of Automobile Manufacturers (ANFAVEA). The best-selling models in Brazil in 2017 were Volkswagen Golf, BMW i3, Toyota RAV4 and Tesla Model X, only the latter is purely electric, while the other ones are hybrid [11, 12].

Figure 1 indicates the sales of electric vehicles. As a result, the demand for home charging systems and commercial charging stations would go higher. In countries like India, Brasil and other emerging economies, the penetration level of electric vehicles is currently low, which is mainly due to two reasons: (i) the high selling price and (ii) due to the availability of limited models. However, penetration of electric vehicles is high in the U.S. and European countries such as the Netherlands, Norway, and others. In addition, penetration level of home charging systems in the U.S. is about 90% among electric vehicle owners compared to the European region, where it is 80% [1, 13].

Asia-Pacific region includes China, Japan, India, Australia, and rest of Asia-Pacific. This region holds strong growth potential for the market of electric vehicles. Currently, China and Japan are the major markets for electric vehicles in Asia-Pacific region. Owing to the high growth potential for electric vehicles, paired with easy accessibility of raw material at a low price, many electric vehicle manufacturers are planning to invest in countries such as China and India.

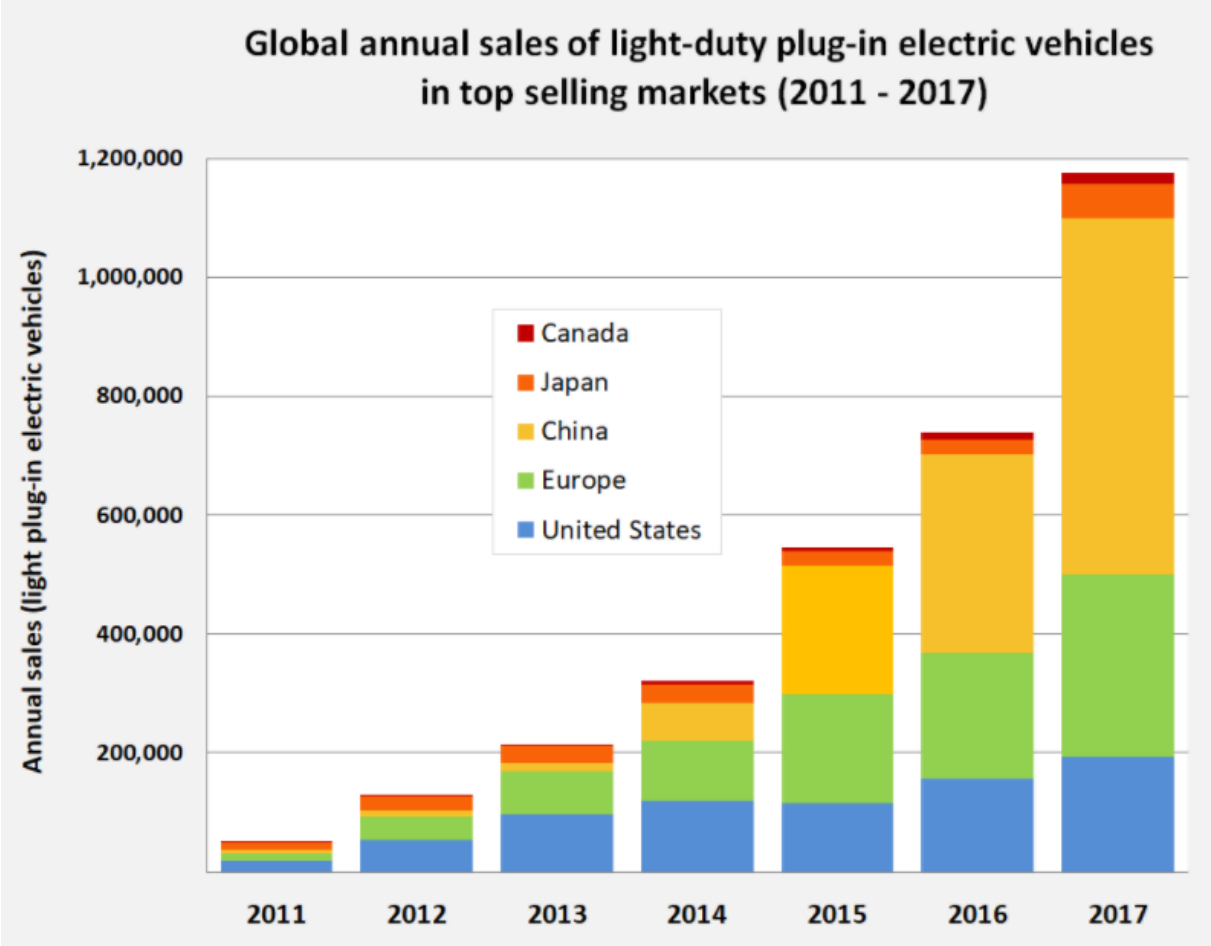

Figure 1 – Annual sales of light-duty plug-in vehicles in the world's top markets between 2011 and 2017 [1]

Modern vehicles make use of technologies such as regenerative braking system (RBS) and Anti-lock braking system (ABS). Regenerative braking system is a technology applicable in both conventional and electric vehicles. The regenerated energy can be stored in batteries, supercapacitors or other devices. ABS allows the wheels of a vehicle to maintain traction while braking, to prevent the wheels from blocking. Hence this way, it helps to avoid uncontrolled skidding. Therefore, ABS is of great importance by providing safety to passengers, maintaining the vehicle steerable.

The growth of the market in the Asia-Pacific region is supplemented by the increase in road safety rules, such as launching vehicle with ABS. For instance, as per Indian government rules, airbag and ABS are compulsory, and hence would be a standard feature in passenger cars from October 2018. Moreover, ABS will be mandatory for motorcycles with more than 125cc engine. Currently, global ABS Market is expected to garner $41 billion by 2022, registering a CAGR of 8.2% over the forecast period 2016-2022 [14].

1.1 Motivation

The safety systems such as Anti-lock Braking System (ABS) and Vehicle Stability Control (VSC), which are essential features in all modern automobiles, are developed continuously.

Researches focus on the technology of regenerative braking working together with friction braking are very limited in the literature [15].

The vehicle stability depends on the driver behavior, which performs basic operation such as steering angle, braking, and throttle application. These are inputs for the process Driver-Vehicle-Environment, as shown in Figure 2. The precision with which these inputs are applied depends upon the driver's level of experience.

The Anti-lock Braking System is an electronic system with sensors that monitors the rotation of each wheel and compares it to the speed of the vehicle.

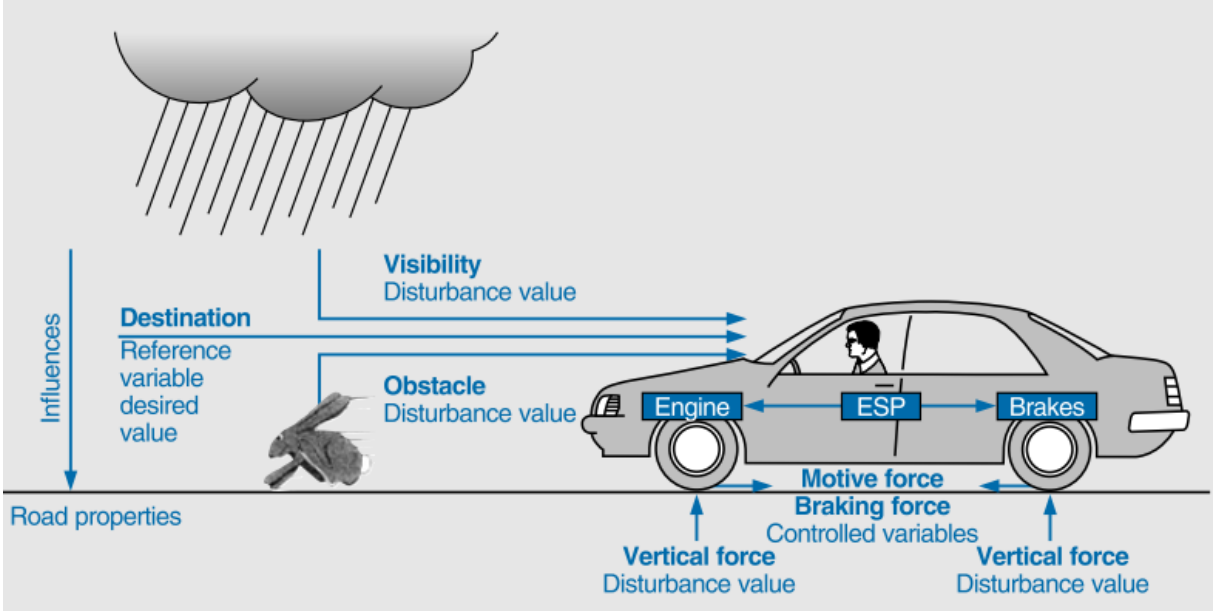

Figure 2 – Overall system of "Driver – Vehicle – Environment" [2]

As the control algorithms for ABS and RBS become more advanced, there is a requirement to accurately predict and understand the forces generated by the response of the tire to road contact, brake torque variations and the interaction of the wheels with the vehicle. Taking advantage of the quick response and accurate control of the electric motor torque, researchers have explored a way to introduce the motor torque into the ABS control, expecting a better control effect. However, these strategies haven't considered the cooperative action between the hydraulic braking system and the regenerative braking system. Therefore, it can be difficult to achieve good braking stability and high regenerative braking efficiency simultaneously [16, 17].

In this regard, this work provides study on the strategy of using regenerative braking system to satisfy the requirements of an electric vehicle with ABS.

1.2 Objective

This study develops a simulation tool and proposes control strategies to improve the performance of ABS applied to electric vehicles. An ABS function is proposed to be included in the electric motor control system to act during regenerative braking. Such a system operates in coordination with the mechanical brake, thus allowing an extension of RBS despite the critical steerability conditions. The vehicle modeling affords an adaptive simulation with RBS and/or ABS based on Simulink/Matlab driven by the induction machine with direct torque control (DTC). The performance analysis considers the capability of the braking system (regenerative plus mechanical) and maintains the commanded torque even if the road presents frictional variations.

1.3 Research Approach

- Literature review of simulations models and VE technologies.
- Detailed mathematical modeling of all the components based on a set of assumptions and requirements.
- Identification of simulation platform, implementation, and integration of models.
- Development of the torque estimation procedure to activate the anti-lock braking systems based on the ground conditions and external forces.
- Detailed analysis of the results of the simulation.

1.4 Thesis Outline

The chapters are organized as follows.

Chapter 2 provides a background of the mathematical modeling and simulation tools to regenerative braking and anti-lock braking system, as well as implementation of base components for torque control applied to the electric vehicles.

In Chapter 3, a comparison between scalar control and a direct torque control with space vector modulation (DTC-SVM) for the development of regenerative braking system is discussed. In addition, it develops a dynamic model of an electric vehicle fitted with a bank of supercapacitors and direct torque control. We will therefore focus on the regenerative braking control system, as well as torque control problems at low speed. This will allow us to base our contribution to regenerative braking control strategies under an adequate friction coefficient between tire and road, in addition to the hard stops.

Chapter 4 contains the study of the model and the dynamic behavior of the vehicle when the surface between tire and ground has a low friction. Henceforth, the simulation results are presented, using the control strategies performed in chapter 3.

Chapter 5 contains the discussions of ABS control to keep the regenerative braking under surfaces with a low grip.

Chapter 6 contains general conclusions and the perspectives for future works.

This thesis regards the studies published in the *2018 IEEE Transportation Electrification Conference and Expo (ITEC)*.

Link: `https://ieeexplore.ieee.org/document/8449954/`

2 Literature Review

This chapter provides a detailed description of the state-of-art in the dynamic modeling and control of an electric vehicle (EV) to make use of technologies for the braking system including the regenerative and anti-locked braking system. The first one provides efficiency in energy-saving on the braking and the latter provides stability to the driver, steering control and shorter stopping distances on some particular surfaces.

The model considers an electric propulsion system that is the heart of electric vehicles. It consists of an electric machine, power converters, and electronic controllers. The electric machine converts electrical energy into mechanical energy to propel the vehicle. Vice versa, the regenerative brake generate electricity that will be sent to an onboard energy storage elements. The power converter is used to supply the electric motor with voltage and current at appropriate conditions. The electronic controller controls the power conversion in order to have the production of torque and proper speed, according to the driver's command. The controllers can be divided into functional units: sensors, interface circuits, and processor (see Figure 3).

2.1 Vehicle Dynamics Model

This work considers the case study of a pure electric passenger vehicle shown in Figure 3. The block diagram shows that the vehicle is driven by an induction machine (IM) with traction on the front-wheels. The IM can work in two states: as a motor or a generator. Supercapacitors (SC) are energy storage elements that are electrically connected with the converter and can be charged and discharged during driving cycles.

For the regeneration process it isn't necessary to consider the batteries, since the role of the supercapacitor bank is be the high power source, what means the energy during acceleration and braking intervals will circulate in such device. The batteries role is to provide long term (average) power.

The braking performance is one of the most important characteristics that affect the vehicle's safety. There are many active safety systems such as Anti-lock braking system (ABS), traction control system (TCS), and electronic stability program (ESP), that regulate the forces at the tires and adapt the vehicle's conditions to the situations according to the driving environment.

Figure 4 shows the components of a conventional vehicle braking system. These components are controlled by a control unit through hydraulic actuators, that press the brake shoes against the drum, which cause braking due to frictional force. Currently, vehicles are equipped with disc brakes since they are more efficient during braking and have a better heat

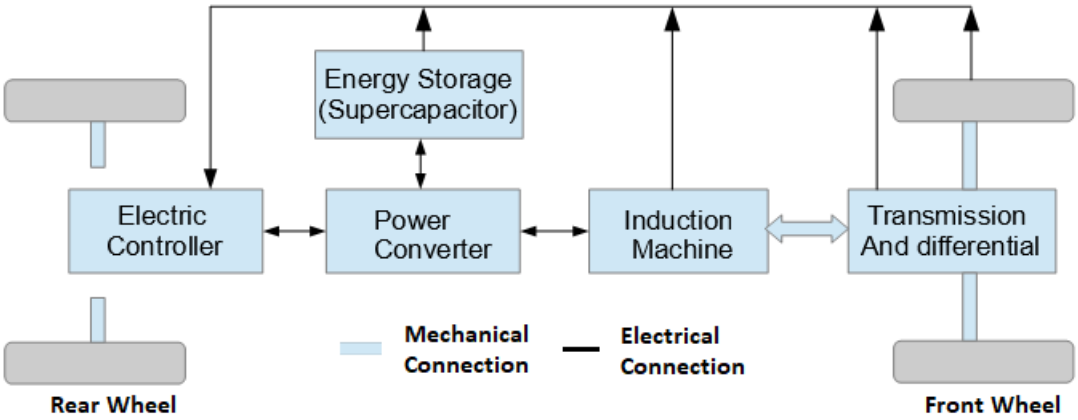

Figure 3 – Configuration of the case-study electric vehicle.

dissipating mechanism [18].

Small vehicle and some medium-sized vehicles are fitted with disk brakes on the front wheels and drum brakes on the rear (drum brakes represent a cost saving). New cars are now fitted exclusively with disk brakes at the front, and there is an increasing trend towards disk brakes for the rear wheels as well [2].

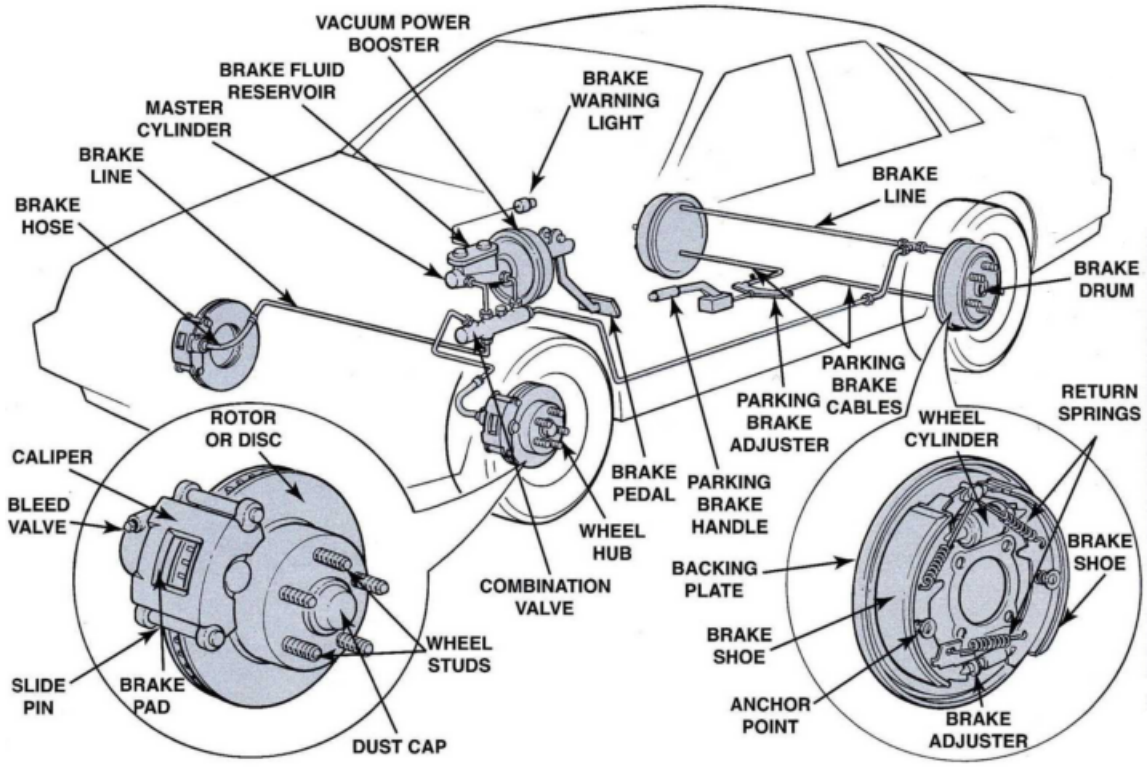

Figure 4 – Conventional vehicle braking system [3].

The force applied to the tires affects the vehicle dynamics and determine the stability and maneuverability of the vehicle, especially under critical driving conditions. The forces and moments of the tires on the road also indicates the intention of the driver command. Generated from the friction between the tire and the texture of the road, the friction coefficient plays

an important role for achieving a proper performance between the tires and the road. Friction coefficient defines the maximum possible acceleration, and more importantly, the minimum braking (stopping) distance as shown in Figure 5.

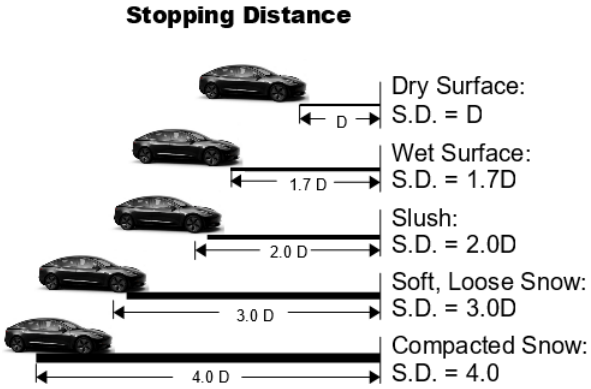

Figure 5 – Vehicle Stopping Distance for different friction conditions [4].

Table 1 shows the average values of tractive effort coefficients on various roads. The traction coefficient is heavily dependent on the roughness, the contact area, and the frictional force pulling or pushing a vehicle's mass.

Table 1 – Average Values of Tractive Effort Coefficient on Various Roads [8]

Surface	Peak Values,μ_p	Sliding Values,μ_s
Asphalt and concrete (dry)	0.8–0.9	0.75
Concrete (wet)	0.8	0.7
Asphalt (wet)	0.5–0.7	0.45–0.6
Grave	0.6	0.55
Earth road (dry)	0.68	0.65
Earth road (wet)	0.55	0.4–0.5
Snow (hard packed)	0.2	0.15
Ice	0.1	0.07

The behavior of a vehicle system and its dynamics involves a balance among the several acting forces. These forces are categorized into tractive (F_t) and road-load (F_{tb}) forces.

The tractive effort appears in the contact area between the driven wheels and the road surface and propels the vehicle forward. It is produced by the torque power plant and transferred through transmission and final drive to the wheels. While the vehicle is moving, there are road-load resistances, that try to stop its movement. These road-load forces include rolling resistance of the tires, the aerodynamic drag force, frictional force of the slope and force due to vehicle inertia.

According to the Newton's second law, equation 2.1 indicates that speed and acceleration depends on tractive effort, road-load force, and on the mass of the vehicle. Vehicle

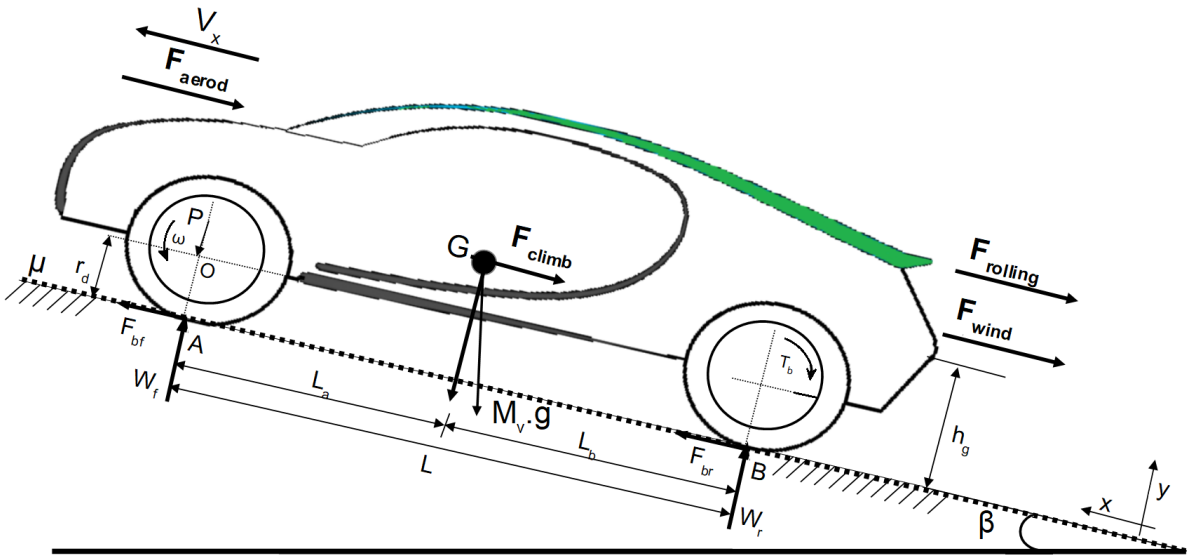

Figure 6 – Electric Vehicle Dynamics.

acceleration can be written as

$$\Sigma F_b - \Sigma F_{br} = \frac{\partial V_x}{\partial t} * \delta M_v \ [N] \tag{2.1}$$

where V_x is the vehicle speed (m/s^2), $\Sigma\, F_b$ is the total tractive effort, $\Sigma\, F_{br}$ is the total resistance, M_v is the total mass, and δ is the mass factor, which is an effect of rotating components on the power train.

The Aerodynamic Drag force (F_{aerod}) takes into account the aerodynamics of the vehicle and is given by:

$$F_{aerod} = 0.5 * \rho * A_f * C_d * (V_x - V_w)^2 \ [N] \tag{2.2}$$

Where, C_d is the aerodynamic drag coefficient, A_f is the frontal area, V_w is wind speed, ρ is the air mass density, and V_x is the vehicle linear speed.

Rolling resistance force ($F_{rolling}$) is the tangential force of normal force (P) on tires and the rolling resistance coefficient (μ_r).

$$F_{rolling} = P * \mu_r = M_v * g * \mu_r * cos(\beta) \ [N] \tag{2.3}$$

The hill-climbing resistance force (F_{climb}) is based on the angle of inclination β and is given by:

$$F_{climb} = M_v * g * sin(\beta) \ [N] \tag{2.4}$$

The linear acceleration force (F_{acc}) is based on the mass of the vehicle (M_v), acceleration/deceleration of the vehicle (α_v), and the vehicle speed (V_x) expressed as following:

$$F_{acc} = M_v.\alpha_v = M_v \frac{\partial V_x}{\partial t} \; [N] \tag{2.5}$$

Based on all these equations the resultant force produces a counteractive torque to the driving motor. The total acting force is given by

$$F_{total} = F_{aerod} + F_{rolling} + F_{climb} + F_{acc} + F_{wind} \; [N] \tag{2.6}$$

2.1.1 Wheel Dynamics

Figure 7 shows the principle of braking force distribution between front and rear wheels, which occurs when brake operations are performed while the vehicle is running on a flat road. The vehicle braking force depends on the vehicle mass (M_v) and acceleration/deceleration of the vehicle (α_v). The relationship between the vehicle braking force (F_v), the front wheel braking force (F_{bf}), and the rear wheel braking force (F_{br}) can be represented as:

$$F_v = M_v.\alpha_v = F_{bf} + F_{br} \; [N] \tag{2.7}$$

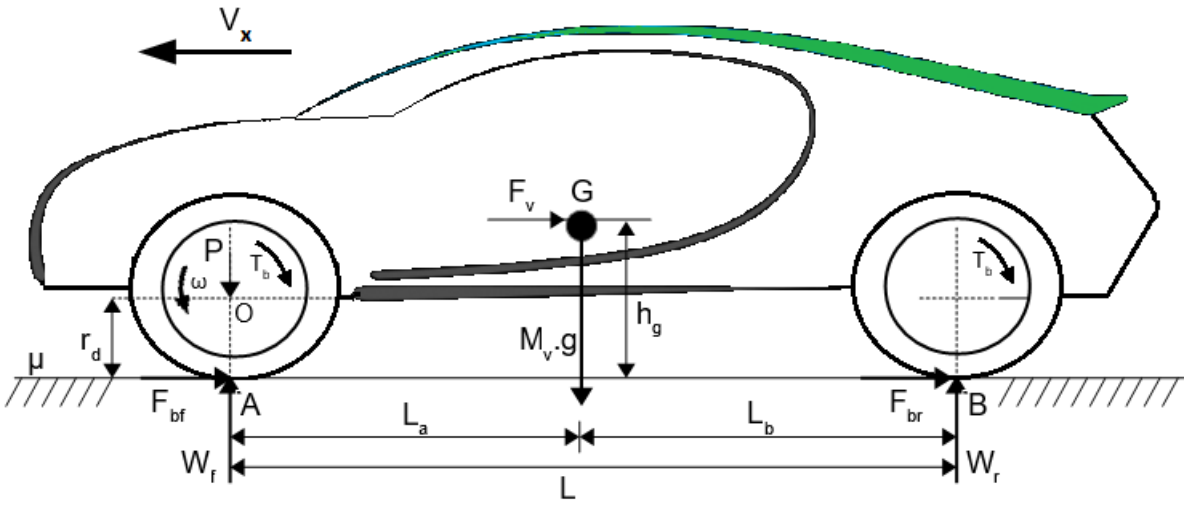

Figure 7 – Load movement which occurs when brake operations are performed while vehicle is running on flat roads.

The load will be shifted from the rear wheels to the front wheels when the brake pedal is stepped on, which will affect the distribution of braking force between front and rear wheels [8, 19]. To estimate the influence of load movement on braking, brake strength z is

defined by the equation 2.8. Where, g is the gravitational acceleration (m/s^2) and (α_v) is the vehicle's deceleration.

$$z = \frac{\alpha_v}{g} \tag{2.8}$$

Thus, the maximum braking forces F_f and F_r which can be generated for the front and rear wheels, are given by Equations (2.9–2.11):

$$F_{bf} = \mu.W_f = \mu.\frac{M_v g(L_b + z.h_g)}{L} \tag{2.9}$$

$$F_{br} = \mu.W_r = \mu.\frac{M_v g(L_a - z.h_g)}{L} \tag{2.10}$$

$$F_{bf} + F_{br} = \mu.M_v g \tag{2.11}$$

Where W_f and W_r are the normal forces on the front and rear wheels, G is the total load of the vehicle and μ represents the friction coefficient between the tire and the road surface. It's possible to determine the braking forces which can make the front and rear wheels lock for each friction coefficient. When the braking force is distributed among the front and rear wheels safe braking is secured, which can be represented as

$$F_{br} = \frac{1}{2}\left[\frac{M_v g}{h_g}\sqrt{L_b^2 + \frac{4h_g L}{M_v g}F_{bf}} - \left(\frac{M_v g L_b}{h_g} + 2F_{bf}\right)\right] \tag{2.12}$$

The ideal braking force distribution characteristics were determined by calculations based on the specifications of a passenger vehicle (see Table 2).

Table 2 – Parameters used for studying at vehicle dynamic

μ	0.4∼1	M_v	1320 kg
L	3 (m)	L_a	1.4 (m)
h_g	0.5 (m)	L_b	1.6 (m)
C_d	0.4 (m)	A_f	3 (m^2)
ρ	1.18 (kg/m^3)	V_w	0 (m/s)
J_w	0.5 (kg/m^2)	g	9.819 (m/s^2)
β	0∼0.174 (rad)	r_d	0.25 (m)

As shown in the Equation 2.9 and Equation 2.12, braking forces F_f and F_r vary with the friction coefficient μ. Thus, in order to distribute braking force according to the ideal curve, we need to obtain the friction coefficient in real time. However, it is difficult to measure

the changing friction coefficient directly. It can be found that the distribution ratio R_f and R_r of the front and rear wheels, does not depend on the friction coefficient [20].

$$R_f = \frac{F_f}{F_f + F_r} = \frac{L_b + z.h_g}{L_a + L_b} \tag{2.13}$$

$$R_r = 1 - R_f \tag{2.14}$$

The vehicle models available are of the following types: general vehicle model, vehicle model of four-wheels, vehicle model of two-wheels and vehicle model of the single wheel. We used the dynamic model with the single wheel in order to describe a suitable braking performance and also to simplify the underlying problem.

The vehicle braking is analyzed on the point A of figure 7. The brake pad is pressed against the brake plate, thus developing a frictional torque. This braking torque results in a braking force at the contact area between the tire and the ground. It is this braking force that tries to stop the vehicle. The traction or braking force is produced by the pneumatic tire and friction coefficient. Depending on the driver's command, this is an acceptable procedure, provided the EV protection devices prevent any exaggerated elevation of temperature and current peaks [21]. The braking forces act on front and rear wheels and can be expressed as the force (F_{bf}) available at the tire-ground contact which depends on the axle torque (T_b) and tire radio (r_d). The wheel reaction force will generate a torque that initiates rolling motion of the wheel, resulting in an angular speed ω. The equations of motion and longitudinal friction of the wheels are:

$$F_v = M_e.\alpha_v = M_e * \frac{\partial V_x}{\partial t} \tag{2.15}$$

$$F_{bf} = \frac{T_b}{r_d} \tag{2.16}$$

$$F_{bf} = \mu P \tag{2.17}$$

$$F_{bf} = \frac{J_w.\dot{\omega} + T_b}{r_d} \tag{2.18}$$

Where M_e is ¼ of the mass of the vehicle (kg), V_x is the vehicle speed (m/s), F_v is the longitudinal friction (N), J_w is the moment of inertia of the wheel (kg·m2), ω is the wheel angular speed (rd/s), r_d is the wheel radius, T_b is the front brake torque (N·m), μ is the coefficient of longitudinal friction, and P is the normal force (N).

2.1.2 Tire Modeling

When the vehicle braking command takes place on a straight-line, the longitudinal speed of wheel is lower than the vehicle speed because of tire deformation and the traction/braking forces exerted on the tire. Hence, the vehicle will slip on the road. Where tire slip is calculated using ω, r_d, and V_x, which represents the wheel angular velocity, the wheel rolling radius, and the vehicle forward velocity for the formula:

$$\lambda(t) = \frac{V_x(t) - \omega(t).r_d}{max(V_x, \omega)} = \frac{V_x(t) - \omega(t).r_d}{V_x} \tag{2.19}$$

The tractive effort coefficient (μ) and tire slip have a relationship as shown in Figure 8. Where $\lambda \ \varepsilon$ [0, 1]. In particular λ= 0 corresponds to a pure rolling wheel and λ= 1 to a locked wheel.

The tractive effort coefficient reaches the maximum value at the peak value, point A, caused by the elasticity of the tire. When the slip ratio (λ) is below point A, the slip can increase the traction force. The peak tractive effort is reached at a slip of $0.15 \sim 0.2$. Once the slip ratio exceeds A, the traction force will decrease as a result of the decrease of adhesive coefficient. This is an unstable condition. Therefore, for normal driving, the slip of the tire must be limited $\lambda \ \varepsilon$ [0, 0.2] to maintain the steering ability. The longitudinal tire force F_{bf} in Equation 2.20 depends linearly on vertical force P and nonlinearly on the friction coefficient. On the asphalt dry surface, the maximum force is larger. However, on the snow road surface, the maximum value is really small. The road-wheel friction coefficient (μ) depends on the road condition (see Table 1).

$$F_{bf}(\lambda, P) = \mu(\lambda)P \tag{2.20}$$

The tire model is the functional relation between the tire adhesion during the braking process and other various parameters. The road-wheel friction coefficient has been developed for many empirical expressions and various parameters are represented by the functional relationship.

The Pacejka's model is also known as 'Magic Formula'. It uses trigonometric functions to fit experimental data with a function. It depends on the longitudinal tire slip (λ), the aligning torque, the combined effects of vertical force (P), road surface (maximum values μ_p) and other conditions. A simplified form of Pacejka's magic formula can be expressed as:

$$\mu_i(\lambda) = Dsin(C\tan^{-1}\left\{B\lambda_i - E[B\lambda_i - \tan^{-1}(B\lambda_i)]\right\}) \tag{2.21}$$

Figure 9 shows tire friction curves, generated by the Pacejka model, for four common road conditions. This static map describes the dependence between slip and friction, additionally it depends on the vehicle speed (V_x).

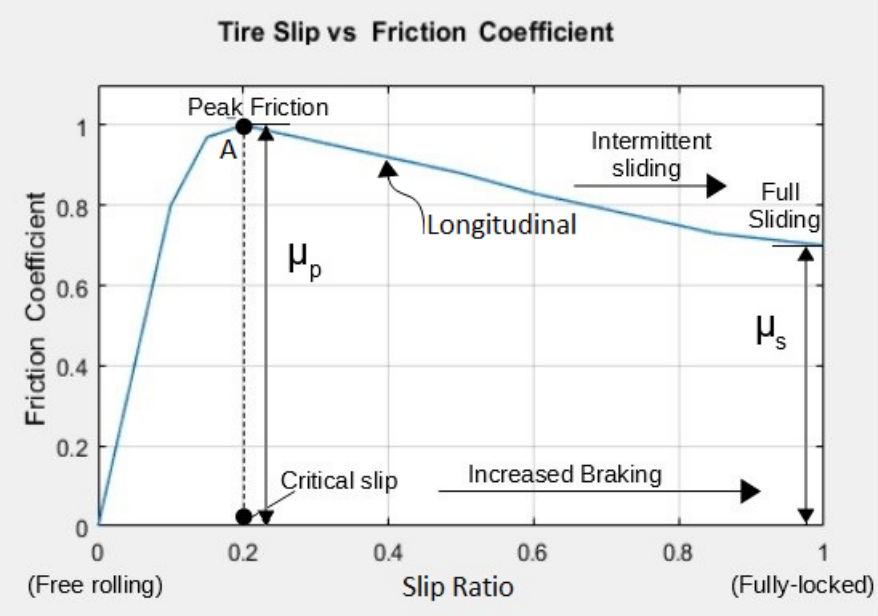

Figure 8 – Longitudinal Slip and the friction coefficient curve of the tire.

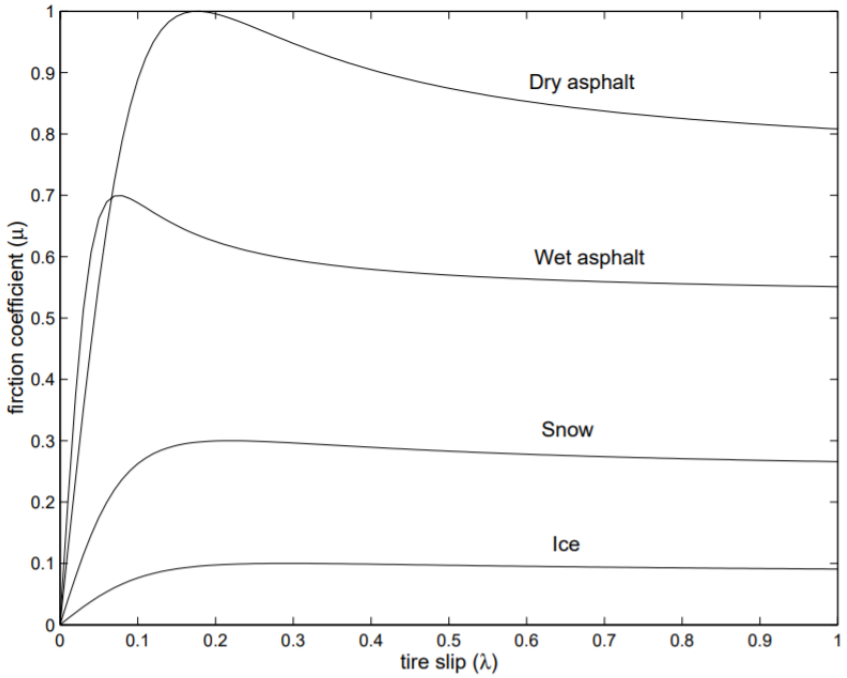

Figure 9 – Tire friction curves.

The nonlinear Magic Formula tire model in Matlab has coefficients by Paceijka for typical road conditions. Magic formula coefficients for typical road conditions are numerical values based on empirical data [5, 22].

Table 3 – Magic Formula Coefficients for different kind of surfaces

Surface	B	C	D	E
Dry	10	1.9	1	0.97
Wet	12	2.3	0.82	1
Snow	5	2	0.3	1
Ice	4	2	0.1	1

This model contains a quite simple description of the slip dynamics for a wheel. It does not capture pitching motion of the car body while braking, suspension dynamics, actuator dynamics, tire dynamics nor camber angle (the tire is consider perpendicular on the road surface) [23].

2.1.3 Induction Electric Machine

A three-phase induction machine (IM) has stator windings in which the alternating supply voltage is applied. The rotor can be composed of a short-circuited cage or windings that allow current flow.

Given the three-phase characteristic of the stator supply and the spatial distribution of the windings, the field produced by the stator is rotating, that is, its resultant has a rotational movement. By transformer effect, the magnetic fields produced by the stator windings induce currents in the rotor. The field produced by the currents induced in the rotor has the same rotational characteristic, always trying to follow the rotating field of the stator. So that, the interaction of both magnetic fields produces the torque that makes the machine to rotate.

If the rotor rotates at the same speed as the rotating field, there will be no induced current since there will be no flux variation through the rotor turns. If there is no current, there will be no torque. From this qualitative analysis, it can be concluded that the production of torque in the machine axis derives from the fact that the speed of the rotor is always different than the speed of the rotating field.

The current induced in the rotor has a frequency which is the difference between the angular frequency of the rotating field and the rotor speed.

In traction, the rotor rotates in the same direction of the rotating field, and as the sliding increases (starting from zero), the torque also increases, practically linearly, while the air gap flux remains constant. The normal operation as a motor occurs in this linear region.

In the regeneration region, the rotor and the rotating field move in the same direction, but the mechanical speed is greater than the synchronous speed, leading to a negative

sliding. This means that the machine operates as a generator, delivering power to the system to which the stator is connected.

The electric machine slip is defined by

$$S = \frac{\omega_s - \omega_m}{\omega_s} \tag{2.22}$$

Where ω_m is the rotor angular speed (rd/s) and ω_s is the stator angular speed (rd/s). The Figure 10 shows a typical torque-speed curve from a sinusoidal voltage source of fixed frequency and amplitude, according to the analysis of its power flow. There are three operating regions:

- Traction (0<s<1)
- Regeneration (s<0)
- Braking (1<s<2)

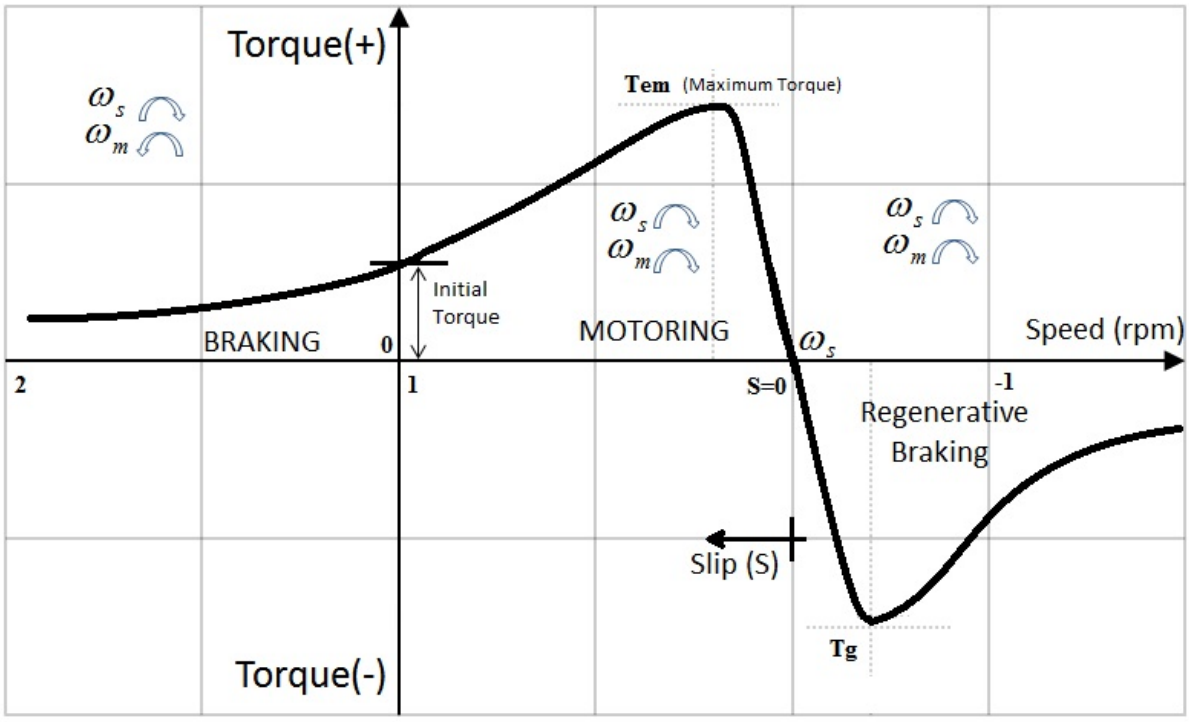

Figure 10 – Characteristic torque-speed of the induction machine.

The developed torque can be expressed by

$$T_{em} = \frac{3.R_r.V_s^2}{s.\omega_s\left[(R_s + R_r/s)^2 + (X_s + X_r)^2\right]} \tag{2.23}$$

Where R_s and R_r represent the resistances of the stator and rotor windings, while X_s and X_r are the stator and rotor leakage reactances, that is, they represent the magnetic flux that do not link both windings.

Figure 11 shows the induction motor drive characteristics when used as the EV propulsion. The transmission gear ratio is designed such that the EV reaches its maximum speed at the maximum induction motor speed.

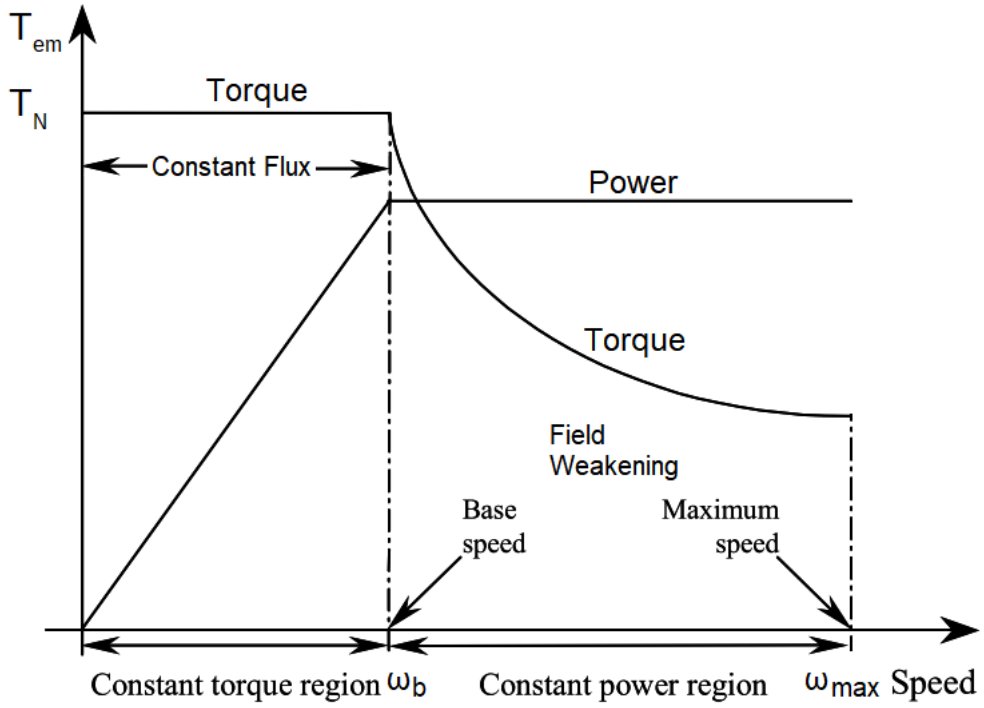

Figure 11 – IM speed range for EV typical.

The IM maximum torque is determined from the motor characteristic curve. Such torque is available below the IM nominal power (P_N). When the IM reaches P_N, it can operate with field weakening, reducing the torque as the speed increases. This is described by

$$T_{em} = \begin{cases} T_N, & \omega_s \leq \omega_b \\ P_N/\omega_s, & \omega_s > \omega_b. \end{cases} \tag{2.24}$$

The IM can operate continuously at the nominal conditions. During short intervals the IM can produce a higher torque. In this study such overload torque will be considered 50% above T_N, i.e., T_{max} =1.5 T_N [24].

When a deceleration is required, torque is transferred from the motor and mechanical brakes to the wheels. The braking torque applied by the motor is converted to electric energy and transferred to the storage device (Supercapacitors).

The regeneration allows to capture (store) part of the kinetic energy that would be converted into heat (wheel discs) during frictional braking in a conventional vehicle. Performing

regenerative braking, when the driver press the brake pedal to reduce the vehicle speed, the electric machine acts as a generator, driven by the wheel or wheel axle. The generated electric energy is absorbed, processed and stored.

2.1.4 Power Converters

DC-AC converters are called as "Inverters". The function of an inverter is to transform a continuous source of electricity (voltage or current) into an alternating quantity, of null mean value. Typically, the induction machine is driven by a variable frequency and voltage inverter with pulse width modulation (PWM).

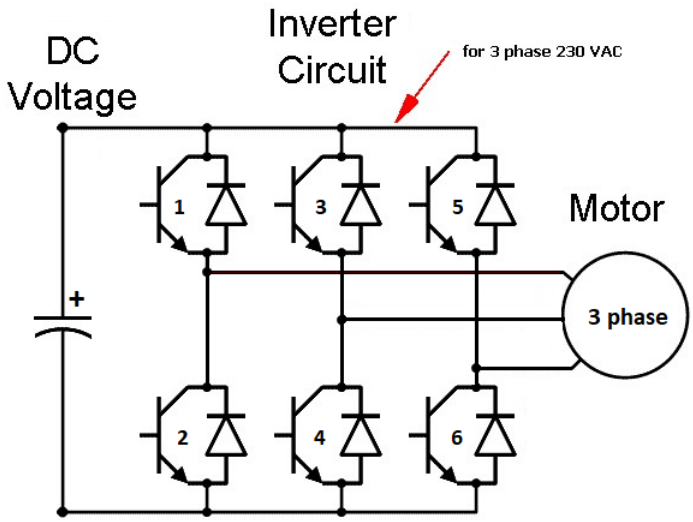

Figure 12 – Machine drive control by Three-Phase Voltage Source Inverter.

DC-DC bidirectional converters are shown in Figure 13. They process the energy transferred from the SC bank and batteries to the DC side of the inverter. The SC bank is used as an auxiliary source to avoid the stress of the batteries due to high current peaks [25, 26].

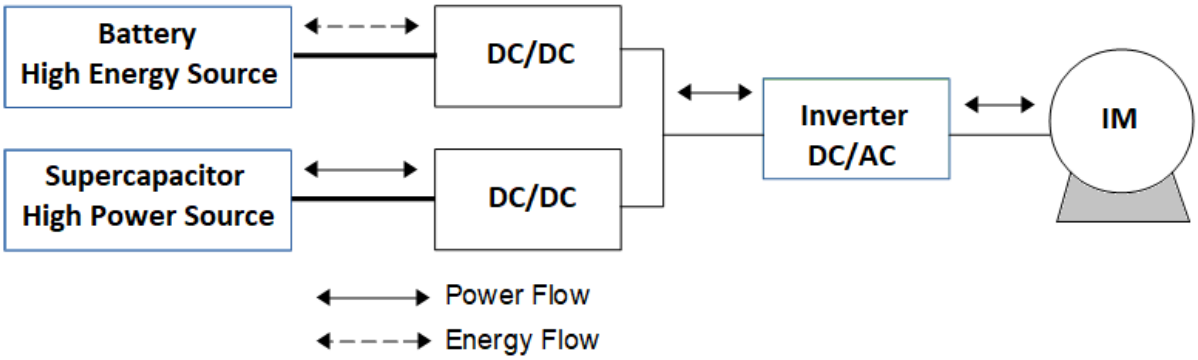

Figure 13 – Power Flow in electric vehicle.

The scalar control imposes a certain combination of voltage and frequency (V/F), in order to maintain the V/F ratio constant, that is, the motor works with approximately constant flux.

The torque developed by the induction motor is directly proportional to the ratio of the applied voltage and the frequency of supply. By varying the voltage and the frequency, but keeping their ratio constant, the torque developed can be kept constant throughout the speed range [8]. It is normally applied when there is no need of fast response to torque command. It's shown in Figure 14.

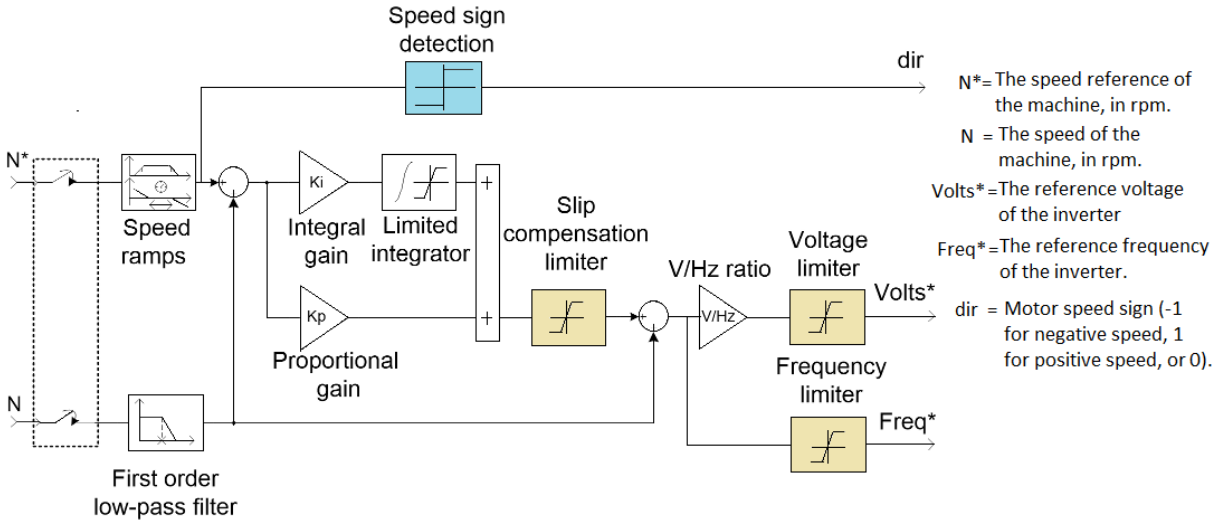

Figure 14 – Speed Controller of V/F control on Matlab/simulink [5].

Space Vector Modulation (SVM) is an algorithm for the control of Pulse Width Modulation (PWM). SVM gives better harmonic response and higher efficiency compared to pulse width modulation techniques. The performance of Space Vector Modulation technique and Sinusoidal Pulse Width Modulation are compared for harmonics, THD and output voltage, It was discussed in [26, 27].

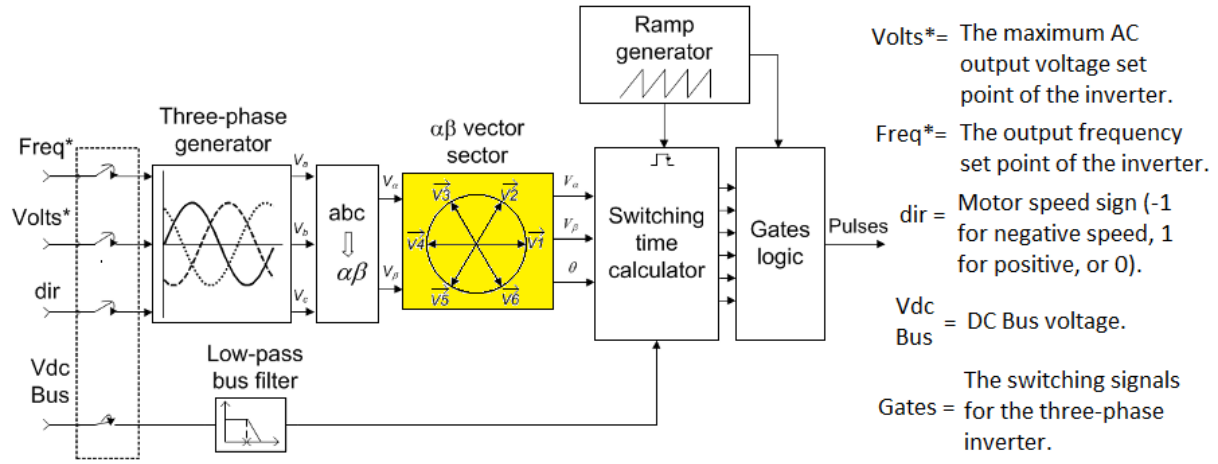

Figure 15 – Space Vector Generator on Matlab/simulink [5].

2.1.5 Torque Control in Electric Vehicle

Two techniques are known for three-phase induction machines, which are: (i) the Field-oriented control (FOC) and (ii) Direct torque control (DTC). The simplicity of DTC allows a good torque control in steady-state and transient conditions as can be seen in Table 4.

Table 4 – Summary of the comparison between FOC and DTC [10]

Properties	DTC	FOC
Dynamic response for torque	Quicker	Slower
Steady-state behaviour for torque, stator flux and currents	High ripple and distortion	Low ripple and distortion
Requirement of rotor position	No	Yes
Current control	No	Yes
PWM modulator	No	Yes
Coordinate transformation	No	Yes
Parameter sensitivity	- For a sensorless estimator: Rs - For a non-sensorless estimator Lsd, Lsq e ψ	Decoupling depends on: Lsd, Lsq e ψ
Switching frequency	Variable, depending on the operating point and during transients	Constant
Audible noise	Spread spectrum, high noise especially at low speed	Low noise at a fixed frequency
Control tuning	Hysteresis bands/PI gains	PI gains
Complexity and processing requirements	Lower	Higher

The DTC is employed in this study together with space vector modulation as shown in Figure 16. The DTC technique is based on the application of a logic table that calculates the correct switching of the inverter, by correcting the torque values and stator flux. DTC-SVM allows achieving a fast torque response and a good closed-loop speed control, if this control loop is desired. However, the DTC requires an intense inverter switching and can produces high torque ripple [26, 28], which is a disadvantage.

Currently, the latest research seeks DTC performance to solve these problems and, at the same time, retains its simple control structure, with the use of improved switching tables, use of comparators with and without hysteresis, at two or three levels, implementation of DTC schemes with constant switching frequency operation, with PWM or SVM, introduction of fuzzy or neuro-fuzzy techniques and use of the sophisticated flux estimators to improve the low speed behavior [27, 29, 30].

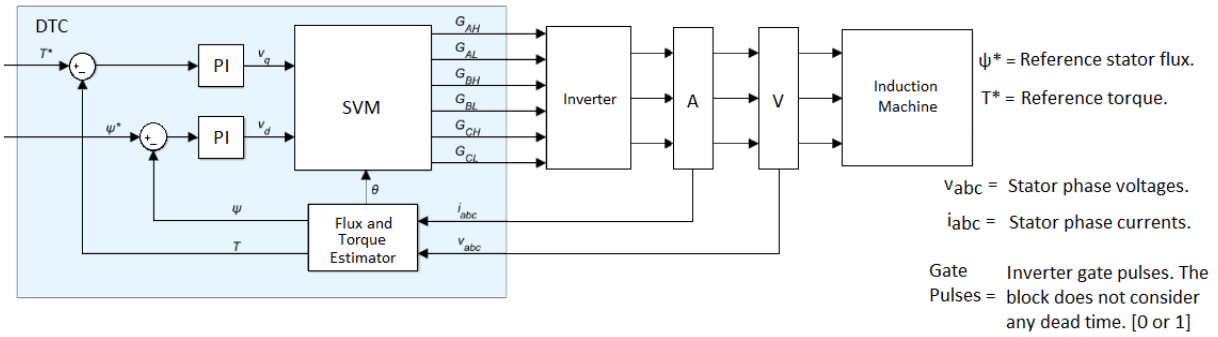

Figure 16 – Configuration of Direct Torque Control on Matlab/simulink [5].

2.2 Regenerative Braking System (RBS)

Braking, for any vehicle, means the application of a force to reduce its speed or stop its movement. The braking distance is the elapsed course between the time the brakes are applied and the time the vehicle comes to the complete stop. The braking friction is used to counteract the forward momentum of a moving vehicle. As the brake pads rub against the wheels or a disc that is connected to the axles, heat energy is created. This heat energy dissipates into the air, wasting the vehicle's kinetic energy as shown in Figure 17. This cycle of friction and wasted heat energy reduces the vehicle's fuel efficiency. Therefore, more energy from the engine is required to replace the energy that was lost in braking the vehicle [31].

Regenerative braking is a technology fitted for extending the vehicle's range. The technology dates the XIX century, when it was developed by M.A. Darracq and presented in France in 1897. Since that system was heavy and bulky, it wasn't attractive at that time [21, 32].

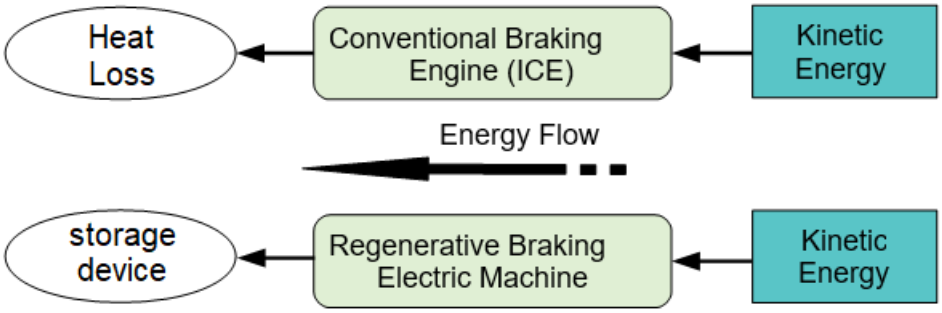

Figure 17 – Energy Flow in Vehicle Braking.

The regenerative braking in EV converts the kinetic energy (E_k) into electrical energy. This energy is stored batteries or supercapacitors and can be used instantaneously or later in accordance to the vehicle's demand.

The following equations allow to evaluate the energy accumulation in the storage elements by using the principle of energy conservation.

$$J_c = b^2 J_w \tag{2.25}$$

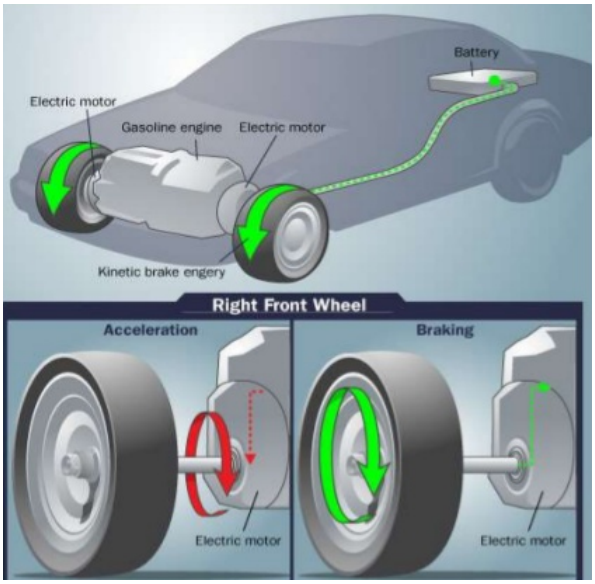

Figure 18 – The electric motor in the braking operation becomes a generator allowing to recover the energy [6].

$$E_k = M_v * \frac{V_x^2}{2} = J_m.\frac{\omega_m^2}{2} + J_c.\frac{\omega^2}{2} \tag{2.26}$$

Where J_w is the wheel inertia ($kg.m^2$), J_c is the load inertia ($kg.m^2$), J_m is the motor inertia ($kg.m^2$), M_v is vehicle mass (Kg), ω_m is motor speed (rd/s), ω is wheel speed (rd/s) and b is the gear ratio.

The first EV with RBS was implemented with DC motor. The use of DC machines in EV is due to its easy control for traction application. This motor provides high torque at low speed. However, the main drawback is the intense maintenance needs due to the brushes and commutator wear [7, 8, 31]. Advances in AC converters and motors allow the use of induction motors, since they show an acceptable performance, in addition to their low cost and robustness [33, 34]. Other motors, as the brushless DC or the Permanent magnet synchronous motor (PMSM), are considered in high performance and conceptual vehicles due to their high cost [35].

We can analyze the torque behavior from Figure 19. In the curve, there are three main factors to take into account: (i) maximum nominal torque T_N (point 1), (ii) maximum motor speed (point 2) and (iii) electric motor power limitation $P_N = T_N * \omega_b$ (see Equation 2.24).

Generally, a regenerative braking system operates in coordination with the traditional friction brake (Mechanical Braking), the reasons are: (i) the regenerative braking torque is not enough to cover the required braking torque; (ii) sometimes the regenerative braking cannot be used to preserve the SC or the battery life, which includes, the high state of charge (SOC) and high temperature of the device [7, 36].

From Figure 19 we can observe that, when the required motor torque is "a", the braking can be achieved only by the electric brake since it's smaller than T_N . Whereas, as the braking torque "b" is larger than maximum motor torque at that speed, the conventional friction brake is demanded to be operated together with the electric brake to supply the missing torque, "c". Similarly, the motor power limitation needs to be taken into account. Thus, the algorithm used and presented in Figure 20 can perform the regenerative and mechanical braking combinedly.

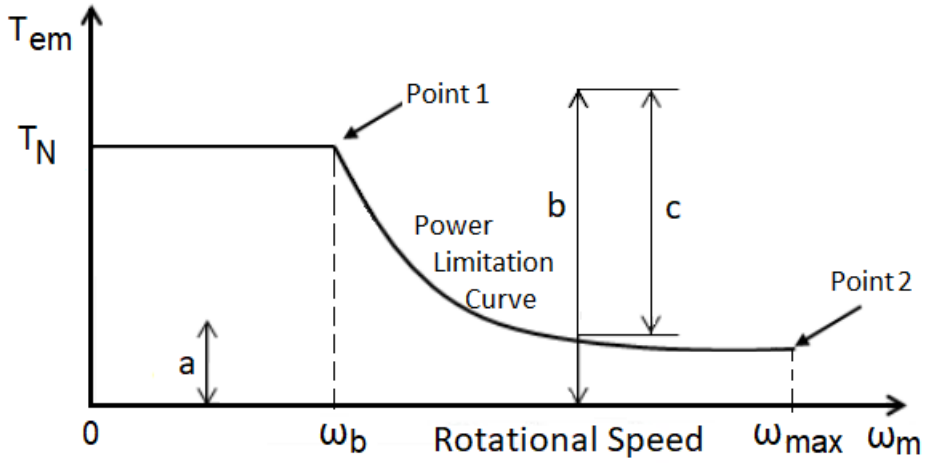

Figure 19 – Electric Motor Torque-Speed Characteristic, valid for traction and braking.

The control structure depicted in Figure 21, is to test the system performance. In this structure, we can observe three input variables which are the driver desired brake torque ($T_{desired}$) and motor speed (ω_m). The outputs are motor current (I) and pressure (ρ) to be applied to electrical and mechanical brake system. The logic control adjusts regenerative braking torque for ensuring the stability of the vehicle in the braking operations with the distribution of the deceleration forces [7, 21, 37].

This work advances the RBS study developed at [21], considering a more precise torque control, the implementation of ABS in both, electric and magnetic brakes.

2.3 Anti-lock Braking System (ABS)

The ABS first began in Germany in 1978 developed by Bosch. In 1986, it was followed by the traction control system (TCS) which extended system capability to the control of wheel spin under acceleration. As a further improvement of driving safety, the electronic stability program (ESP) was introduced in 1995, which integrated the functions of ABS with TCS. The ABS is shown in Figure 22.

ABS acts in hazardous driving conditions, in which it is possible to lock the wheels under braking. Possible causes of such locking include wet or slippery road surfaces, and abrupt reaction by the driver (unexpected hazard). As a result, the vehicle can become uncontrollable,

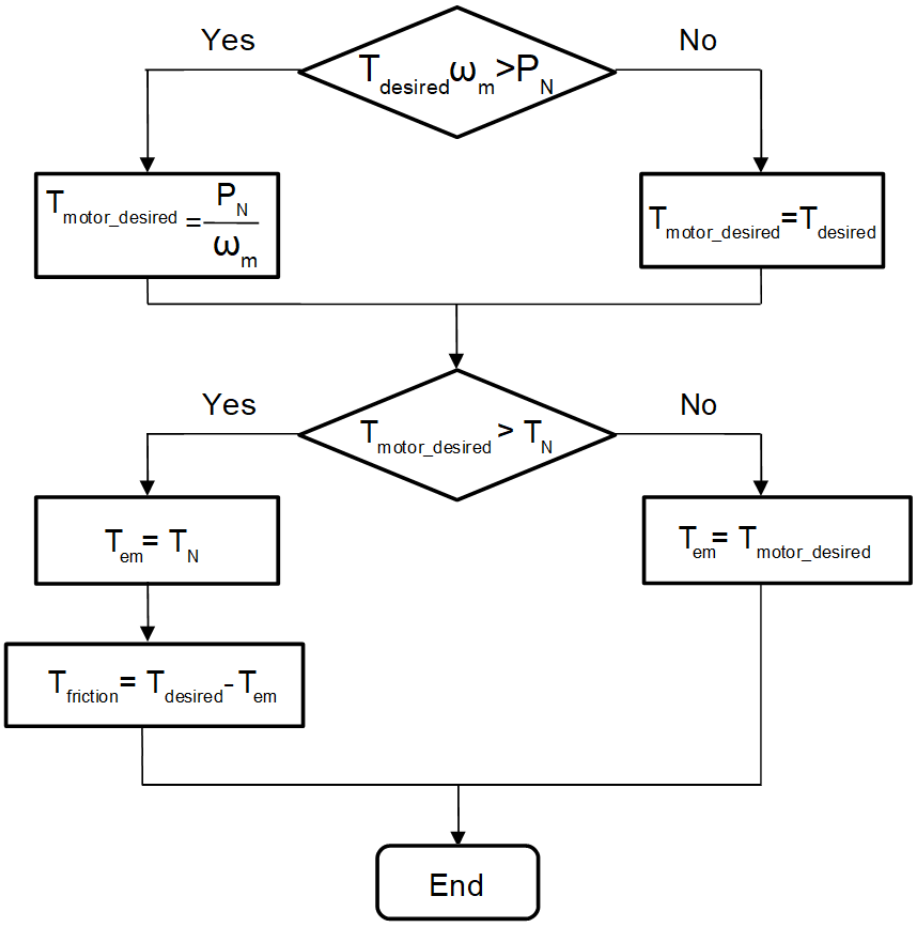

Figure 20 – Brake torque allocation flow chart.

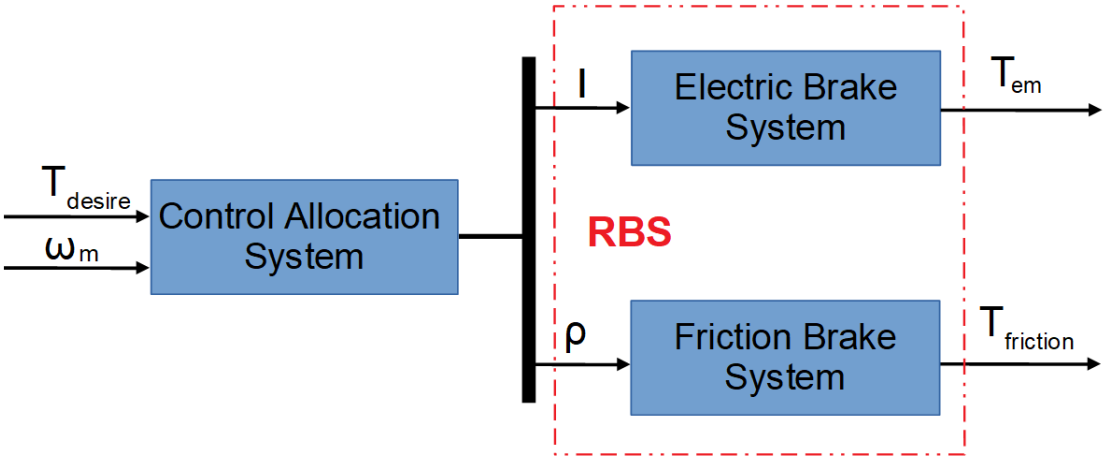

Figure 21 – Brake system with control allocation module.

and may go into a slip and/or leave the road. In this context, the anti-lock braking system detects if one or more wheels are about to lock up under braking and, if so, makes sure that the brake pressure remains constant or is reduced. By doing so, it prevents the wheels from locking up and the vehicle remains steerable. As a consequence, the vehicle can brake or stop quickly and with safety, reducing the danger of skidding.

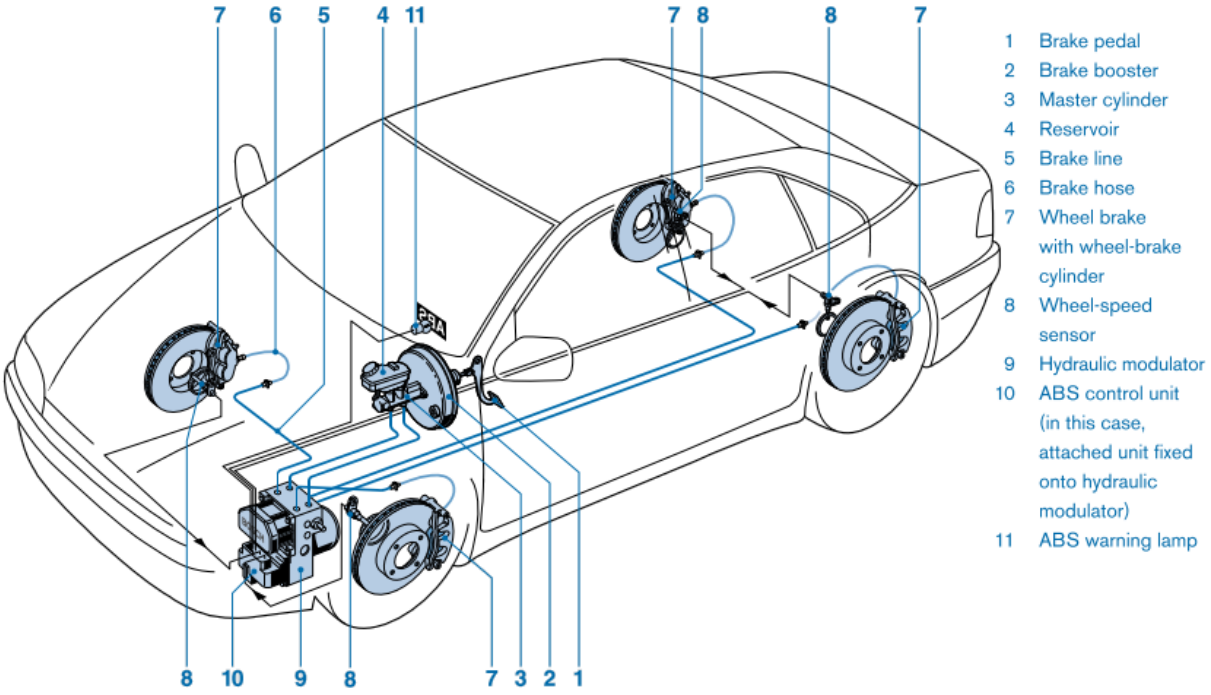

Figure 22 – Braking System with ABS [2].

The ABS is designed to achieve maximum negative acceleration by preventing the wheels from locking up. It consists of three parts: sensors, electronic control unit (ECU) and actuator (pressure regulator). The mathematical model of the ABS is composed of four parts: the vehicle dynamics model, the tire model, brake system model and control system, as is shown in Figure 23.

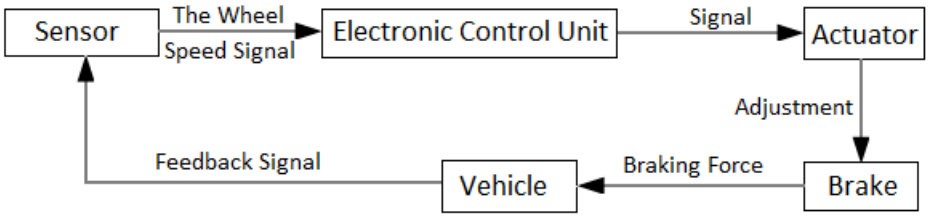

Figure 23 – The components of automobile anti-lock system.

The ABS is based on several measures. The main source of information is the angular speed of the vehicle's wheel, that is constantly being controlled. As second the speed of the vehicle or the angular acceleration of the wheel, must be available.

There are different kinds of ABS algorithms: those based on logic switching from wheel acceleration information and wheel slip regulation. A third kind uses both, wheel slip and wheel acceleration measurements. This algorithm is able to stabilize globally and asymptotically the wheel slip around any prescribed set-point, both in the stable and unstable regions of the tire. Moreover, it gives precise bounds on the gains of the control law for which stability is proved mathematically [38, 39].

Most of the command algorithms for ABS are based on a combination of two control, which are described below [7]:

- **Wheel Slip Control** - In this method, the wheel slip is continuously calculated through wheel speed and vehicle speed sensors and the value is sent as a state to the ABS controller. The control action commands the actuator to get the wheel slip equal to the desired value. The ABS control algorithms must be robust and operate under varying surface conditions. Slip control systems are known to work well for non-decreasing force conditions.
- **Wheel Acceleration Control** - The concept of an ABS based on the measurement of angular acceleration of the wheel is implemented, using a rule-based approach. In this system, the braking cycle is designed to operate in three states: 1. Apply 2. Hold 3.Release. The ABS controller is supplied with an exhaustive look-up table that accounts for different braking scenario. This table is essentially a set of threshold values for wheel deceleration and slip ratios that would decide the brake state during the prediction and re-selection stage. In a typical system, the ABS would activate when the wheel deceleration drops below a specific value. The brake states are continuously regulated such that the wheel deceleration and slip are within the provided thresholds. This method is considered to be an indirect way of controlling wheel slip because it requires careful adjustment of wheel acceleration thresholds to achieve optimum performance.

The performance characteristics of the ABS system under operating conditions would respond due to the 'Magic Formula' tire model in accordance with the tire friction curves characteristics based on road conditions to calculate the applied force at a locked wheel, which is divided in two regions static and kinetic friction as shown in Figure 24.

The operation of an ABS is centered on the longitudinal force versus slip characteristic of a tire. The force generated at the contact patch is dependent on the slip ratio. This is the braking force that is generated in the direction opposite to the motion of the vehicle. Figure 25 shows the different steps taken by the ABS in terms of braking force and pressure of the hydraulic actuator which results in immediate application of highest guaranteed braking force. Once this is reached, the force is slowly increased until instability occurs and the braking force is consequently reduced. The last known stable braking force is applied as soon as wheel slip is in the stable region.

The RBS strategy is crucial for energy recovery and braking performance. Figure 26 depicts in blocks a complete system where RBS and ABS work together. It can be observed that the output ABS system sends a signal to the allocation controller to adjust the electric braking torque, which depends on the friction coefficient (μ).

Figure 27 shows simulation results of emergency (hard) braking without ABS, on a surfaces with low friction coefficient. In this case, the driver brake command applies maximum

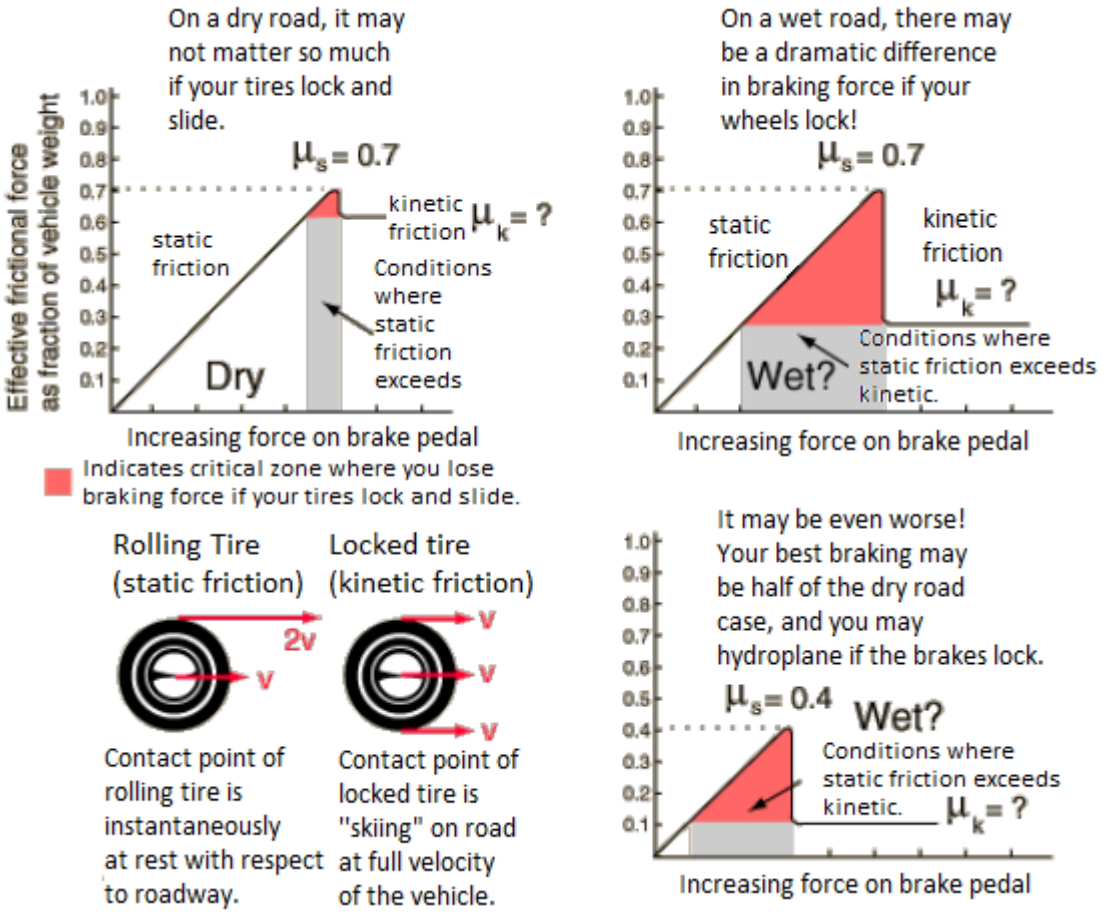

Figure 24 – Coefficent of friction at different road conditons [4].

torque which leads the vehicle to instability by the lack of grip between the tire and the road.

Figure 28 shows the simulation results, where the driver commands a sudden hard braking on a road with varying adhesive coefficients. While the commanded braking force is less than the maximum braking force that the ground surface can support without the wheel being locked, the actual braking force follows the commanded one. However, when the commanded braking force is greater than the maximum braking force that the ground can support, the actual braking force follows the maximum allowed value (in a period of 0.5 to 1.5 s). Consequently, the wheel slip ratios can be controlled in a proper range (usually < 25%). The vehicle gains directional stability and shorter braking distance.

Researches in [7, 39, 40] detailed that the friction between road and tire is a nonlinear function of wheel slip. The slip ratio to achieve an ideal braking shall be maintained at 15% to 25%, thereby gaining a sufficient large lateral force to maintain steering capability. Therefore, maximum negative acceleration can be achieved by a suitable control system for wheel slip regulation at its optimum value. In addition, investigations for ABS and RBS consider two things, the first one is to minimize the braking distance, the second is the maximum recovery of energy.

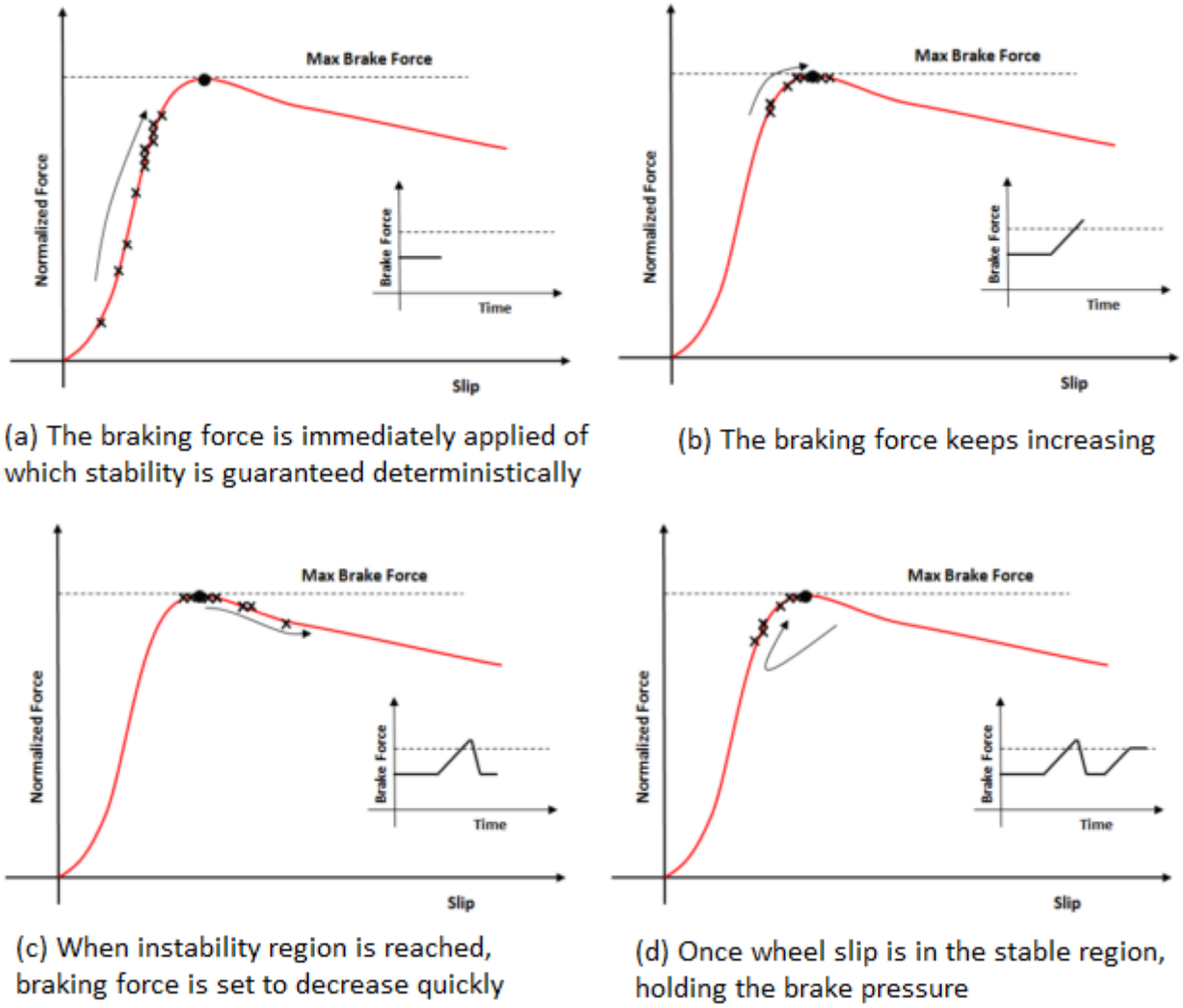

Figure 25 – The different steps taken by the ABS controller [7].

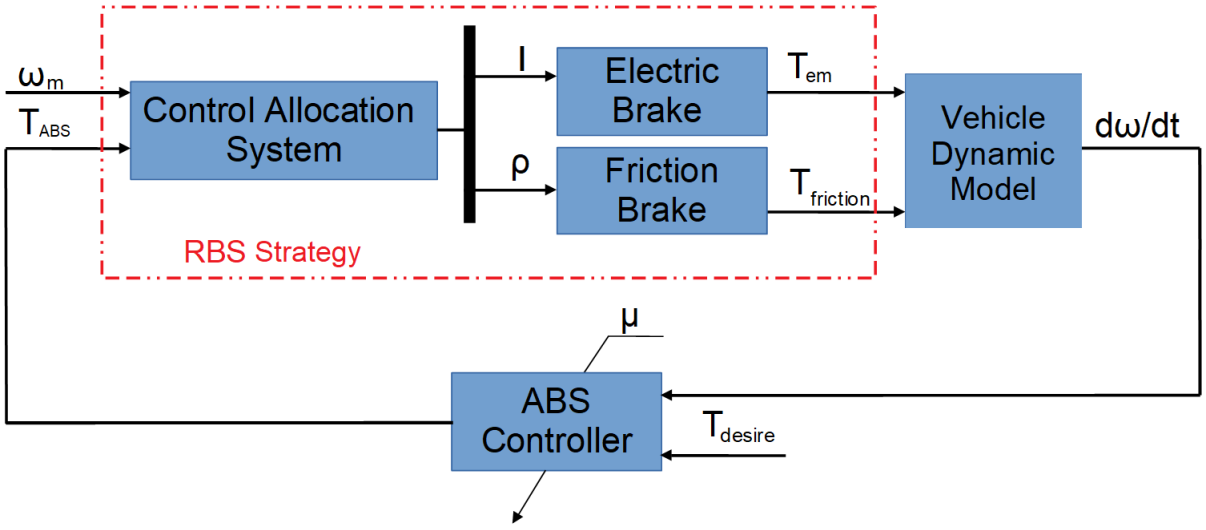

Figure 26 – Cooperative work of regenerative and mechanical braking, equipped with ABS.

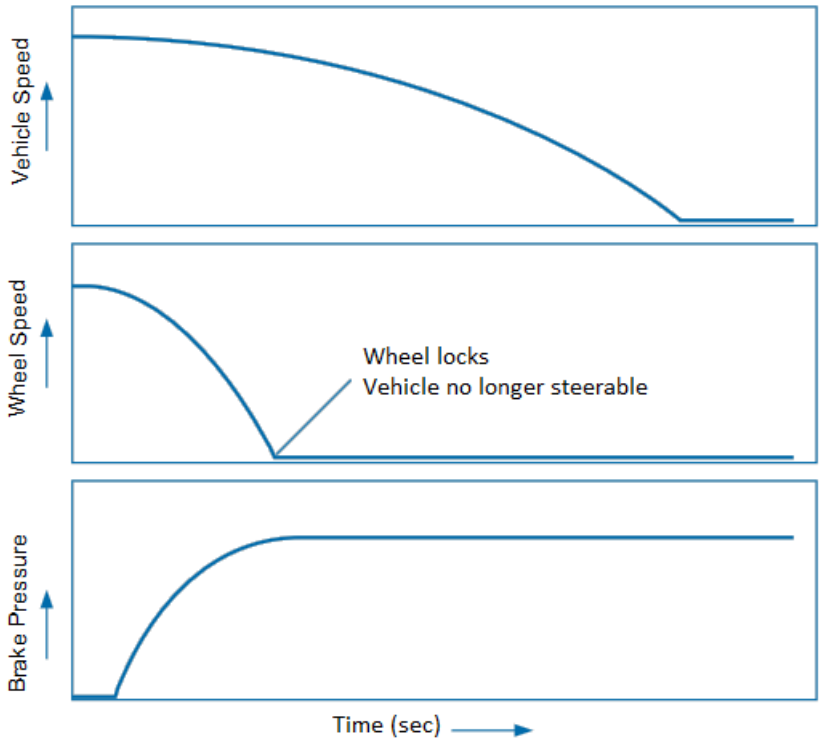

Figure 27 – Braking without ABS on surfaces without good grip [2].

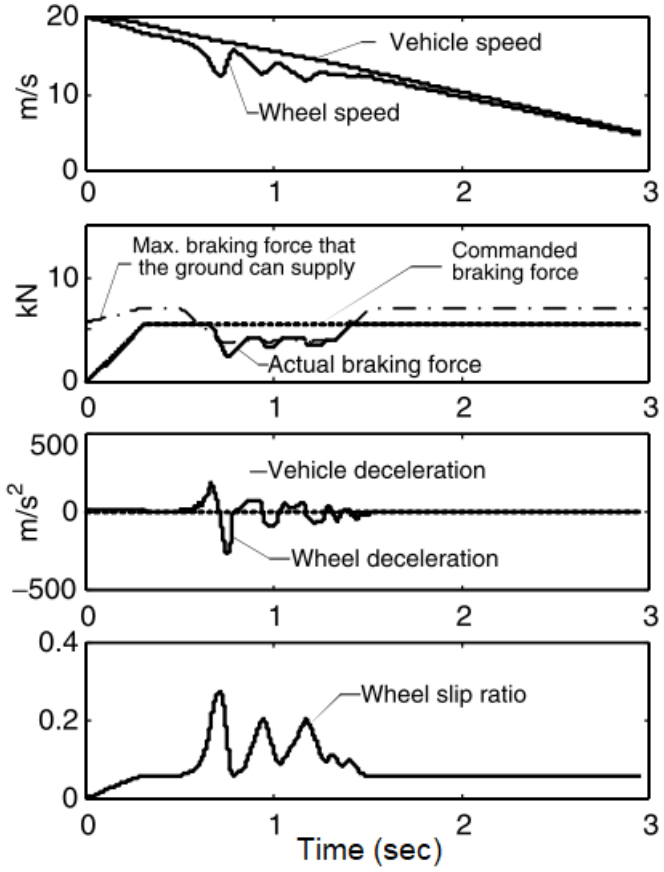

Figure 28 – Braking with ABS (Front Wheels) on surfaces without good grip [8].

3 Regenerative Braking Control System

Regenerative Braking System (RBS) is a technology to recover energy of EV and HEV, on braking. The electrical and mechanical braking combination is necessary to obtain braking performance of the vehicle at any circumstance [7, 21].

This chapter presents the dynamic modeling of an EV on flat and downhill surfaces. It is built and simulated on MATLAB 8.9(R2017a)/Simulink. In order to obtain the model, we detail the required subsystems. However, the model faces nonlinearities and uncertainties such as in mass, center of gravity of the vehicle and road condition, that affect the model.

RBS can be developed using an electric machine that is rigidly connected to the front wheels.

The configuration of the EV case study is shown in Figure 3 with traction in two-front-wheels. Two torque control methods are considered for driving the induction machine with space vector modulation (SVM): (i) V/F scalar control and (ii) DTC.

3.1 Computational Model

The acceleration and braking vehicle performances depend on the available power-train and vehicle mass. Additionally it must consider the user safety and comfort [2, 21].

In urban application, the speed is limited. In this study we consider three situations:

- Level 1: 35 km/h or 323 rpm,
- Level 2: 50 km/h or 461 rpm,
- Level 3: 65 km/h or 600 rpm.

In a light vehicle like the 'Gold city' electric vehicle, the deceleration does not exceed 5 m/s^2 due to the deceleration rate, which usually the vehicle brakes most of the time, considered to charge electric accumulators is from $0.5m/s^2$ to $4.5m/s^2$. Thus, the values defined and considered in the following simulations are:

- Level 1: 1,5 m/s^2 low,
- Level 2: 2,5 m/s^2 medium,
- Level 3: 3,5 m/s^2 high.

The vehicle total mass is 1320kg, however, it was reduced to 660kg at simulations for maintaining a deceleration in according with the defined high deceleration above and maximum mechanical torque applied at braking, as shown in [18].

Table 5 shows the induction machine model parameters, used in the simulation.

Table 5 – Induction Machine Parameters

Nominal Power (P_N)	37 kW (50 HP)
Frequency	60 Hz
Nominal Torque(T_N)	200 N.m
Stator Resistance (R_s)	0.025 ohm
Rotor Resistance (R_r)	0.23 ohm
Stator Inductance (L_s)	0.22 mH
Rotor Inductance (L_r)	0.87 mH
Mutual Inductance (L_m)	3.79 mH
Moment of Inertia (J_m)	0.5 kg.m^2
Pole Number (p)	4

Table 6 shows the torque values for the so called "hard brake", that corresponds to the maximum torque that can be applied to the wheels.

As already defined, T_{max}=1.5 T_N. However, to avoid motor overheating during long braking intervals, the motor torque is limited to 240 Nm (T_{Lim}).

Table 6 – EV Parameters

Gearbox Ratio	1 : 2.5
IM Maximum Torque (T_{max})	300 Nm
IM Limit Torque (T_{Lim})	240 Nm
Wheel Maximum Torque	750 Nm

The electric power supply is a supercapacitor bank (17F) with initial condition of 380V.

3.1.1 Shutdown Criteria of the Electrical Braking

Figure 29 shows a block diagram based on scalar control, in a flat surface, to perform the study. The "Vehicle Dynamic" block and a speed profile block were added. These simulations depict a completely electrical braking behavior.

Consequently, the parameters in the vehicle dynamic block were accordingly changed to maintain a maximum deceleration at braking, as shown in Table 7

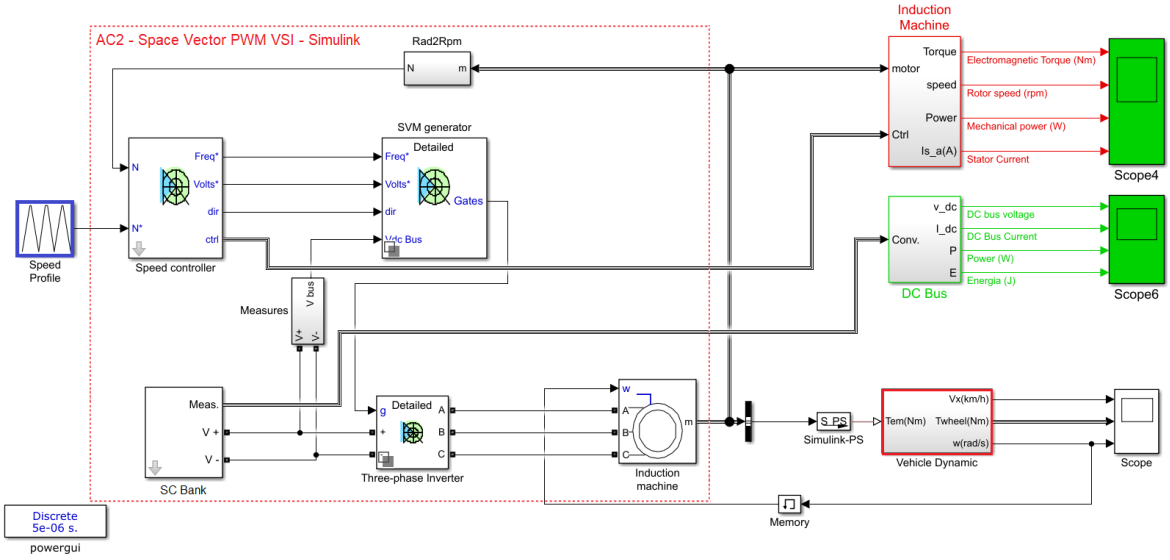

Figure 29 – EV Base Model System with Scalar Control.

Table 7 – Vehicle Dynamic Parameters

Vehicle Mass (m)	660 kg
Path Inclination	0 deg
Rated vertical load	1700 N
Peak longitudinal force at rated load	2500 N
Slip at peak force at rated load	10%

Figure 30 shows the simulation results. The motor accelerates until reach the cruise speed (1350 rpm), when the torque reduces to maintain the speed constant. The braking process starts at t=5 s. The torque becomes negative as well as the supply power. The motor follows the speed reference but, at low speed, that corresponds to a low inverter frequency, the torque becomes oscillatory, affecting the deceleration. Another important fact is that the supply power becomes positive. This means that the powertrain losses overcome the power recovery, making the regenerative procedure useless.

Such results indicate the regenerative braking must be interrupted before the effective vehicle stop. The final braking will be performed by the mechanical brake.

The torque at the wheel axis is limited to 750 Nm, that corresponds to 300 Nm at the motor axis.

Such devices uses a brake disk. The applied force that results the desired torque is given in Equation 3.1.

$$F_N = \frac{J_C.\alpha_v}{2.D_r.r_d.\mu} \tag{3.1}$$

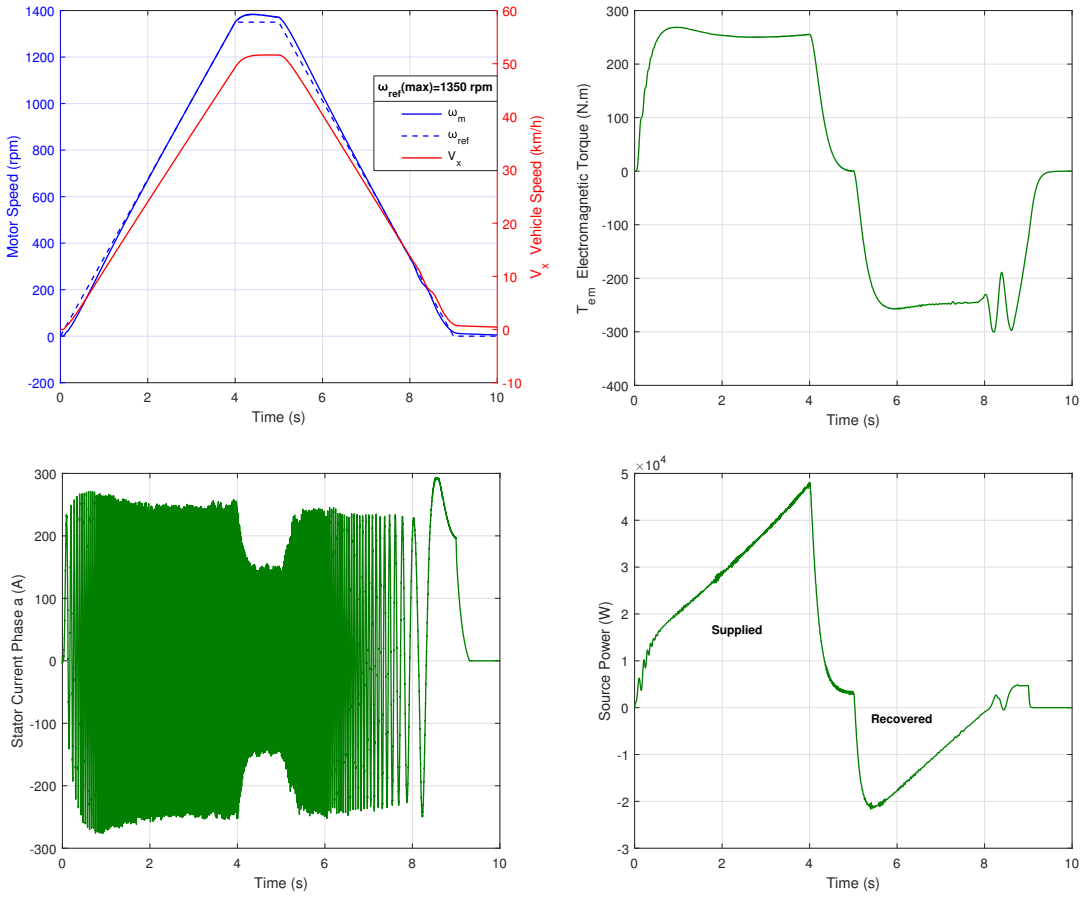

Figure 30 – Simulations of the driving cycle with Regenerative Braking.

Where J_C is the load inertia ($kg.m^2$), α_v is the vehicle's deceleration, D_r is the brake disk radio (m), r_d is the wheel radio (m), and μ is the friction coefficient.

3.2 Strategy to Control Brake

3.2.1 Strategies to the Scalar Control

A closed loop torque control is added. During the braking, the inverter reference is 5% less than the corresponding motor speed applied by the SP_Control block. This way the induction machine slip is negative, resulting a negative torque. The inverter turns-off at low speeds, avoiding the torque oscillations. Then, Mechanical Torque block applies a friction torque to maintain the same deceleration, as is shown in Figure 31.

For the braking stage, the speed reference changes accordingly to the brake pedal and 95% of the motor speed is used as reference.

The torque control block includes two PI regulators. One regulates the speed and produces the torque reference. The second controls the torque loop.

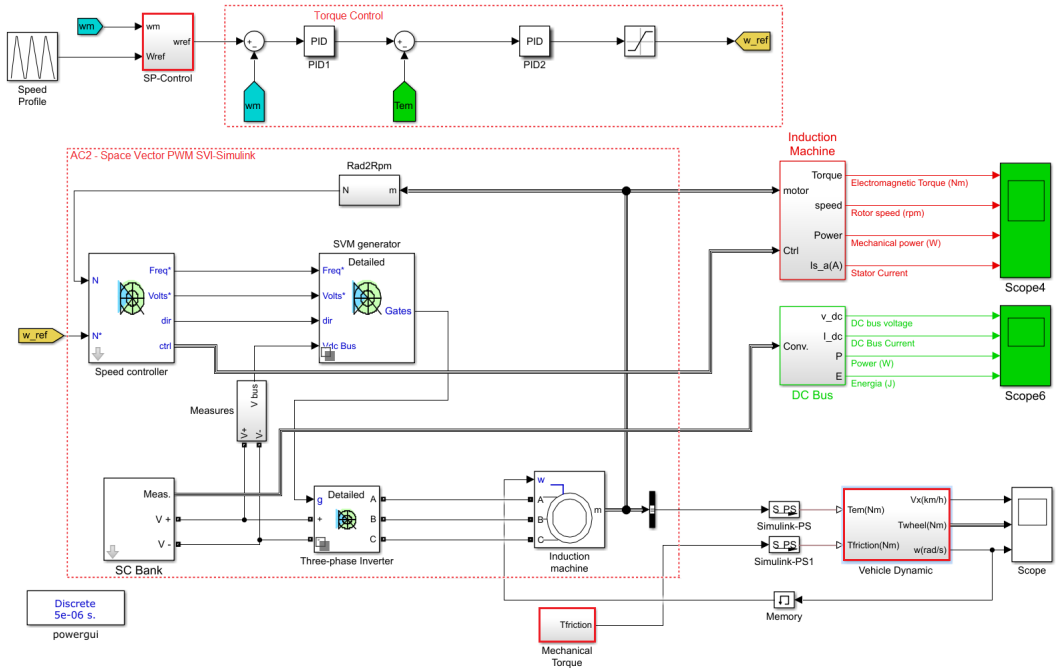

Figure 31 – EV Model System with Scalar Control for driving cycles studies.

It is necessary to know if the required torque is greater than electric motor limit torque. The use of the block "Mechanical Torque" is divided into two parts: (i) Brake1" and (ii) Brake2" to apply friction torque according to the torque demand, as shown in Figure 32.

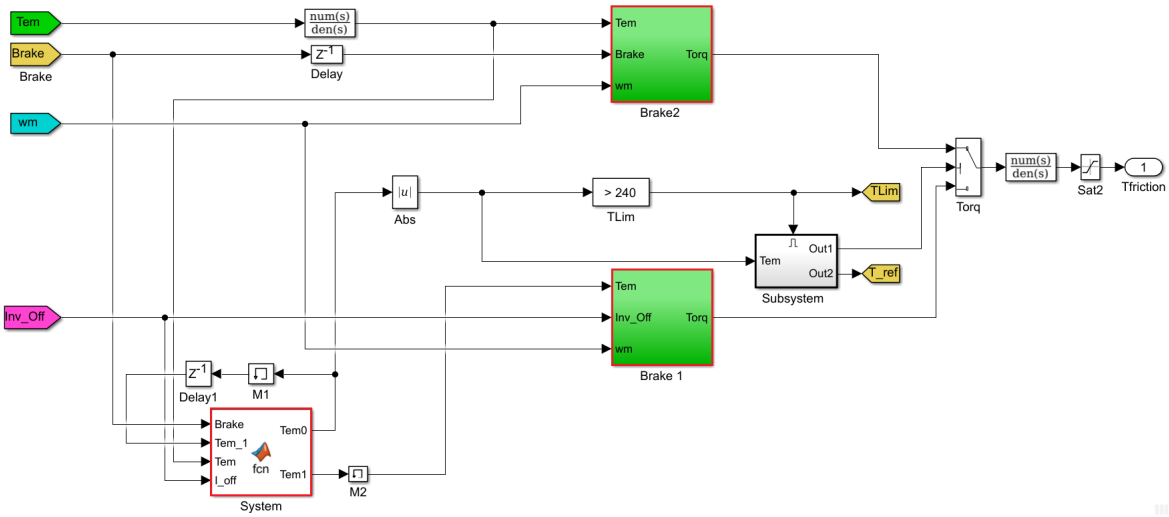

Figure 32 – The Block "Mechanical Torque" used to Scalar Control.

Figure 33 depicts the flow diagram for two strategies ("Brake1" and "Brake2") to scalar control. The torque developed by the induction motor is directly proportional to the ratio of the applied voltage and the frequency of supply. By varying the voltage and the frequency, but keeping their ratio constant, the torque developed can be kept approximately constant.

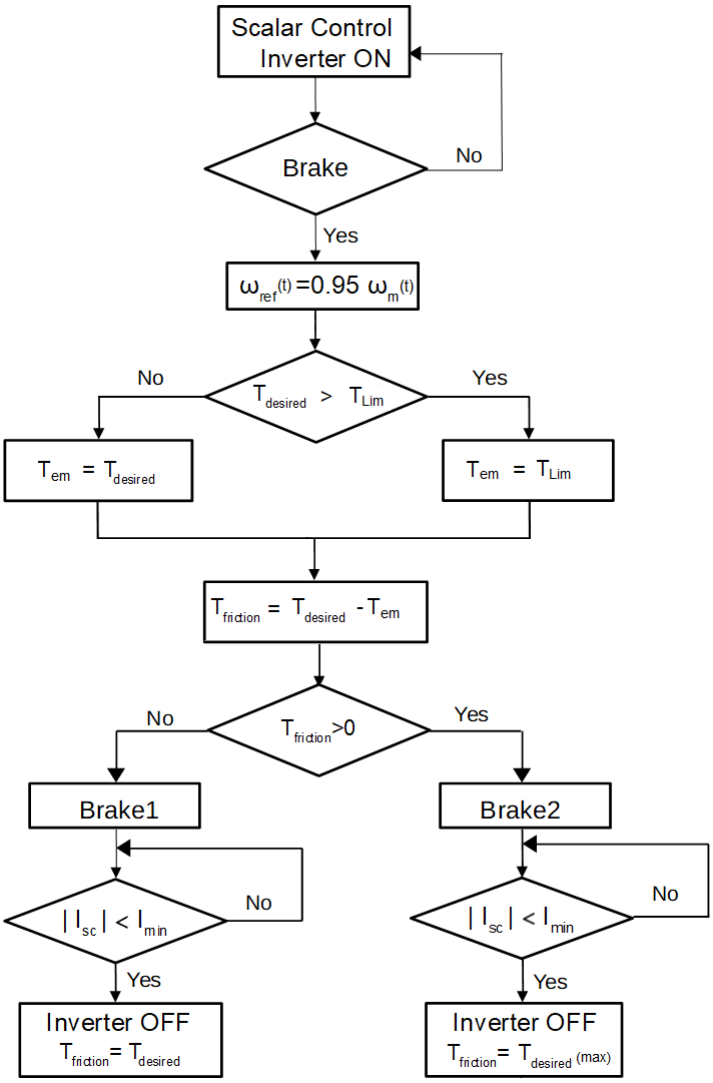

Figure 33 – Flow Diagram to Scalar Control.

In Brake1 mode the initial friction torque is 0, for a maximum speed reference ω_{ref}. The electrical brake is performed with the desired torque while the current in the SC bank is greater than a minimum value. When the inverter turns-off, the desired torque is applied by the friction brake, maintaining the deceleration and the stability of the vehicle.

In the Brake2 mode the friction torque is greater than zero for a maximum speed reference ω_{ref}. The desired torque is divided between the electrical and the mechanical system. When the regenerative brake losses efficacy, the inverter turns-off and the friction torque assumes the full torque.

Figure 34 shows the comparison of both braking strategies on a dry and flat surface.

The Brake1 has a longer braking distance than Brake2, due to the fact that brake demand is lower. The reference speed is applied while the inverter is working.

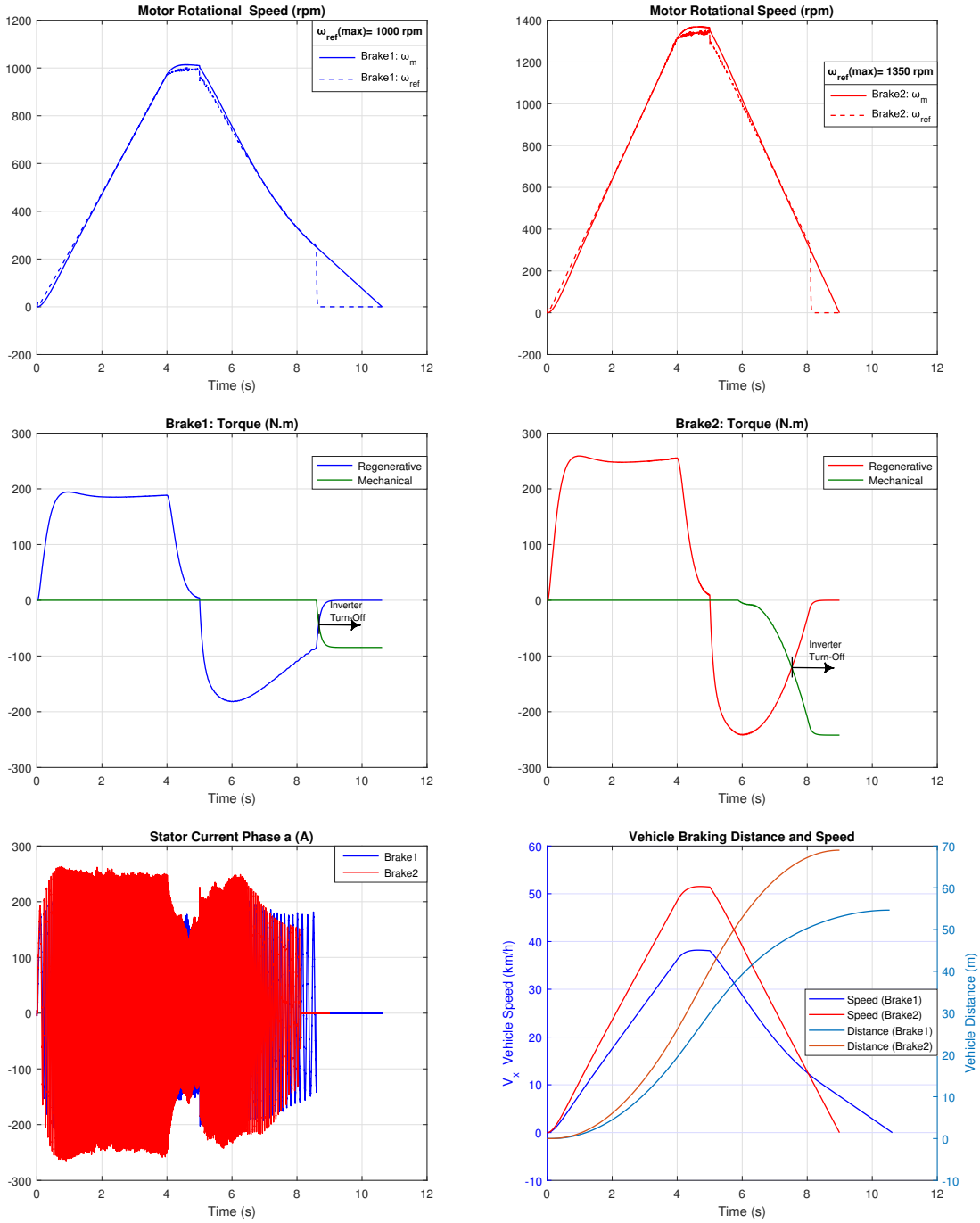

Figure 34 – Simulation V/F Control on flat surface: Brake1 mode at left column and Brake2 mode at right column.

As shown in Figure 34, Brake1 mode, the braking torque is variable. This occurs because the scalar strategy defines a speed reference 5% lower than the motor speed. This results a variable slip and, consequently, a variable braking torque. To improve the torque regulation would be necessary to change the speed reference, what doesn't make sense in a simple control strategy as is the scalar control. This will be used in the following DTC strategy.

Figure 35 shows the inverter DC bus voltage (where the SC Bank is connected). The recovered energy in Brake1 is lower than Brake2 since the initial kinetic energy is lower.

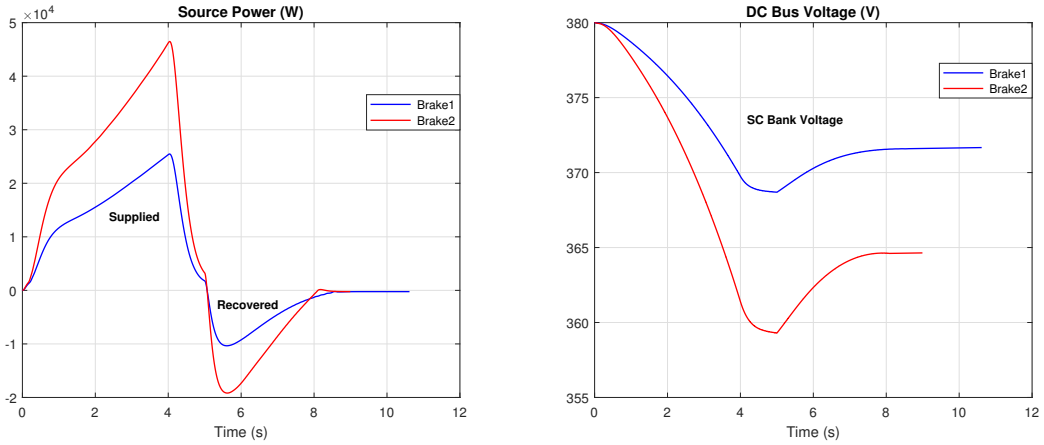

Figure 35 – Comparison of strategies for electric braking: electric behavior.

Table 8 shows the electrical quantities of the two braking strategies for a flat surface with scalar control.

Table 8 – Quantities for Regenerative and Mechanical Braking

Parameters	Brake1	Brake2
Brake Peak Power (kW)	10.35	19.18
Recovered Energy (kJ)	18.53	32.70

3.2.2 Strategies for DTC

The direct torque control structure is depicted in the "AC4-SVM" red box, shown in the Figure 36.

The block "Sist" represents the vehicle commands (acceleration and brake). The electrical parameters and the dynamics of the vehicle are the same as for scalar control.

Let us consider the intense braking of the vehicle, in which the system uses the motor limit torque of 240 Nm.

Direct torque control (DTC) is based on two PI controllers for torque and flux, which allows better response to the driver's command.

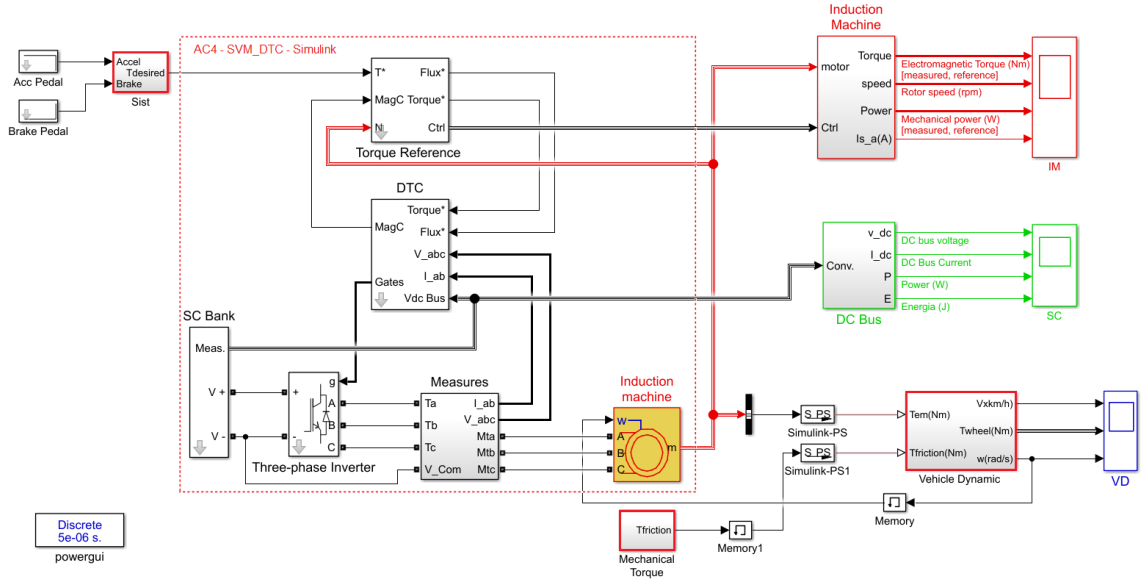

Figure 36 – EV Model System with DTC Control for driving cycles studies.

It's possible to brake with both, electric and mechanical brakes, in order to achieve maximum torque on the wheels, maintaining the criterion of turning off the electric brake if the motor current is minor than a minimum current, as shown in Figure 37.

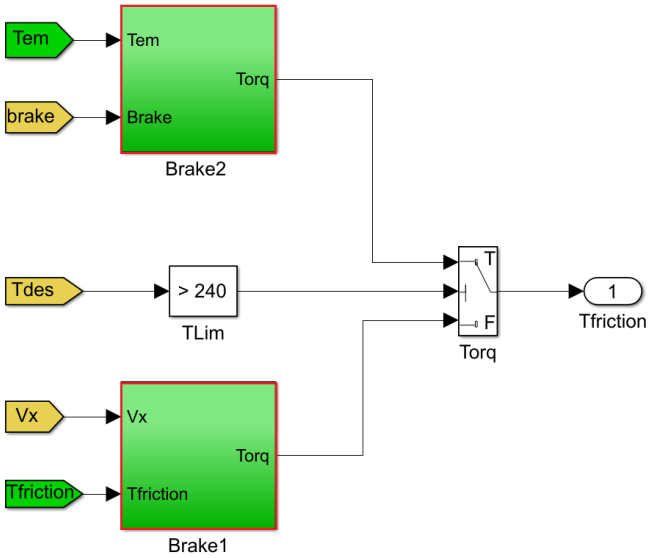

Figure 37 – "Mechanical Torque" block used to define the friction torque.

Figure 38 shows the flow diagram of the braking strategies, "Brake1" and "Brake2". The desired torque or torque demand is made by the brake pedal, according to the motor speed vs. torque curve. If the desired torque is greater than the motor limit torque, it is necessary to add the mechanical torque.

Brake1 is performed when the electric brake is enough. The mechanical brake is applied only when the inverter turns-off.

Brake2 uses both, the electric and the mechanical brakes concurrently.

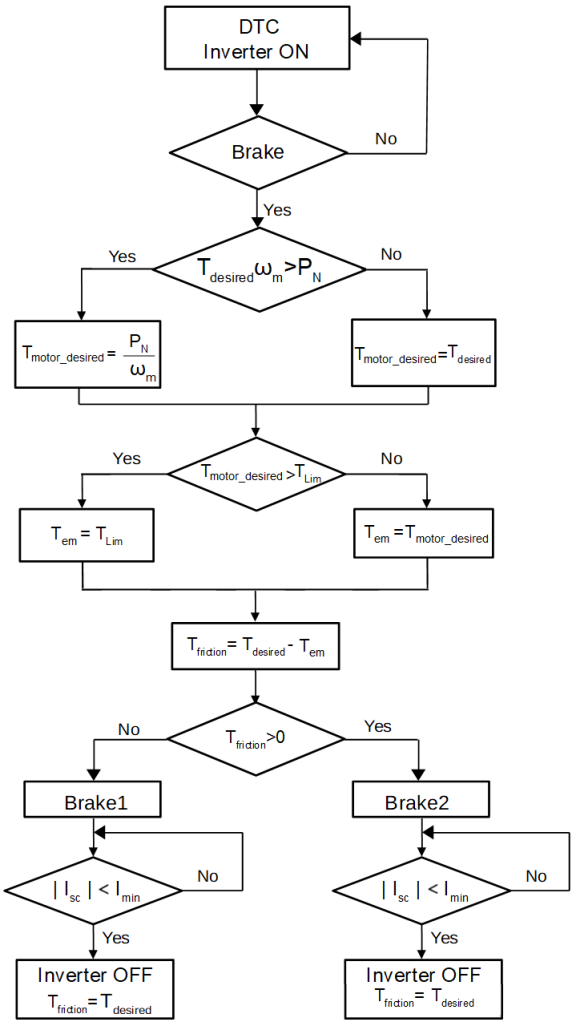

Figure 38 – DTC Flow of Logic Diagram.

The Figure 39 shows simulations when the brake commands 60% of the maximum motor torque (Brake1). If the command corresponds to 100% or more the strategy is Brake2.

For the Brake1, the regenerative energy is greater than Brake2 as the mechanical brake is not applied. The braking distance of the vehicle for the Brake1 is 14.25m, since the deceleration is lower than Brake2 and it takes longer time to stop the vehicle.

Figure 40 shows a comparison of recovered energy for both cases. It can be observed that more energy is recovered by Brake1 than Brake2, since both start with the same kinetic energy.

Table 9 – Quantities for Regenerative and Mechanical Braking on flat surface

Parameters	Brake1	Brake2
Brake Peak Power (kW)	16.95	16.60
Recovered Energy (kJ)	30.12	15.40

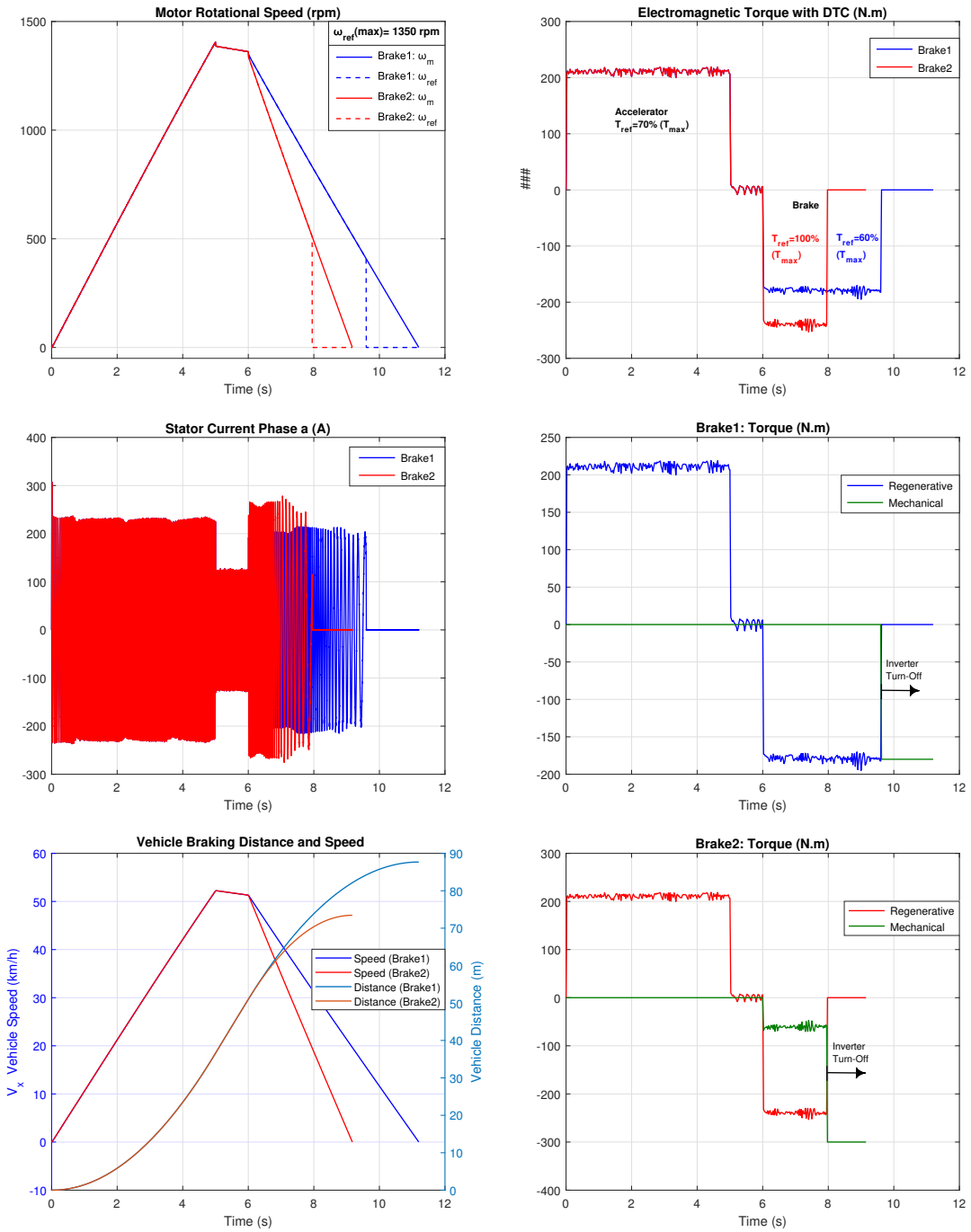

Figure 39 – DTC Simulation on a flat surface.

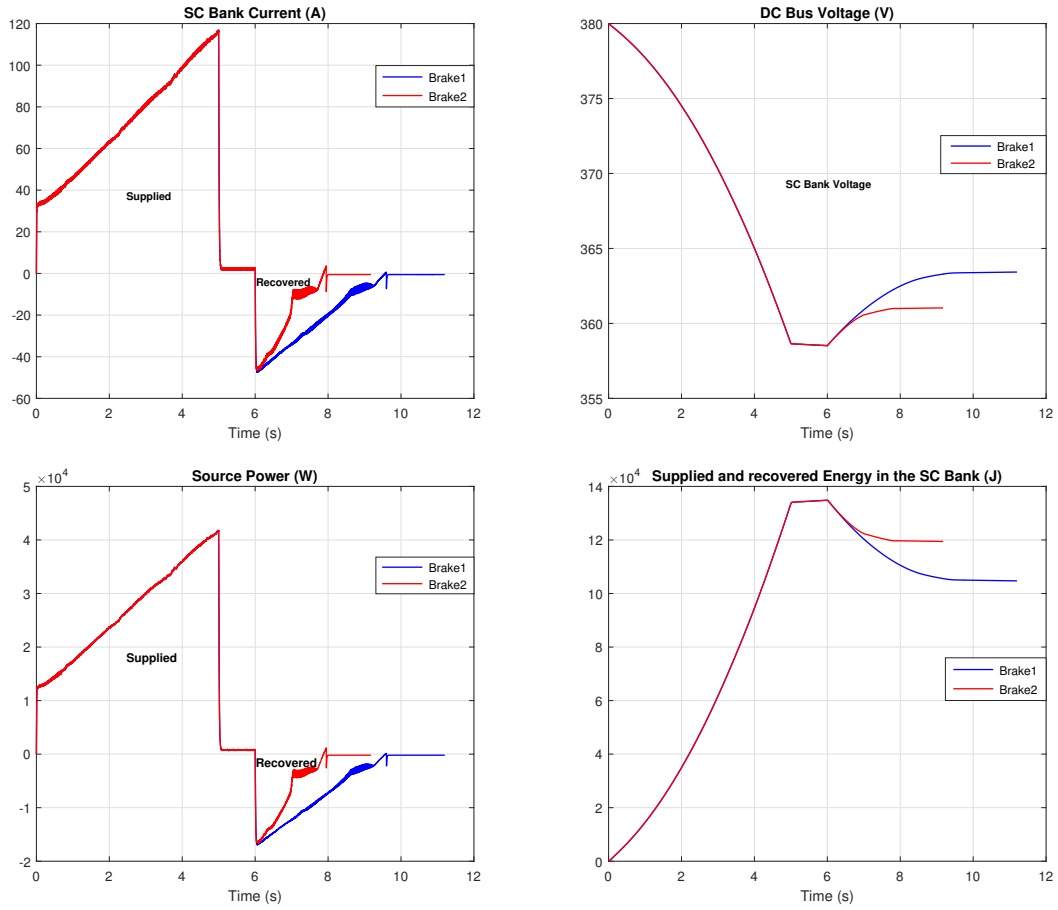

Figure 40 – Electrical Simulation DTC on flat surface.

As the DTC presents a superior behavior compared to the scalar control, due to the precise torque regulation, the following studies consider only DTC systems.

- **Downhill surface (-10deg)**

  Figure 41 shows braking during downhill and on the flat surface to compare the traction and braking in both cases, maintaining a fixed coefficient of friction as for a dry surface.

  In both cases the reference torque changes from an initial braking torque of 60% to 100% of the maximum motor limit torque.

  Figure 42 shows that in downhill surface more energy is recovery since the kinetic energy is summed to the potential energy.

3.2.3 Flat surface with Variable Friction Coefficient: Wet-Snow

In this section, the EV tires are exposed to a variable friction coefficient (VFC) on a flat surface, as shown in the diagram of the Figure 43.

According to the Paceijka model for typical road conditions, the system considers two VFC (wet and snow).

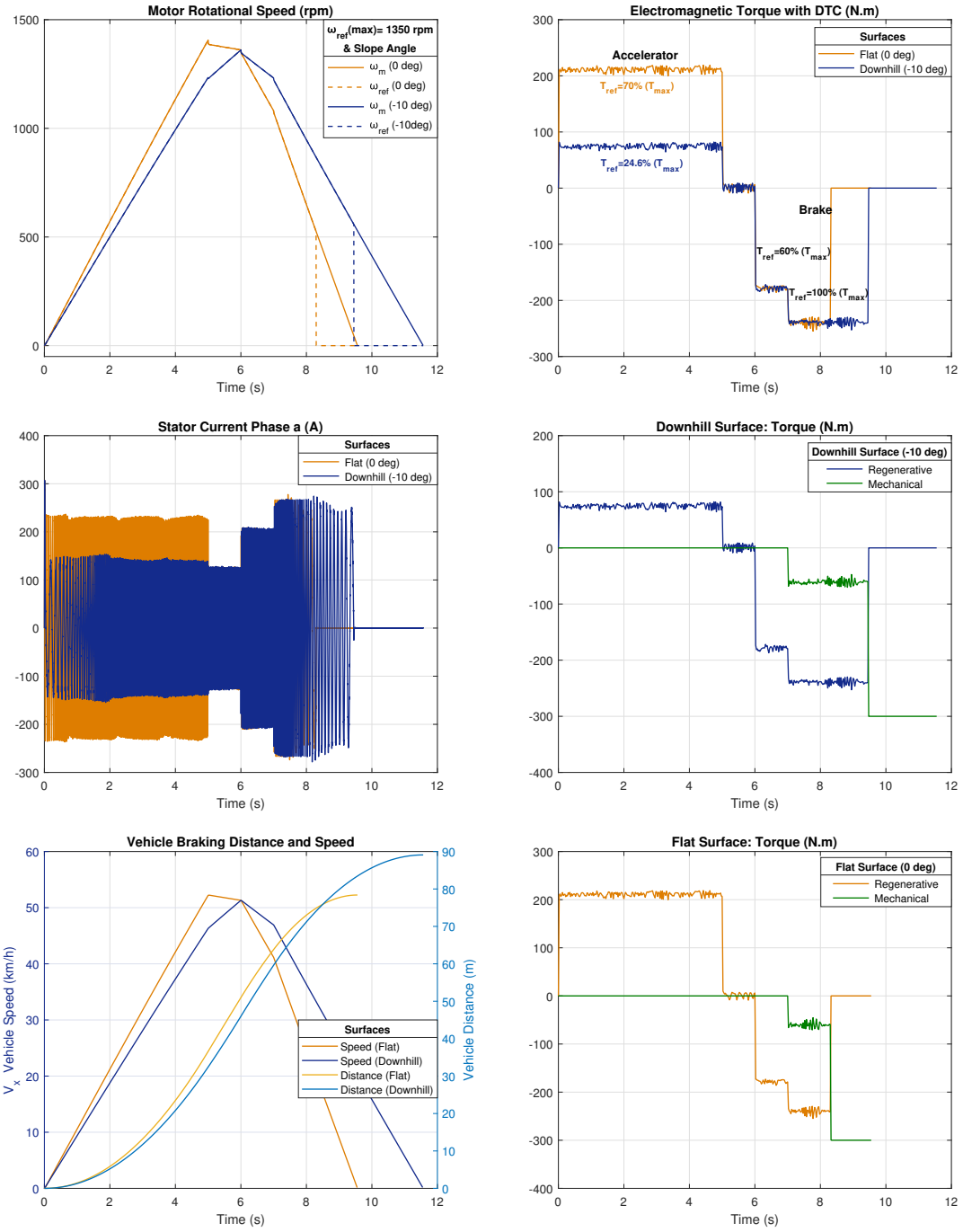

Figure 41 – DTC Simulation on Flat and Downhill Surfaces.

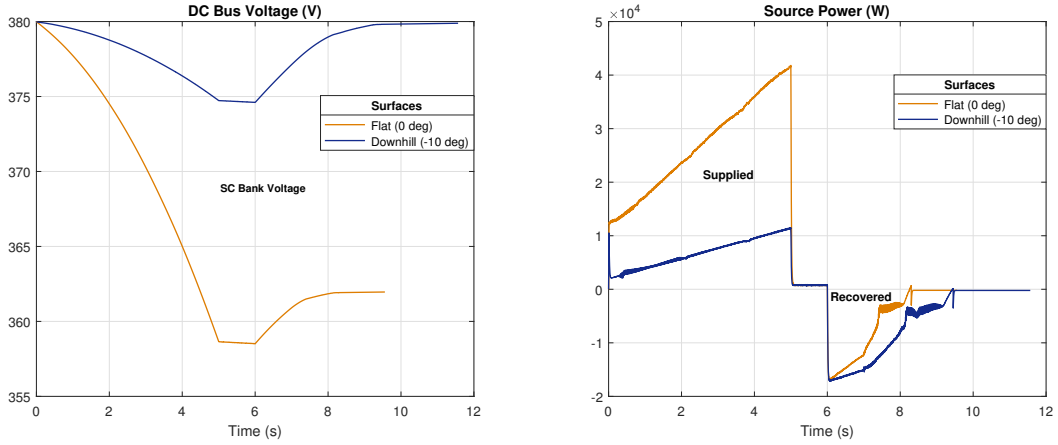

Figure 42 – Electrical Simulation of DTC on flat and downhill surfaces.

Figure 43 shows the "friction" block responsible for changing the surface characteristic. The vehicle is initially exposed to wet surface that changes to a snowy surface while braking, as shown in Figure 44.

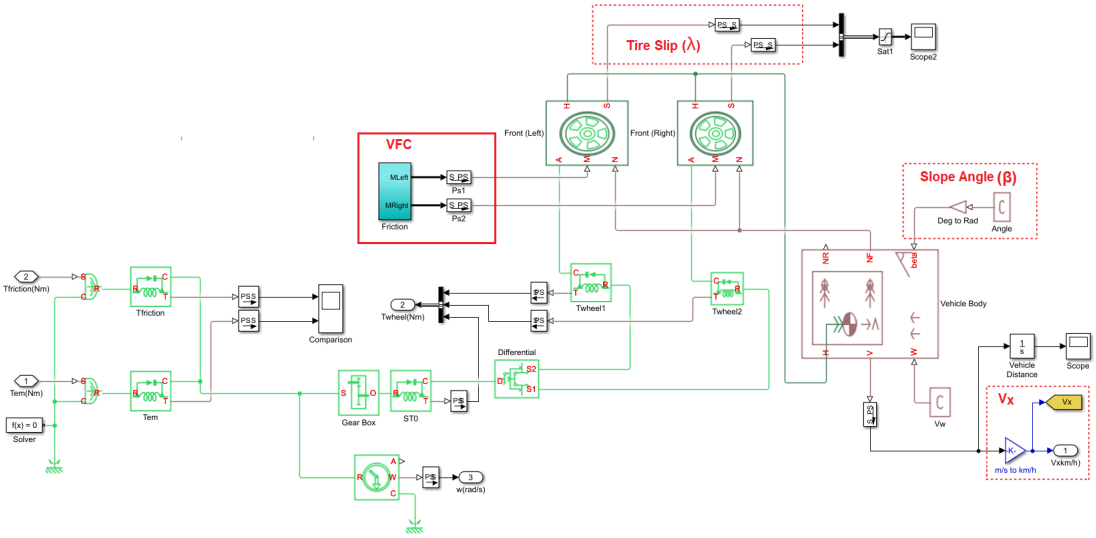

Figure 43 – Modeling vehicle dynamics with VFC

The study considers the change affects both traction wheels (frontal tires). Furthermore, it can be used in other cases as well, for example if the change affects one side of the vehicle (left or right wheel).

- **Inverter Turns-off before VFC: Wet-Snow**

  Let's consider the case when the inverter will be disconnected at the starting stage of the deceleration. For example, because of SC is fully charged. The driver's demand requires a torque greater than the motor limit torque, making necessary to use mechanical torque (strategy Brake2).

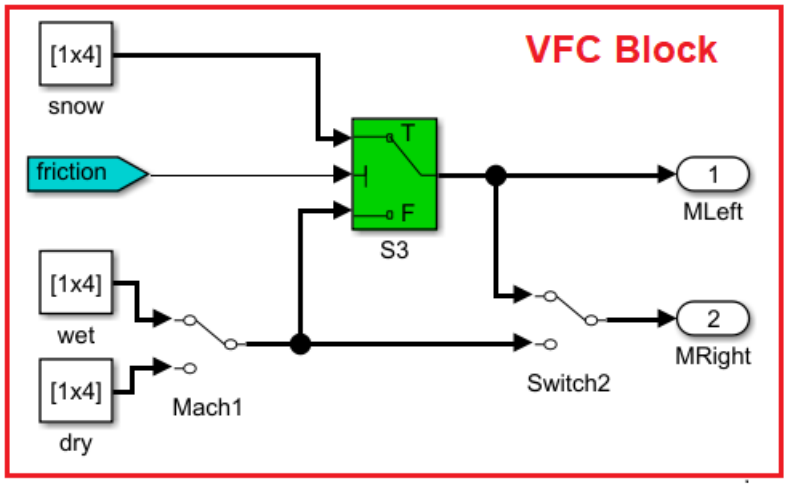

Figure 44 – Modeling VFC from Wet to Snowy surface

As shown in Figure 45, the vehicle starts the braking on a wet surface. As the torque demand is 100%. Brake2 strategy is applied.

When the inverter is turned-off, only mechanical braking is applied, maintaining the desired torque. Then the tires leave the wet surface and enters on the snow surface.

The tires do not maintain the contact with the ground, leading to an uncontrolled driving. The slide of the tire with the ground is analyzed as a slip variation, and shows that it is outside the 0.2 limit (negative for braking) indicating, the tires lose friction with the ground.

- **Inverter Turn-off after VFC: Wet-Snow**

  In this study, the behavior under variable friction coefficients for regenerative braking and mechanical braking, concurrently, is analyzed on a flat surface. The analyses also count on a demand of 100% brake, and the Brake2 strategy is used.

  As shown in Figure 46 the inverter is turned-off when the regenerated power changes signal, due to the change of the surface from wet to snow.

  Although the vehicle receives the desired mechanical torque, the vehicle does not stop with the applied torque. On the contrary, it takes the vehicle to instability, where the tires lose contact with the ground.

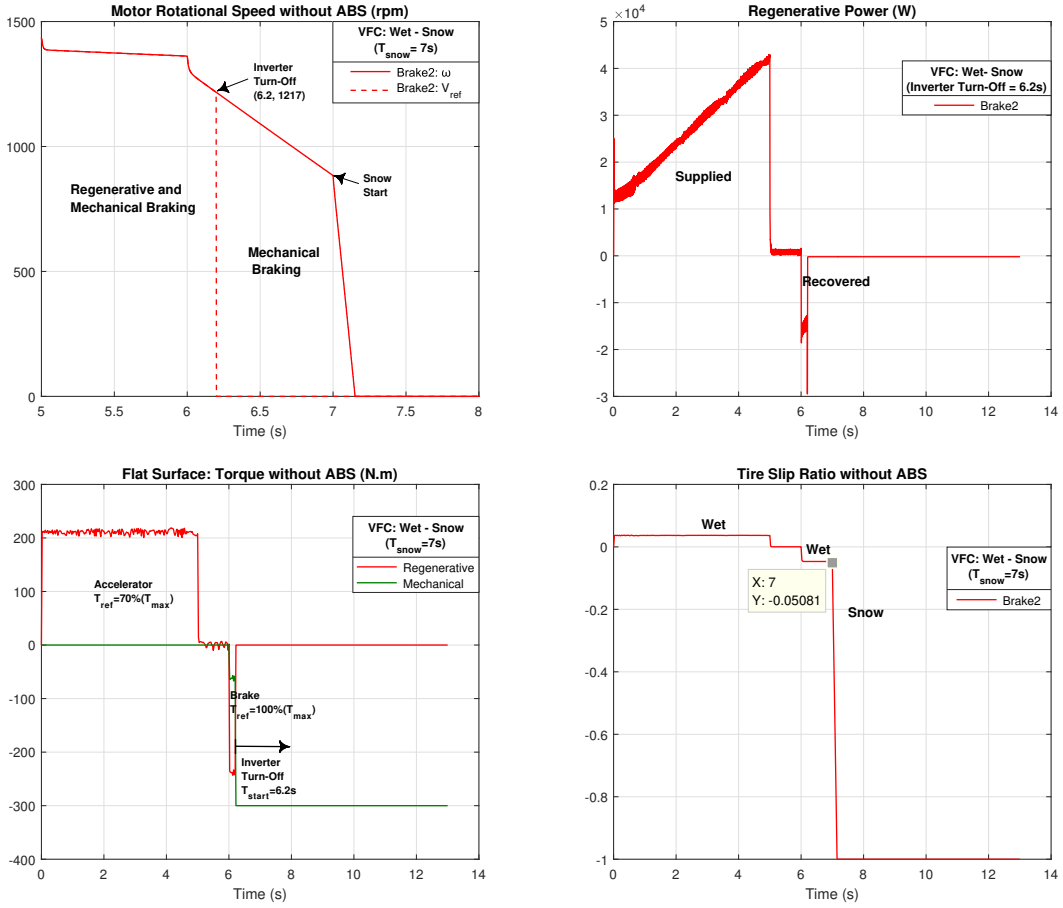

Figure 45 – Simulation for a turned off Inverter before VFC without ABS.

Table 10 shows a comparison of the vehicle's behavior for the variable surface in both cases: the combination of regenerative and mechanical braking and with the use of mechanical braking alone.

Table 10 – Quantities for Inverter Shutdown Before/After without ABS

Parameters	Inverter Turn-Off Before	Inverter Turn-Off After
Brake Peak Power (kW)	29.50	15.80
Recovered Energy (kJ)	4.40	11.20
Electrical Finish Time (s)	6.2	7.15

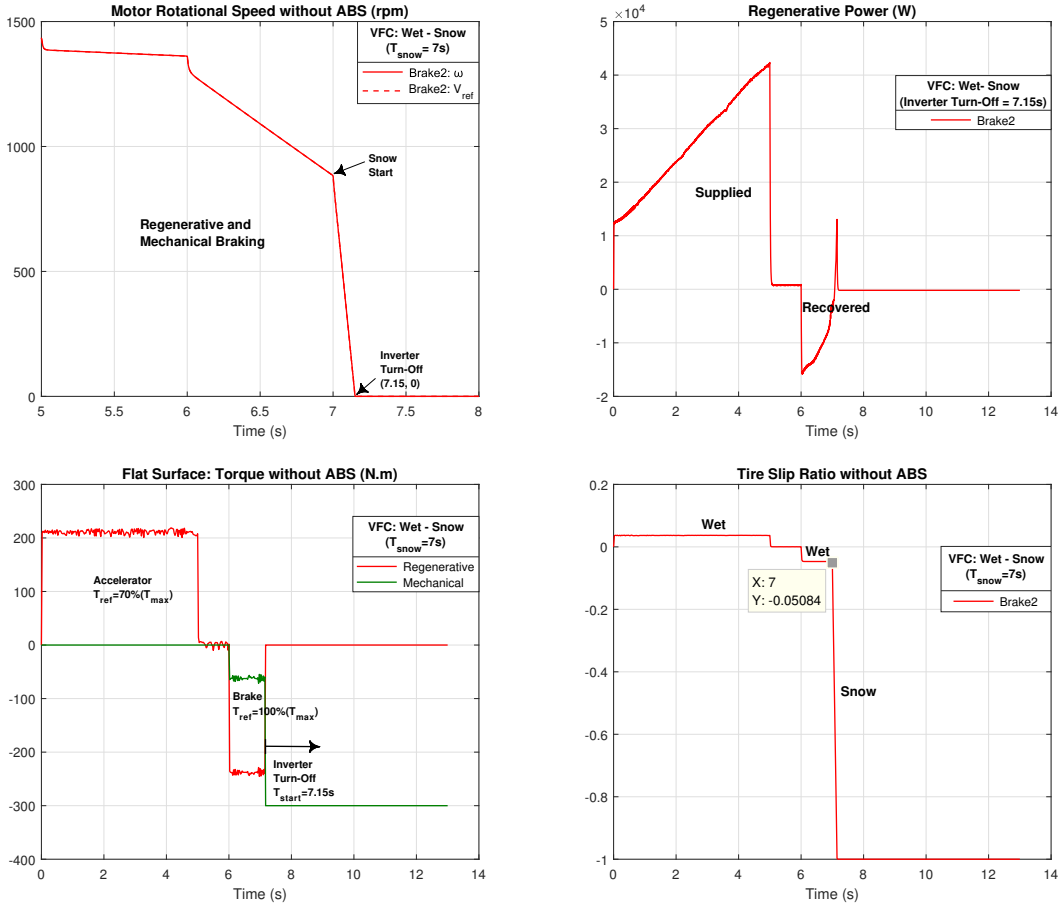

Figure 46 – Simulation for a turned off Inverter after VFC without ABS.

3.3 Conclusions

This chapter has reviewed the key aspects of regenerative and mechanical braking, analyzing and comparing different braking strategies, as well as how it affects the driver's maneuver in severe braking.

The simulation of the vehicle model is an important part of this study which analyzed control techniques and strategies to be used and applied to an induction machine [41].

For the braking of a light vehicle, it is necessary to have a robust control system whith direct torque control, a good option to control the induction motor due to its focus at torque control.

If the coefficient of friction between the ground and the tires varies during braking, then one or more of a vehicle's wheels can lock (begins to skid) where the probability that an accident occurs in consequence of braking distance increases, and the loss of steering control.

4 Anti-lock Braking System Control

This chapter is based on a braking with DTC, carried out on a flat surface. The vehicle dynamic model is the same as presented in chapter 2. The mechanical brake acts together with the regenerative brake.

The MATLAB wheel model has an entry that allows to simulate various road friction curves by using Paceijka model. A locked-up wheel results low road handling force and minimal steering force. In addition, the slide values for stopping/traction force are proportionally higher than the slide values for cornering/steering force. Figure 47 depictes the behavior of one wheel on the road. When there are multiple wheels in an axle group, the wheel slips may differ, but each one behaves as is shown. The greater the number of tires, the greater the maximum horizontal forces and the greater the load carrying capacity [42].

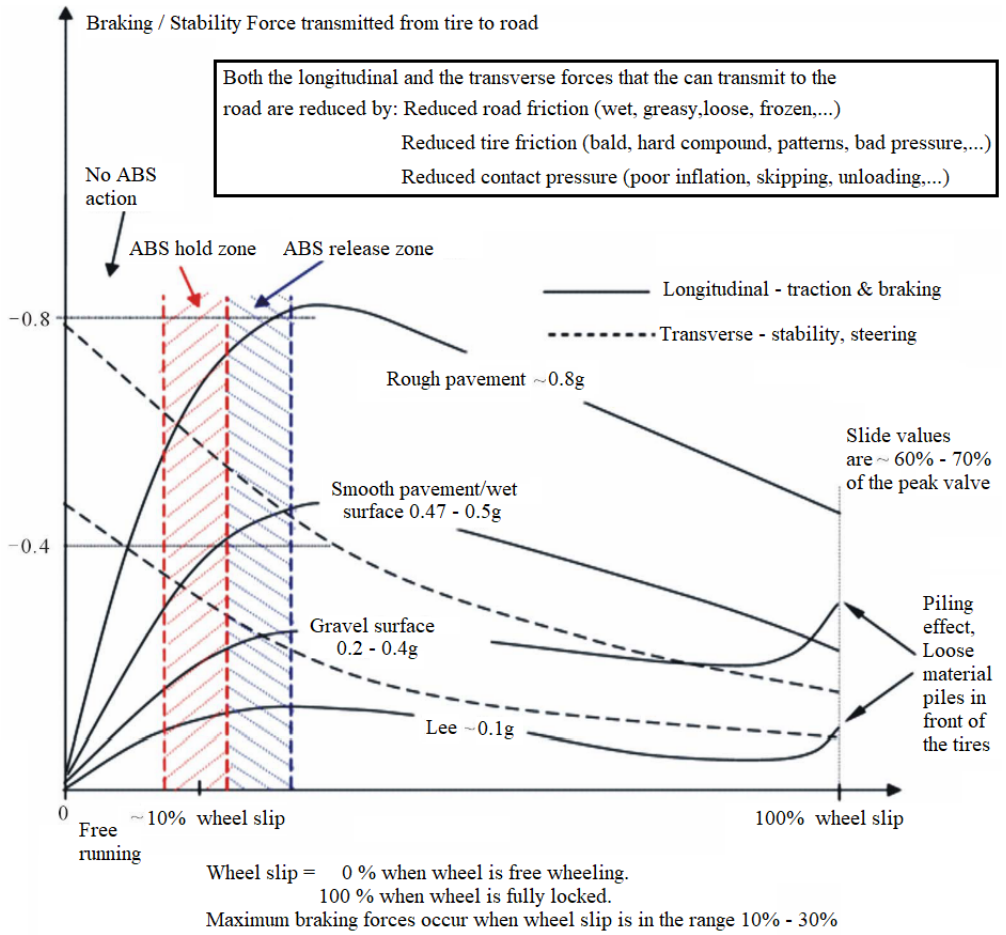

Figure 47 – Relationship between braking coefficient and tire slip at tire-road interaction [9].

Figure 48 shows a configuration suitable to the layout of the brake lines connecting the master cylinder and the brakes due to legal requirements that demand to incorporate a dual-circuit force transmission system (include the transmission medium, hoses, pipes and, on some

systems, a pressure regulating valve for limiting the braking force at the rear wheels) of braking system in which the deviation in the weight distribution is rearward. This design involves a division of the front axle/rear axle split, whereby circuit (1) operates the front brakes and the circuit (2) operates the rear brakes. The ABS control is carried out only for the front wheels due to configuration leading to secondary-braking effectiveness [2].

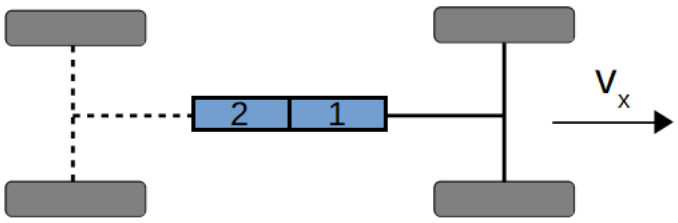

Figure 48 – Brake-circuit Configuration.

The use of ABS helps to keep the wheels working even with severe changes on the road that affect the driving, since the static friction is less than the dynamic friction. Therefore, the proposed ABS strategy makes use of both mechanical and electrical brakes. The analysis consider two cases: (i) mechanical ABS and (ii) ABS Mode with RBS.

Following the approach [15, 22], we explore the concepts of ABS function, mechanical ABS, and RBS to develop control strategies ABS mode with RBS, which considers the motor torque introduce into an antilock brake system (ABS) control, expecting a better control effect to store the electric energy at braking. Our dynamic model with the quick response and accurate control of the motor torque at braking explore and propose a distributed torque strategies.

4.1 Friction Torque Control Strategies with ABS

The ABS control strategy must be able to capture in real time the transient behavior of the friction force, observed during the longitudinal sliding of the wheel.

Figure 49 shows the logic diagram for the ABS for driving conditions on a flat surface. During the braking process, the wheels are exposed to a surface with low coefficient of friction. As a consequence they tend to block.

The diagram identifies the slippage of the vehicle through the calculation of the Slip (λ). Figure 47 shows when slippage is greater than 0.25, the ABS control must be active to unlock the wheels.

4.1.1 Strategy for Mechanical ABS on a flat surface

Figure 50 shows the basic structure of the ABS control. Advanced ABS systems uses accelerometers to improve the process performance [43].

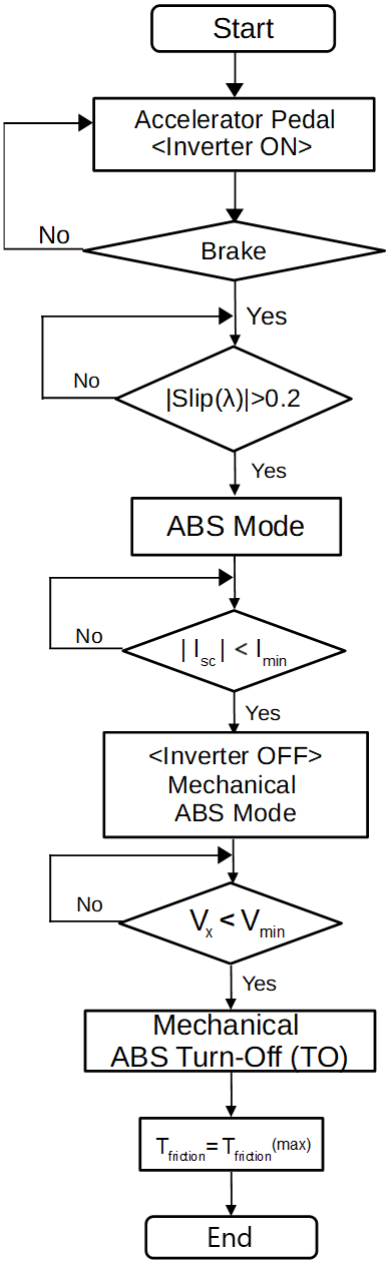

Figure 49 – Logic Diagram of Control Strategy of electric and mechanical ABS.

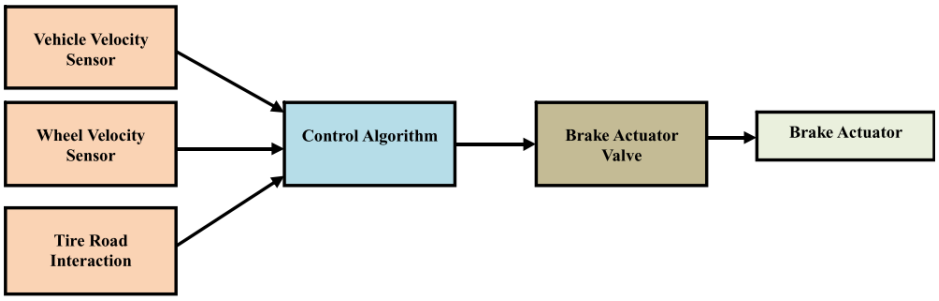

Figure 50 – Block representation of an ABS [9].

The braking procedure with ABS is simulated verifying two strategies (i) Bang-Bang Controller and (ii) PI Controller.

At very low speed (5km/h) the ABS is turned-off because it loses controllability. The mechanical brake continues to apply the friction torque until the complete stop [9, 40].

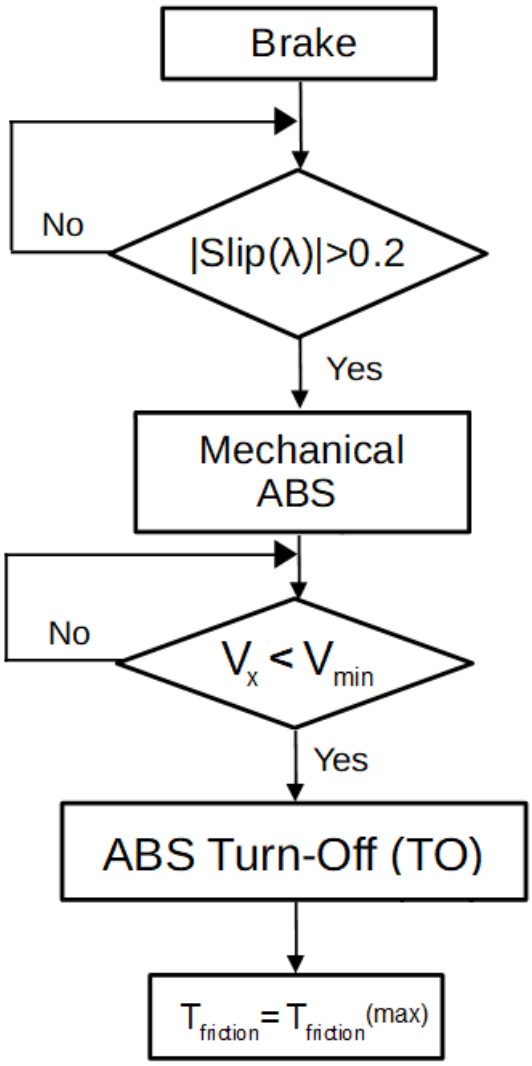

Figure 51 – Logic Diagram of Mechanical ABS

- **Strategy 1: Mechanical ABS**

  Figure 52 and Figure 53 show the block diagram of the bang-bang controller. The bang-bang controller is also known as hysteresis controller. The "Brake1" and "Brake2" blocks make the decision between the control strategies studied at chapter 3 to apply a friction torque. The Brake2 block output is used to define the torque demand at severe braking.

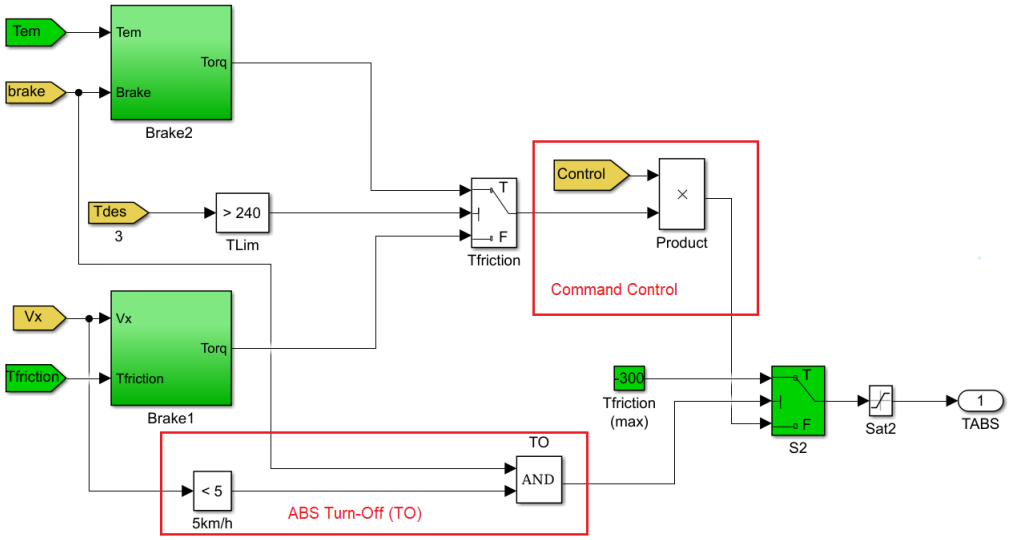

Figure 52 – The block of Command Control for Mechanical ABS

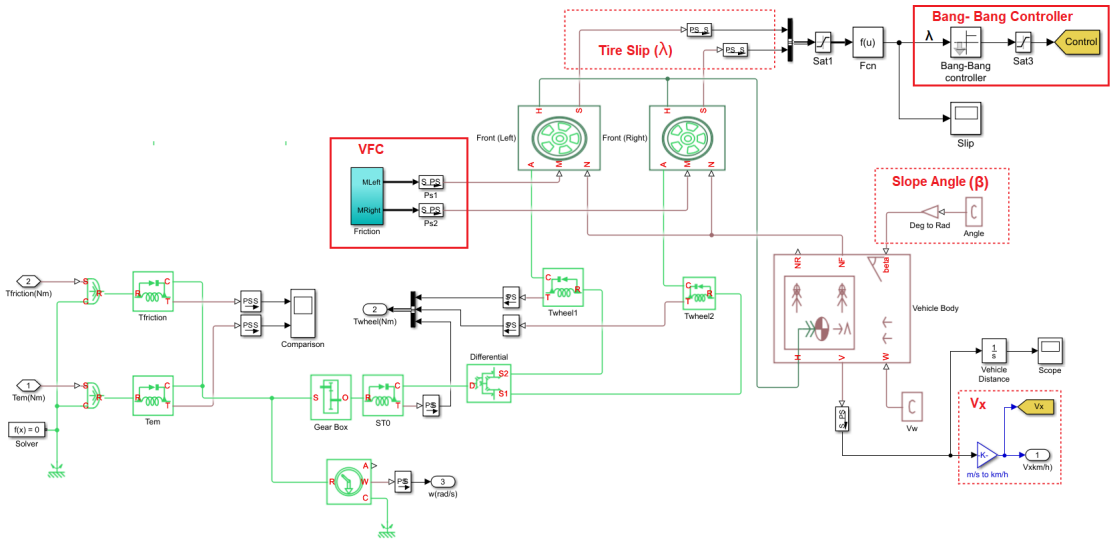

Figure 53 – "Bang-Bang Controller" block into "Dynamic Vehicle" block

Figure 54 shows the structure of the controller. While the slip (λ) in between the limits ($\pm$ 0.2), what means the tire-road friction is adequate, the desired torque is applied to the wheels.

When the slip surpass the limit, indicating the wheel will lock, the output torque command becomes zero, allowing the wheel to continue spinning.

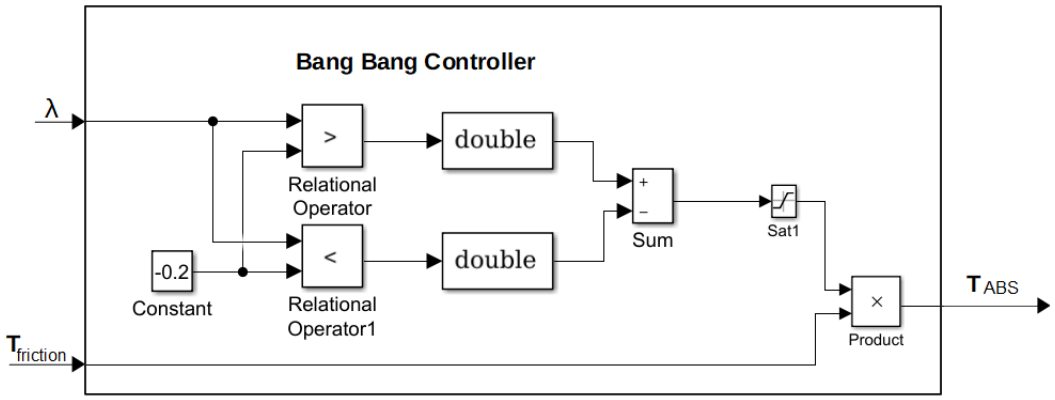

Figure 54 – Command Control with the Bang-Bang Controller

Figure 55 shows a driving cycle. The motor accelerates with constant torque (210 Nm) until 1350 rpm. Then the torque goes to zero and the speed reduces due to the vehicle losses. At t=6 s the brake procedure starts, initially with the regenerative brake (240 Nm) plus the mechanical brake (60 Nm). At t=6.2 s the inverter is turned-off and only the mechanical brake assumes the deceleration (300 Nm). At t=7 s there is a change in the road surface from wet to snow. The lower friction makes the wheel starts to lock, quickly reducing the speed.

Figure 55c shows the torque in the wheel for the same driving cycle. Note that at low speed the bang-bang controller produces a high frequency commutation, what is impossible to be followed by the ABS electromechanical command. Such undesired behavior explain the strategy of turning-off the ABS at low speed.

Figure 55d shows the ABS system recognizes the high slip and acts on the mechanical brake, alternating the application of full torque or zero torque. The objective is to maintain the slip value limited to $\pm$ 0.2. At low speed ($5km/h$), at t= 11.8 s, the ABS is turned off, the wheel locks and the vehicle stops at t= 12.6 s.

- **Strategy 2: Mechanical ABS**

  The PI control method reduces the applied torque in order to maintain the optimal slip that allows unlocking of the wheels as shown in the structure of Figure 56.

  Figure 57 shows the generation of the torque to be applied to the wheel with the PI controller. The output of the PI block is a continuous value between 0 and 1. Such output multiplies the torque reference produced by the driver command, subject to the limitations

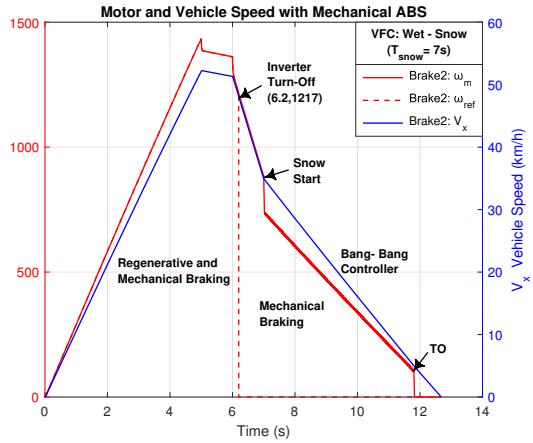

(a) Motor and Vehicle Speed

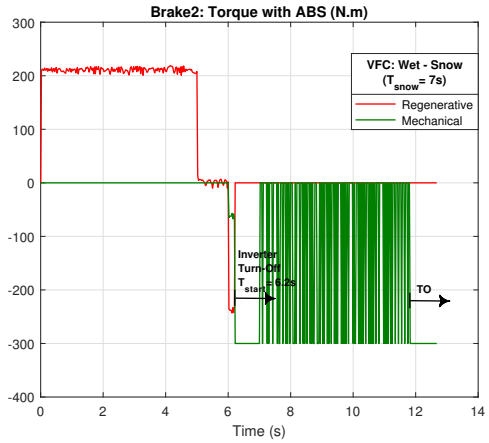

(b) Torque (Brake2 Mode)

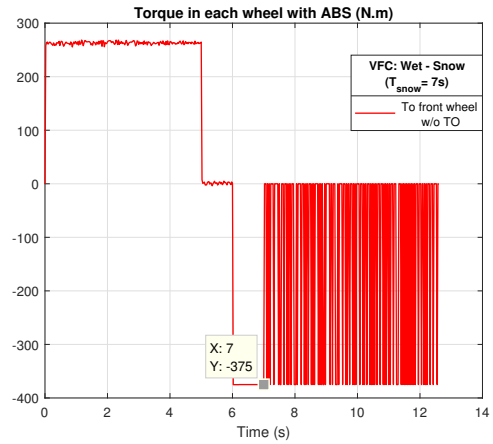

(c) Torque in each wheel

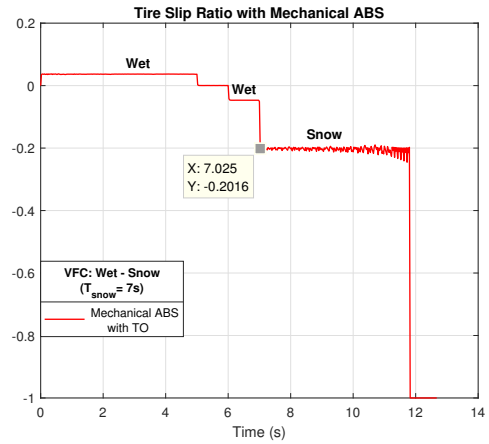

(d) Tire Slip

Figure 55 – Mechanical ABS with Bang-Bang Controller

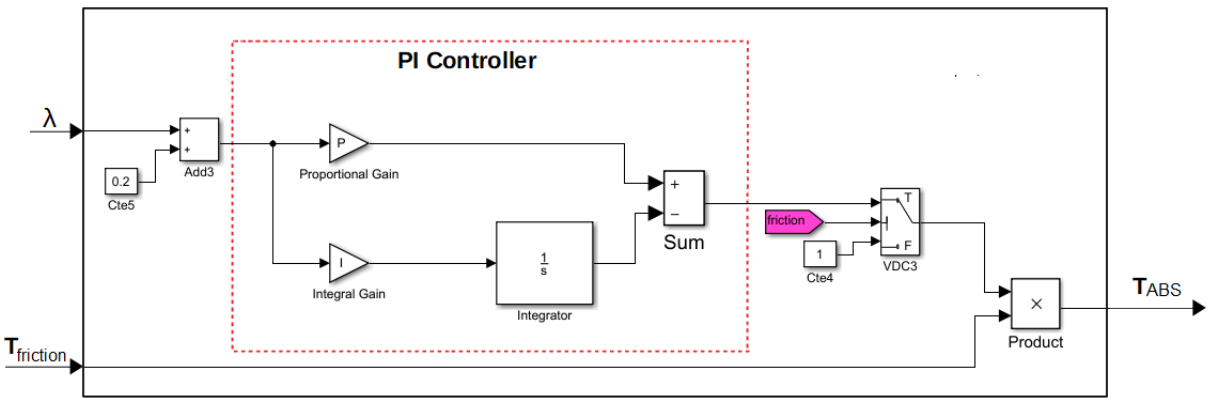

Figure 56 – Structure of the PI Controller

described in chapter 3. While the slip is in the range $\pm$ 0.2 the ABS is not active. Detected the high slip the PI starts to regulate the braking torque in order to maintain the desired slip. At very low speed (5 km/h) the ABS is turned-off and the final braking uses the full torque.

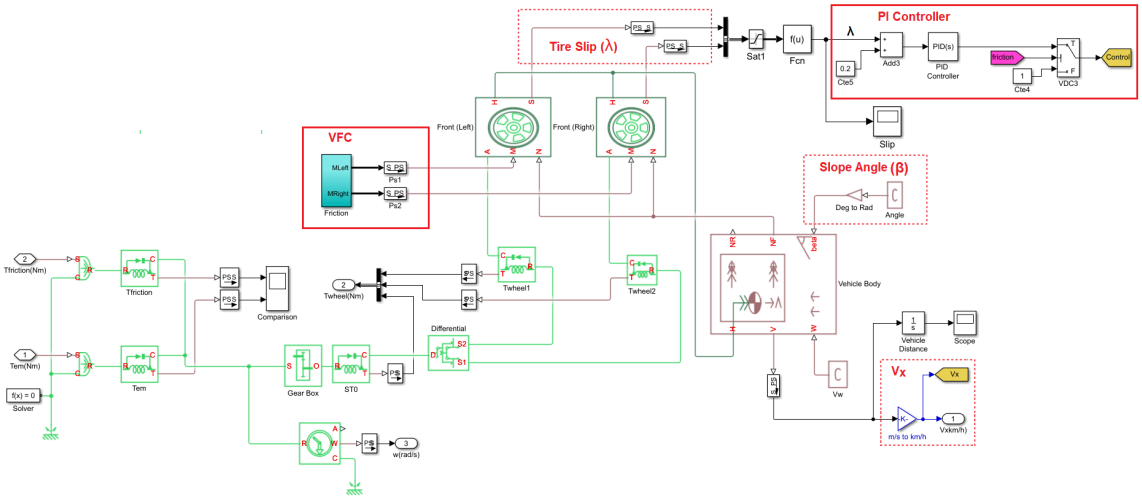

Figure 57 – Braking torque definition with PI Controller

Figure 58 repeats the previous test, now with the PI controller. The events sequence is: from t=0 s, the vehicle accelerates with a torque of 200 Nm, until the motor reaches 1350 rpm; the torque is reduced to zero and the speed decreases due to the friction and aerodynamic losses; at t=6 s regenerative (240 Nm) and mechanical (60 Nm) brakes are applied; at t=6.2 s the inverter is turned-off and the mechanical brake assumes alone; at t=7 s the road condition changes from wet to snow leading the wheel to increase the slip; the PI immediately acts to reduce the applied torque (around 110 Nm) maintaining the vehicle controllability; at t= 11.9 s, when the vehicle speed is 5km/h, the ABS is turned-off and the final braking uses the full torque. As can be seen in Figure 58d such procedure is necessary to avoid the torque oscillation that would appear in very low speed.

4.2 Regenerative Braking System with ABS Mode

Since the regenerative braking is an important aspect of EV, it is necessary to co-ordinate it with the mechanical brake, as well as to implement ABS procedures also in the regenerative brake.

Figure 59 indicates the braking procedures including mechanical and regenerative braking, both with ABS functionalities. While the slip is in the acceptable range ($\pm$ 0.2) the braking command follows the procedures presented in chapter 3. If the slip increases the ABS is activated in the RBS and, if necessary, in the friction brake. The electrical brake operates until the regenerated current (measured in the DC bus of the inverter) becomes lower than a limit. At this value the regenerated power becomes zero, brake assumes, with its ABS, until a minimum

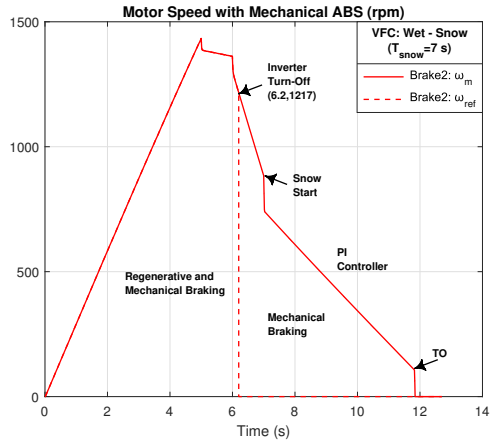

(a) Motor speed

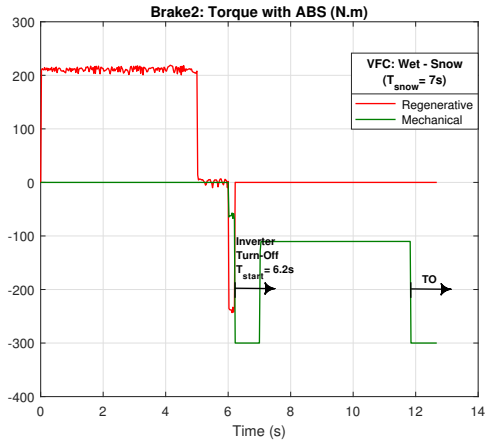

(b) Torque with ABS

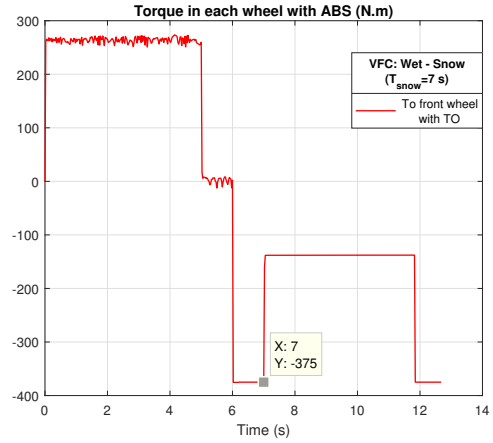

(c) Torque to front wheel with TO

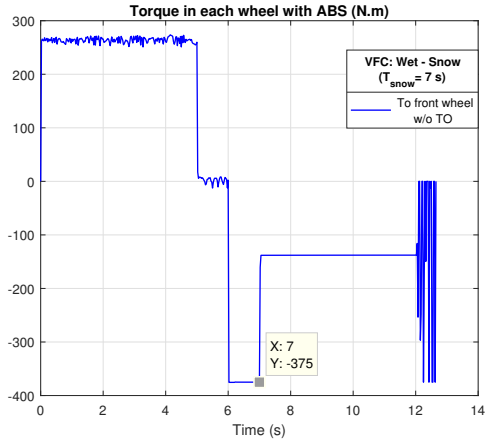

(d) Torque to front wheel without TO

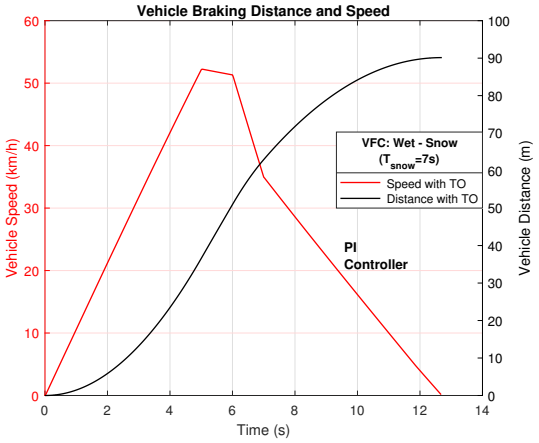

(e) Vehicle Braking Distance and Speed

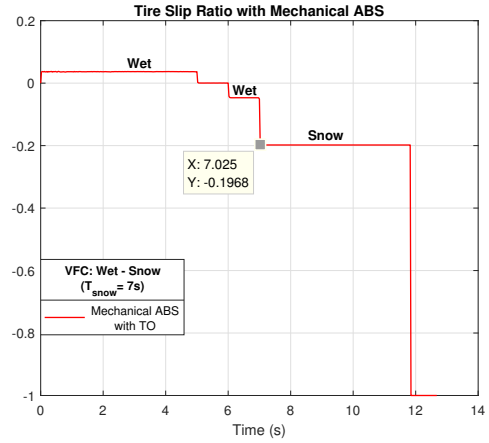

(f) Tire Slip

Figure 58 – Mechanical ABS with PI Controller

speed. To avoid oscillations in the friction brake, the ABS is disabled and the final braking is done with the simple application of the mechanical brake.

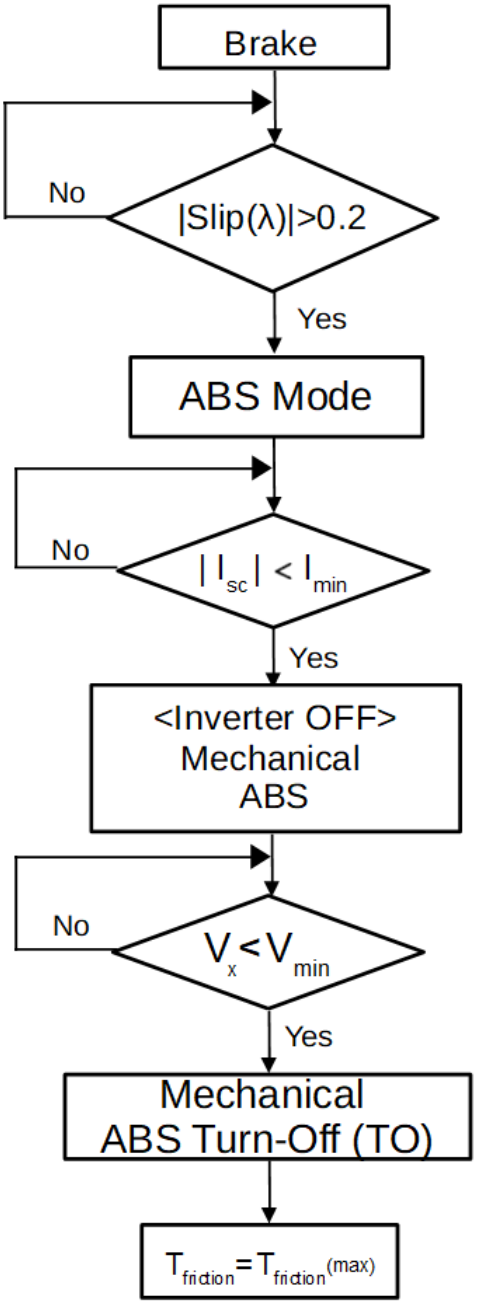

Figure 59 – Flux Diagram for ABS Mode with RBS

- **RBS with ABS Mode: Strategy 1**

  As shown in Figure 60, strategy 1 consider the ABS implemented in the RBS uses a PI controller in order to adjust the electromagnetic torque to a level that maintain the vehicle controllable, what means the slip must be in the range $\pm$ 0.2. The mechanical ABS is activated when necessary and uses the bang-bang method.

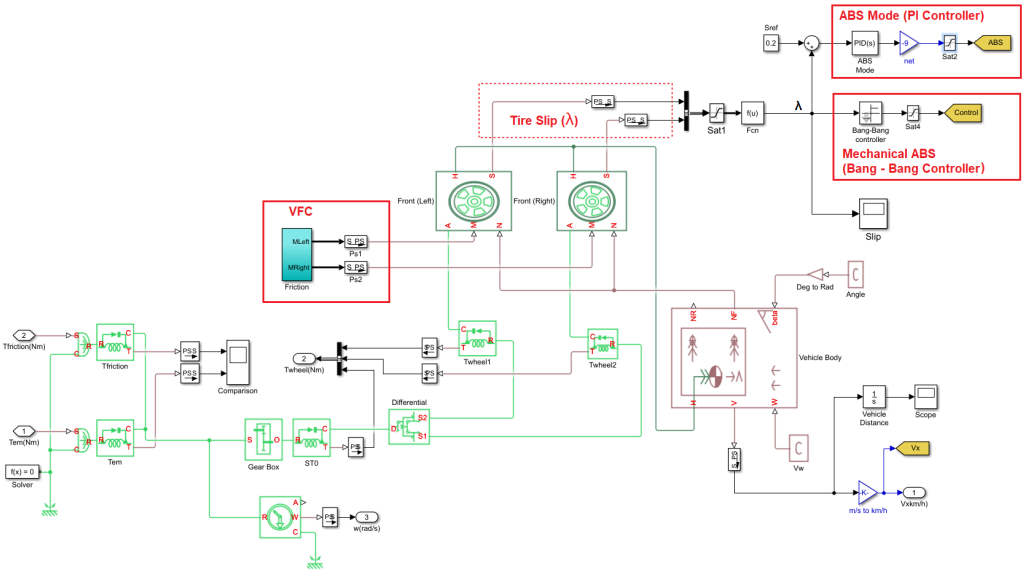

Figure 60 – Block diagram for RBS with ABS Mode

Figure 61 shows the results for the same events described previously. At t=6 s the driver applies the brake command. As the torque is too high (300 Nm), the motor produces 240 Nm, its limit, and the mechanical brake complete the torque. At t=7 s the road condition changes from wet to snow, and the wheel tends to lock. Immediately the motor torque reduces to approximately 110 Nm regulate the slip. As this value is lower than the limit, the mechanical brake does not operate. At t=10 s the inverter is turned-off, since the regeneration stops.

The mechanical brake assumes the torque, and the bang-bang controller maintains the vehicle under control. When the ABS starts to oscillate fastly it is disabled and the final stop occurs with friction maximum torque.

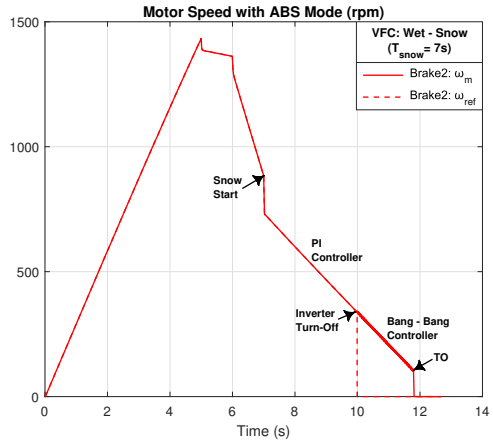

(a) Motor speed

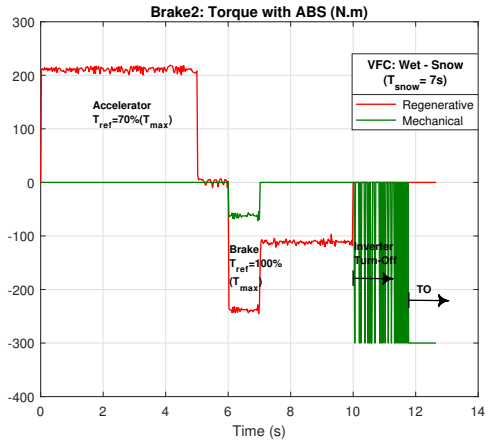

(b) Torque with ABS

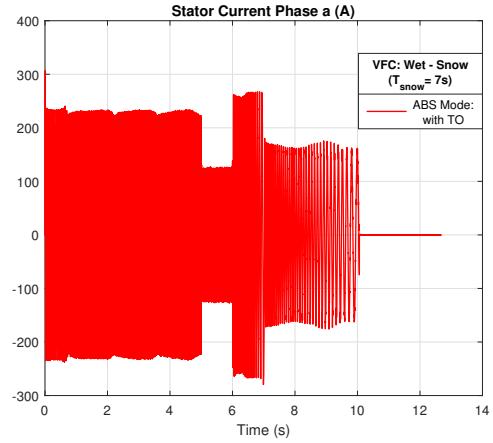

(c) Stator Current Phase a

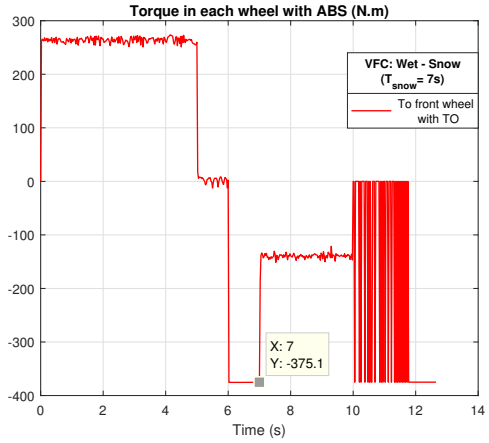

(d) Torque to front wheel with TO

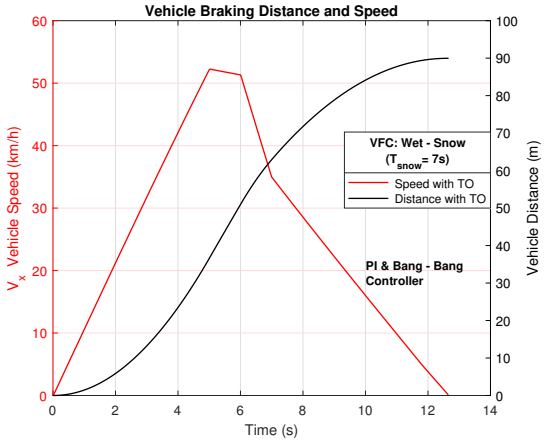

(e) Vehicle Braking Distance and Speed

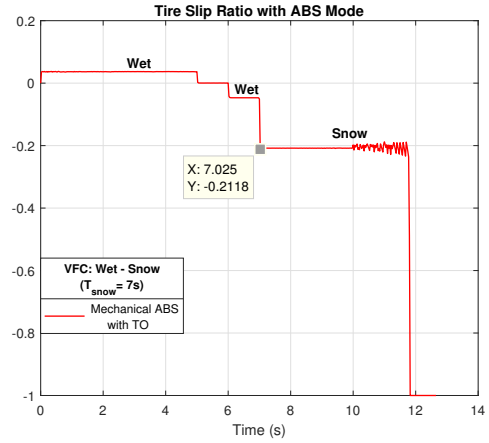

(f) Tire Slip

Figure 61 – Simulation Results for ABS Mode with RBS and Strategy 1

- **RBS with ABS Mode: Strategy 2**

  Figure 62 shows the ABS strategy when both, electromagnetic and mechanical brakes are regulated by the respective PI controllers.

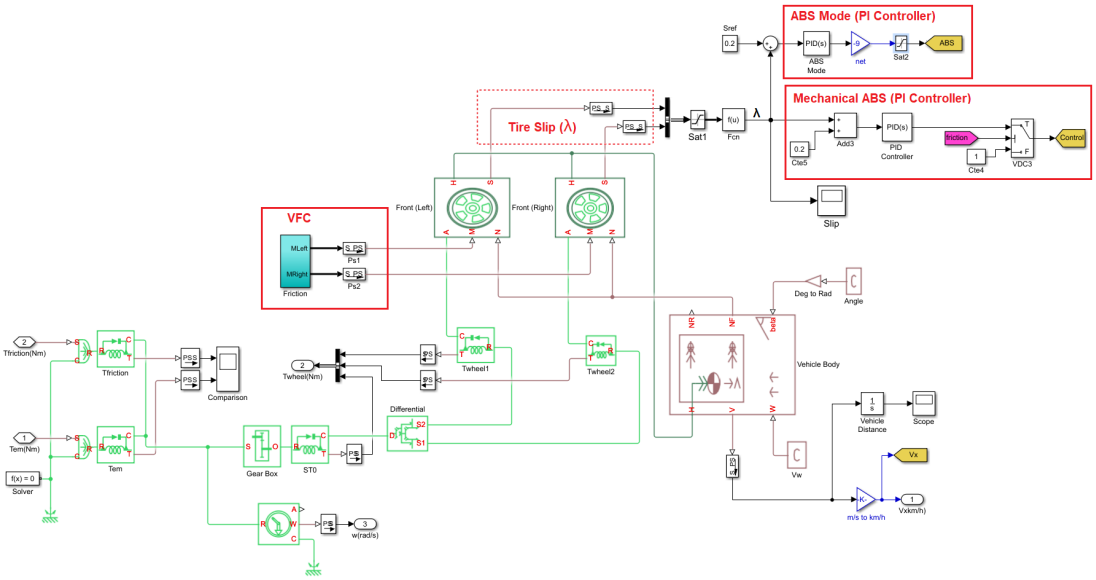

Figure 62 – Block diagram for ABS Mode and PI Controller

Figure 63 shows that for strategies 1 and 2 the regeneration is the same, since the inverter operates under equal conditions.

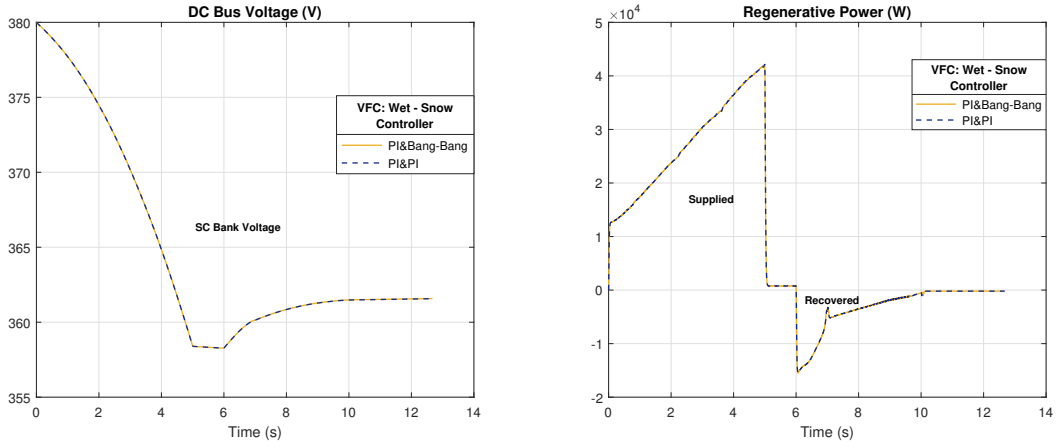

Figure 63 – Electrical Simulation Results to Compare Strategies

Figure 64 shows the results with strategy 2. The only difference is that, with a PI controller applied to the friction brake, there is a continuity in the torque when the inverter is turned-off. The other behaviours are as explained for Figure 61.

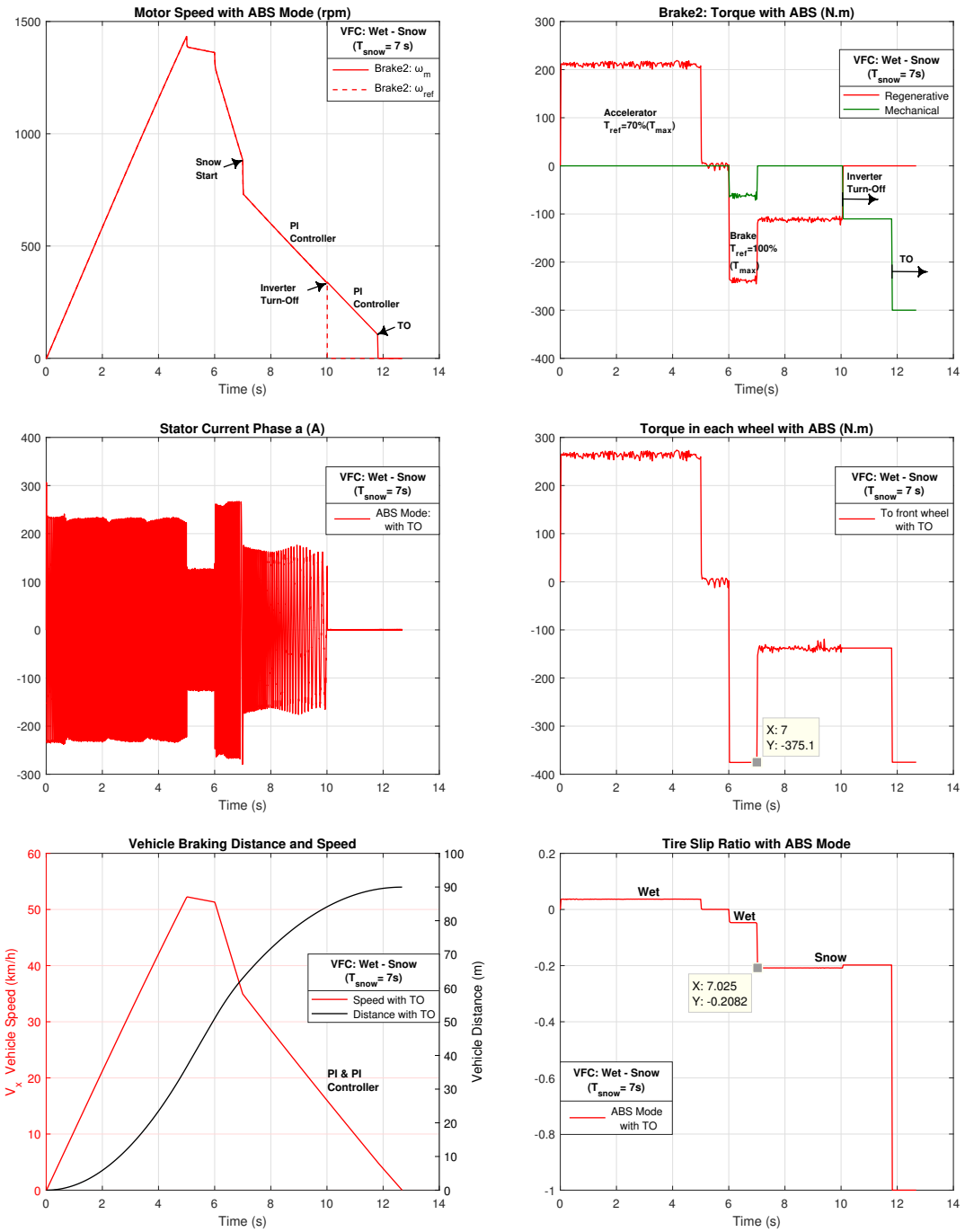

Figure 64 – Simulation Results of ABS Mode with RBS and Strategy 2

4.2.1 Complex Drive Cycle

Figure 65 and Figure 66 show additional simulations exploring the behavior of the proposed ABS strategy in more complex situations. In these cases there are two changes in the road condition: from wet to snow (at t= 7s) and from snow to wet (at t= 9s).

The left column shows a "Brake1" case, in which the brake demand is achieved using only the regenerative brake. The right column shows a "Brake2" case, in which the brake is shared between electrical and mechanical actions while the demand is ever the regenerative limit. In both cases the ABS control is able to regulate the wheel slip (Figure 66) during the show condition. All the already implementations regarding the inverter and ABS turn-off procedure are maintained.

4.3 Conclusions

This chapter has presented the key aspects of the ABS Mode applied to the regenerative braking, combined with the strategies of using the mechanical ABS, when a low coefficient of friction is detected. The ABS avoids the blocking of the wheels and maintain the vehicle control.

The PI controller applied to maintain the desired glide between the wheels and the ground allow a reduction of the electromagnetic torque to get the slip limited to the acceptable range, for any of the tested road conditions. It was shown that the mechanical ABS must be turned-off at low speed to avoid instabilities in this brake, as well as the regenerative brake must be disabled when the regeneration loses efficacy.

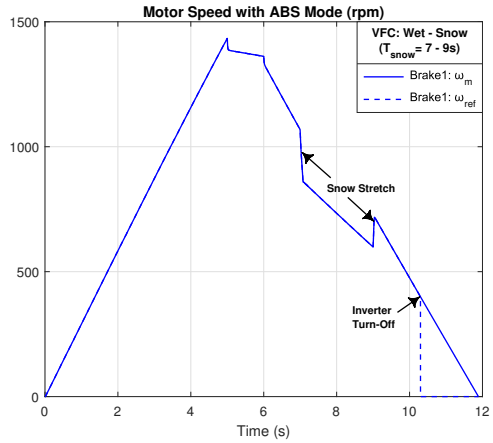

(a) Brake1: Motor Speed

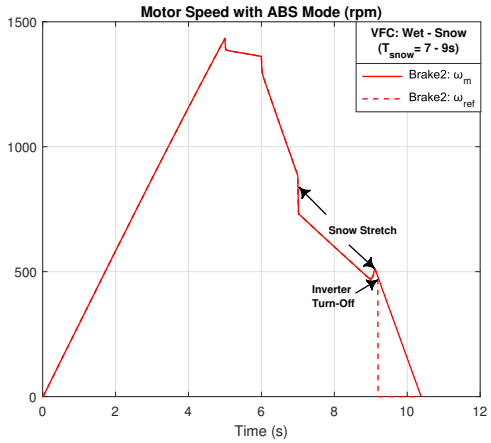

(b) Brake2: Motor speed

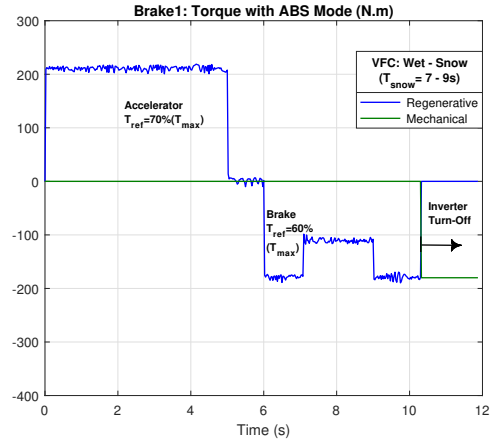

(c) Brake1: Torque with ABS Mode

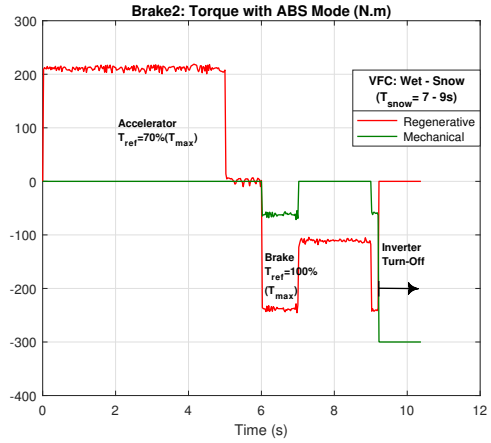

(d) Brake2: Torque with ABS Mode

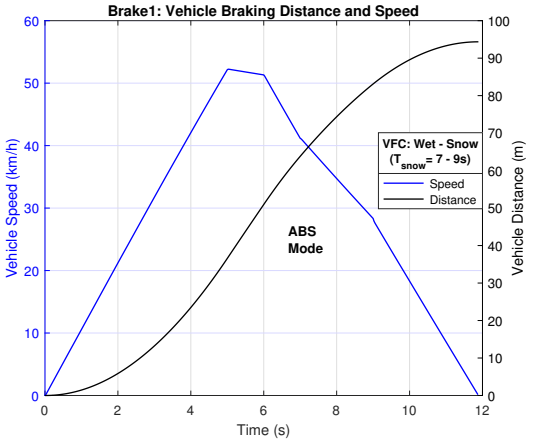

(e) Brake1: Vehicle Braking Distance and Speed

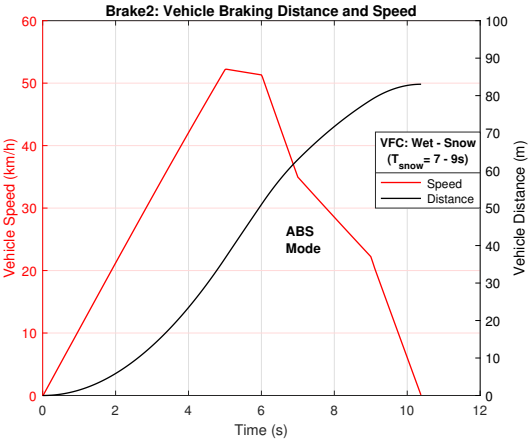

(f) Brake2: Vehicle Braking Distance and Speed

Figure 65 – RBS and ABS with Braking Strategy 1-2

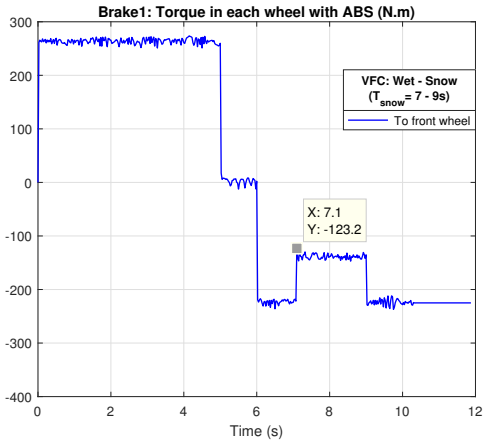

(a) Brake1: Torque to front wheel with ABS

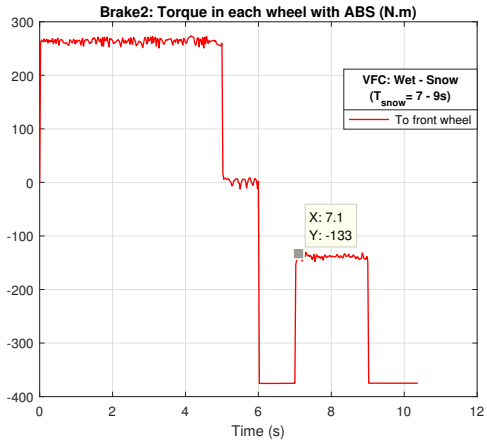

(b) Brake2: Torque to front wheel with ABS

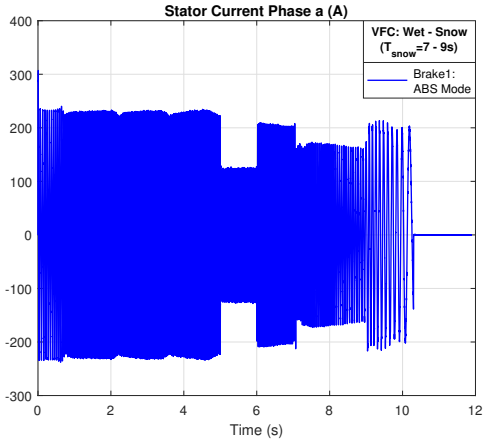

(c) Brake1: Stator Current Phase a

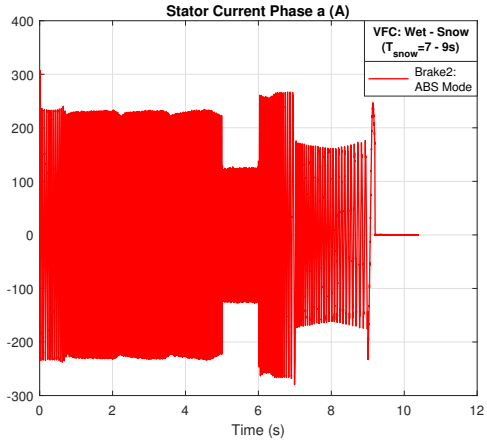

(d) Brake2: Stator Current Phase a

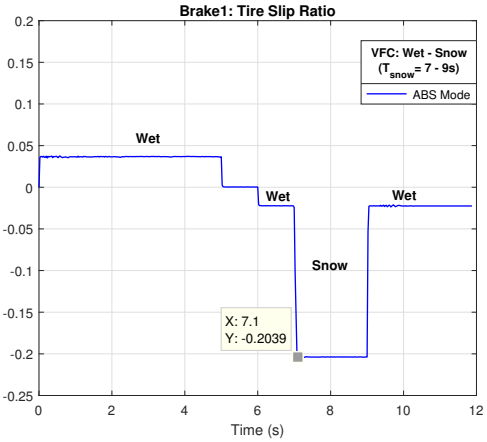

(e) Brake1: Tire Slip

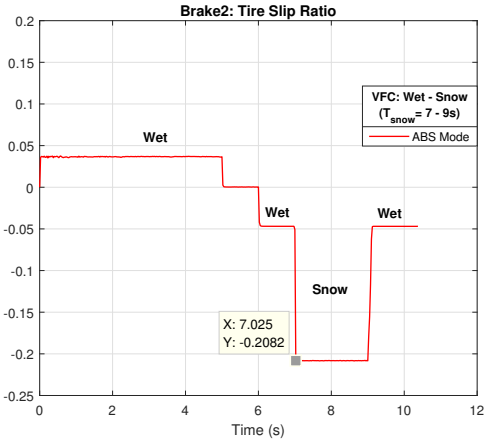

(f) Brake1: Tire Slip

Figure 66 – RBS and ABS with Braking Strategy 1-2

5 Conclusions and Perspectives

This thesis has analyzed the braking process of electrical vehicles, including mechanical (friction) and electrical (regenerative) brake systems, with emphasis in the ABS procedures.

The main contribution is the electric vehicle modeling driven by a single induction machine in a passenger vehicle. From the improved dynamic model was incorporate electrical and mechanical control strategies at same simulation. The use of direct torque control (DTC) allowed us to obtain an adequate procedure of braking. Further, the shutdown procedures between RBS and ABS at low-speed afforded to improve the performance electric (RBS) and mechanical (Mechanical ABS).

As presented in Chapter 2, the studies were carried out based on simulations, including detailed models for the main parts of the system: vehicle dynamic, induction motor with direct torque control, SVPWM inverter and power supply (supercapacitor bank), wheel/tire model, including the interaction with the ground, etc.

In Chapter 3 it was developed the base model, including the procedures for mechanical and regenerative braking. Scalar and direct torque controllers were tested. Due to its superior precision of the DTC method has been applied in the sequence of the research. Also the limitations of the torque in the wheels and in the electric motor were considered, as well as the strategy to share the desired torque (commanded by the driver) between the mechanical and electric devices. Also in this chapter it was presented strategies for the identification of excessive slip, what imposes the application of the ABS. It was identified that it is necessary to disable the regenerative brake when the current measured at the inverter DC bus becomes near to zero. Beyond this value the energy regeneration loses efficacy and the system loses surpass the recovered energy. Additionally, the simulation results have showed that there is an oscillation on the mechanical ABS at low speed, making necessary to turn-off the ABS command below a minimum speed.

Finally, Chapter 4 analyses the system response for more complex conditions, specially the sudden change in the road-tire interaction that would produce wheel locking during braking. The ABS strategies presented in Chapter 3 have showed to be quite effective for maintain the possible braking torque without blocking the wheels. The sudden change from a wet road to a snowy surface, and viceversa, shown the coordination between both brake systems operate correctly, assuring the vehicle can be conducted by the driver.

Clearly there are many additional studies that should be carried out for improving these results. Among them it is possible to indicate:

- Implementation of an experimental setup, initially in the laboratory, in the sequence in an EV, in order to evaluate in a real situation the efficacy of the proposed strategies;
- As an intermediate step, a hardware in the loop simulation would allow longer simulations with more realistic commands and situations;
- Improvement in the EV model to include the cases of four wheel traction, with independent motors in each wheel;
- Deeper discussion about the slip identification and quantification for any kind of road surface;
- Introduce different driving cycles, including curves and the consequent tangential forces;
- Adaptive control procedures regarding the EV mass variation, tire conditions (pressure, roughness,etc).
- Improvement the mechanical brake modeling, including the valve behavior and the transition between electrical and mechanical systems.

Bibliography

[1] "Electric car use by country," 2018. [Online]. Available: https://en.wikipedia.org/wiki/Electric_car_use_by_country#cite_note-Global2011_2015-20

[2] Konrad Reif, *Brakes, Brake Control and Driver Assistance Systems*, 2014.

[3] Srikanth Veppathur Sivaramakrishnan, "Discrete tire modeling for anti-lock braking system simulations," Master's thesis, Virginia Polytechnic Institute and State University, USA, 2013.

[4] M. W. Al-Grafi, M. K. Mohamed, and F. A. Salem, "Analysis of vehicle friction coefficient by simulink with Matlab," *International Journal of Control, Automation and Systems*, 2013.

[5] "The mathworks inc, simscape library." [Online]. Available: https://www.mathworks.com/help/search.html?qdoc=simscape+library&submitsearch=

[6] P. Gupta, A. Kumar, and S. Deb, "Regenerative Braking Systems (Rbs) (Future of Braking Systems)," *International Journal of Mechanical And Production Engineering*, 2014.

[7] W. Li, "Abs control on modern vehicle equipped with regenerative braking," Master's thesis, Delft University of Technology, USA, 2010.

[8] M. Ehsani, Y. Gao, and et al., *Modern electric, Hybrid Electric, and Fuel Cell Vehicles*, second edition ed., U. C. Pres, Ed., 2008.

[9] A. Aly, Z. El-shafei, and et al., "An Antilock-Braking Systems (ABS) Control: A Technical Review," *Intelligent Control and Automation*, 2011.

[10] X. Garcia, B. Zigmund, A. Terlizzi, and et al., "Comparison between foc and dtc strategies for permanent magnet synchronous motors," *Advances in Electrical and Electronic Engineering*, 2006.

[11] "Electric car market statistics," 2018. [Online]. Available: http://www.nextgreencar.com/electric-cars/statistics/

[12] "Brasil tem potencial para vender 150 mil carros elétricos ao ano," 2018. [Online]. Available: https://epocanegocios.globo.com/Tecnologia/noticia/2018/02/brasil-tem-potencial-para-vender-150-mil-carros-eletricos-ao-ano.html

[13] "Electric vehicle charging system market," 2016. [Online]. Available: https://www.alliedmarketresearch.com/electric-vehicle-charging-systems-market

[14] "Anti-lock braking system abs market," 2016. [Online]. Available: https://www.alliedmarketresearch.com/anti-lock-braking-system-ABS-market

[15] L. Zhang, L. Yu, N. Pan, and et al., "Cooperative control of regenerative braking and friction braking in the transient process of anti-lock braking activation in electric vehicles," *Proceedings of the Institution of Mechanical Engineers, Part D: Journal of Automobile Engineering*, 2015.

[16] "Automotive regenerative braking system," 2016. [Online]. Available: https://www.alliedmarketresearch.com/automotive-regenerative-braking-system-market

[17] J. Guo, J. Wang, and B. Cao, "Regenerative braking strategy for electric vehicles," *2009 IEEE Intelligent Vehicles Symposium*, 2009.

[18] Aliandro Henrique Santos, "A contribution to the study of friction brakes for application in regenerative braking," Ph.D. dissertation, School of Mechanical Engineering, State University of Campinas. (in Portuguese) Brazil, 2009.

[19] G. Xu, W. Li, and et al., "An intelligent regenerative braking strategy for electric vehicles," *in Energies 2011, 4, 1461-1477;doi: 10.3390/en4091461*, 2011.

[20] K. Ma, L. Chu, and et al., "Study on Control Strategy for Regenerative Braking in a Pure Electric Vehicle," *2nd International Conference on Electronic Mechanical Engineering and Information Technology (EMEIT-2012)*, 2012.

[21] M. G. S. P. Paredes, "Braking regenerative in electric vehicle driven an induction motor: Study, simulation and implementation (in portuguese)," Master's thesis, State University of Campinas, Brazil, 2013.

[22] G. Yin and X. Jin, "Cooperative control of regenerative braking and friction braking for a hybrid electric vehicle," *Proceedings of the Institution of Mechanical Engineers, Part D: Journal of Automobile Engineering*, 2013.

[23] Stefan Solyom, "Synthesis of a model-based tire slip controller," Ph.D. dissertation, Department of Automatic Control,Lund Institute of Technology,Sweden, 2002.

[24] Y. Guan, Z. Q. Zhu, and et al., "Difference in maximum torque-speed characteristics of induction machine between motor and generator operation modes for electric vehicle application," *Electric Power Systems Research*, 2016.

[25] G. Guidi, T. M. Undeland, and Y. Hori, "Optimized power electronics interface for auxiliary power buffer based on supercapacitors," *2008 IEEE Vehicle Power and Propulsion Conference, VPPC 2008*, 2008.

[26] H. D. Desai and D. Bhanabhagvanwala, "Comparative analysis between scalar control and direct torque control methods for induction motor drives," *International Journal of Current Engineering and Scientific Research*, 2015.

[27] G. Buja and M. Kazmierkowski, "Direct Torque Control of PWM Inverter-Fed AC Motors—A Survey," *IEEE Transactions on Industrial Electronics*, 2004.

[28] C. Lascu, I. Boldea, and F. Blaabjerg, "A modified direct torque control for induction motor sensorless drive," *IEEE Transactions on Industry Applications*, 2000.

[29] N. Idris and A. Yatim, "Direct torque control of induction machines with constant switching frequency and reduced torque ripple," *IEEE Transactions on Industrial Electronics*, 2004.

[30] D. Casadei, F. Profumo, and et al., "FOC and DTC: Two Viable Schemes for Induction Motors Torque Control," *IEEE Transactions on Power Electronics*, 2002.

[31] Yoichi Hori, "Future vehicle driven by electricity and control—research on four-wheel-motored uot electric march ii," *IEEE Transactions on Industrial Electronics*, 2004.

[32] S. J. Clegg, "A Review of Regenerative Braking Systems," *Institute of Transport Studies, University of Leeds*, 1996.

[33] V. Brazis, L. Latkovskis, and L. Grigans, "Simulation of trolleybus traction induction drive with supercapacitor energy storage system," *in Latvian Journal of Physics and Technical Sciences*, 2010.

[34] M. G. S. P. Paredes, J. A. Pomilio, and A. A. Santos, "Combined regenerative and mechanical braking in electric vehicle," *Brazilian Power Electronics Conference (COBEP)*, 2013.

[35] Z. Zhang, X. Zhang, and et al, "A high-efficiency energy regenerative shock absorber using supercapacitors for renewable energy applications in range extended electric vehicle," *Journal of Applied Energy*, 2016.

[36] A. Ferreira, J. Pomilio, and et al., "Energy Management Fuzzy Logic Supervisory for Electric Vehicle Power Supplies System," *IEEE Transactions on Power Electronics*, 2008.

[37] L. Cai and X. Zhang, "Study on the control strategy of hybrid electric vehicle regenerative braking," *2011 International Conference on Electronic Mechanical Engineering and Information Technology Study*, 2011.

[38] W. Pasillas-Lepine and A. Loria, "A new mixed wheel slip and acceleration control based on a cascaded design," *IFAC Symposium on Nonlinear Control Systems*, 2010.

[39] Tianku Fu, "Modeling and performance analysis of abs systems with nonlinear control," Master's thesis, Concordia University, Canada, 2010.

[40] J. Wang, J. Qiao, and Z. Qi, "Research on control strategy of regenerative braking and anti-lock braking system for electric vehicle," *2013 World Electric Vehicle Symposium and Exhibition (EVS27)*, 2013.

[41] R. De Oliveira, L. Mattos, and et al., "Regenerative Braking of a Linear Induction Motor used for the Traction of a Maglev Vehicle," *Brazilian Power Electronics Conference (COBEP)*, 2013.

[42] P. Hart, *ABS Braking Requirements*, A. Hartwood Consulting Pty Ltd, Ed., 2003. [Online]. Available: https://www.techylib.com/en/view/odecrack/abs_braking_requirements_stage_3

[43] S. Miller, B. Youngberg, and et al., "Calculating Longitudinal wheel slip and Tire parameter using GPS velocity," *Proceedings of the American Control Conference Arlington*, 2001.

[44] G. Goodwin, S. Graebe, and M. Salgado, *Control System Design*, first edition ed., Pearson, Ed., 2000.

[45] M. Farasat and E. Karaman, "Speed sensorless electric vehicle propulsion system using hybrid foc-dtc induction motor drive," *Electrical Machines and Systems (ICEMS), 2011 International Conference on*, 2011.

[46] M. Zhou, Z. Gao, and H. Zhang, "Research on regenerative braking control strategy of hybrid electric vehicle," *Proc. of IEEE 2011 The 6th International Forum on Strategic Technology*, 2011.

[47] Edson Bim, *Máquinas Eléricas e Acionamento*, Elsevier, Ed., 2009.

[48] M. Yoong, Y. Gan, G. Gan, and et al., "Studies of regenerative braking in electric vehicle," *Proc. of IEEE Conference on Sustainable Utilization and Development in Engineering and Technology*, 2010.

[49] A. Murthy, D. Magee, and D. Taylor, "Vehicle braking strategies based on regenerative braking boundaries of electric machines," *IEEE Transportation Electrification Conference and Expo (ITEC)*, 2015.

[50] K. Kawashima, Y. Hori, and T. Uchida, "Stabilizing control of vehicle motion using small ev driven by ultra capacitor," *IECON Industrial Electronics Conference*, 2005.

[51] O. Tur, O. Ustun, and R. Tuncay, "An Introduction to Regenerative Braking of Electric Vehicles as Anti-Lock Braking System," *2007 IEEE Intelligent Vehicles Symposium*, 2007.

[52] X. Wang and Q. Wang, "Modeling and Simulation of Automobile Anti-Lock Braking System Based on Simulink," *Journal of Advanced Manufacturing Systems*, 2012.

[53] C. Tannoury, F. Plestan, and et al., "Tyre effective radius and vehicle velocity estimation: A variable structure observer solution," *International Multi-Conference on Systems, Signals and Devices*, 2011.

[54] S. Pay and Y. Baghzouz, "Effectiveness of battery-supercapacitor combination in electric vehicles," *IEEE Bologna PowerTech Conference Proceedings*, 2003.

[55] B. Tabbache, A. Kheloui, and M. Benbouzid, "Design and Control of the Induction Motor Propulsion of an Electric Vehicle," *IEEE Vehicle Power and Propulsion Conference*, 2010.

[56] C. Goia, L. Popa, and et al., "Supercapacitors used as an energy source to drive the short urban electric vehicles," *Advanced Topics in Electrical Engineering (ATEE), 2011 7th International Symposium on*, 2011.

[57] P. Poure, F. Aubepart, and F. Braun, "A design methodology for hardware prototyping of integrated AC drive control: application to direct torque control of an induction machine," *Proceedings 11th International Workshop on Rapid System Prototyping. RSP 2000. Shortening the Path from Specification to Prototype*, 2000.

[58] S. Basu, T. M. Undeland, and G. Guidi, "Voltage and current ripple considerations for improving ultra-capacitor lifetime while charging with switch mode converters," *2007 European Conference on Power Electronics and Applications, EPE*, 2007.

[59] M. Bian, L. Chen, Y. Luo, and K. Li, "A Dynamic Model for Tire/Road Friction Estimation under Combined Longitudinal/Lateral Slip Situation," 2014. [Online]. Available: http://papers.sae.org/2014-01-0123/

[60] André Augusto Ferreira, "Energy management supervisory system of multiple power sources for electric vehicle applications (in Portuguese),State University of Campinas, Brazil," Ph.D. dissertation, 2007.

[61] W. Penny and P. Els, "The test and simulation of ABS on rough, non-deformable terrains," *Journal of Terramechanics*, 2016.

[62] J. Rodriguez, J. Pontt, C. Silva, S. Kouro, and H. Miranda, "A Novel Direct Torque Control Scheme for Induction Machines with Space Vector Modulation," *IEEE 35th Annual Power Electronics Specialists Conference (IEEE Cat. No.04CH37551)*, 2004.

[63] I. Takahashi and T. Noguchi, "A New Quick-Response and High-Efficiency Control Strategy of an Induction Motor," *IEEE Transactions on Industry Applications*, 1986.

[64] Giuseppe Guidi, "Energy management systems on board of electric vehicles, based on power electronics," Ph.D. dissertation, Faculty of Information Technology, Mathematics and Electrical Engineering, Norwegian University of Science and Technology, Norway, 2009.

[65] H. Xiaoliang and H. Yoichi, "Energy Management Strategy Based on Frequency - Varying Filter for the Battery Supercapacitor Hybrid System of Electric Vehicles," *EVS27 International Battery, Hybrid and Fuel Cell Electric Vehicle Symposium*, 2013.

[66] R. Maia, M. Silva, R. Araújo, and U. Nunes, "Electrical vehicle modeling : A fuzzy logic model for regenerative braking," *Expert Systems with Applications*, 2015.

[67] J. Kolar, H. Ertl, F. Zach, V. Blasko, V. Kaura, and R. Lukaszewski, "A novel concept for regenerative braking of PWM-VSI drives\nemploying a loss-free braking resistor," *Proceedings of APEC 97 - Applied Power Electronics Conference*, 1997.

[68] Jin-Woo, Jung, "Space Vector Simulink," *Pace Pacing And Clinical Electrophysiology*, 2005.

[69] G. Guidi, T. M. Undeland, and Y. Hori, "An interface converter with reduced VA ratings for battery-supercapacitor mixed systems," *Power Conversion Conference*, 2007.

[70] Kiyotaka Kawashima, "Vehicle Stabilizing Control Using Small EV Powered only by Ultra Capacitor," *IEEE International Workshop on Advanced Motion Control*, 2006.

[71] S. M. Patil and S. R. S. Prabaharan, "Embedded Control Scheme of Stand-Alone Regenerative Braking System using Supercapacitors," *Indian Journal of Science and Technology*, 2015.

[72] S. Mehta and S. Hemamalini, "A Dual Control Regenerative Braking Strategy for Two-Wheeler Application," *Energy Procedia*, 2017.

[73] X. Yu, T. Shen, and et al., "Regenerative Braking Torque Estimation and Control Approaches for a Hybrid Electric Truck," *2010 American Control Conference Marriott Waterfront, Baltimore, MD, USA*, 2010.

[74] Yoichi Hori, "Motion Control of Electric Vehicles and Prospects of Supercapacitors," *IEEJ Transactions on Electrical and Electronic Engineering*, 2008.

[75] Brian Su-Ming, Fan, "Modeling and Simulation of A Hybrid Electric Vehicle Using MATLAB / Simulink and ADAMS," Master's thesis, University of Waterloo, Canada, 2007.

[76] G. F. Mauer, "A Fuzzy Logic Controller for an ABS Braking System," *IEEE Transactions on Fuzzy Systems*, 1995.

[77] W. Li, X. Wang, and et al., "Modeling and Simulation of Automobile Braking System Based on Kinetic Energy Conversion," *2008 IEEE Vehicle Power and Propulsion Conference (VPPC)*, 2008.

[78] "Toyota recalls thousands of prius cars worldwide," 2010. [Online]. Available: http://news.bbc.co.uk/2/hi/business/8505402.stm

APPENDIX A – Vehicle Braking Systems

An overall vehicle has an active system safety that helps to prevent accidents and makes a preventative contribution to safety. The following are some examples:

- ABS (Antilock Braking System)
- TCS (Traction Control System) and,
- ESP (Electronic Stability Program)

These safety systems stabilize the vehicle's response in critical situations and thus maintain its steerability. Apart from their contribution to vehicle safety, exist currently systems such as Adaptive Cruise Control (ACC) that essentially offer added convenience by maintaining the distance from the vehicle in front by automatically throttling back the engine or applying the brakes, whereby it is necessary to be fitted with a radar system, cameras, and other sensors.

In addition, each vehicle also has passive safety systems, as well as are designed to protect vehicle occupants from serious injury in the event of an accident. They reduce the risk of injury and thus the severity of the consequences of an accident. Examples of passive safety systems are the seat-belts required by law and airbags which can be fitted in various positions inside the vehicle such as in front of or at the side of the occupants. For more information see [2].

A.1 Classification of vehicle braking systems

The entirety of the braking systems on a vehicle is referred as braking equipment. Vehicle braking systems can be classified on the basis of

- design and
- method of operation

Designs are based on legal requirements on commercial vehicles, the braking equipment also includes a continuous-operation braking system that allows the driver to keep the vehicle at a steady speed on a long descent.

The methods of operation depend on whether they are operated entirely or partially by human effort or by another source of energy.

The braking control system should be capable of ensuring that the vehicle retains its handling stability and steerability on all types of road surface, from dry roads with good adhesion to black ice.

Therefore, an ABS system must meet a comprehensive range of requirements, in particular all the safety requirements associated with dynamic braking response and the braking-system technology.

An ABS system should utilize the available adhesion between the tires and the road surface under braking to the maximum possible, giving handling stability and steerability precedence over minimizing braking distance. It should not make any difference to the system whether the driver applies the brakes violently or gradually increases the braking force to the point at which the wheels would lock. This system is operated by hydraulic power (which is based on fluid pressure) transmitted by hydraulic means. The brake fluid is stored in energy accumulators (hydraulic accumulators) which also contain a compressed gas (usually nitrogen). The gas and the fluid are kept apart by a flexible diaphragm(diaphragm accumulator) or a piston with a rubber seal (piston accumulator). A hydraulic pump generates the fluid pressure, which is always in equilibrium with the gas pressure in the energy accumulator. A pressure regulator switches the hydraulic pump to idle as soon as the maximum pressure is reached. Since brake fluid can be regarded as practically incompressible, small volumes of brake fluid can transmit large brake-system pressures.

A.2 Brake-circuit configuration

Legal requirements demand that braking systems incorporate a dual-circuit force transmission system. According to DIN 74 000, there are five ways in which the two brake circuits can be split as is shown in Figure A.1. It uses the following combinations of letters to designate the configurations: II, X, HI, LL and HH. Those letters are chosen because their shapes roughly approximate to the layout of the brake lines connecting the master cylinder and the brakes. Of those five possibilities, the II and X configurations, which involve the minimum amount of brake piping, hoses, disconnectable joints and static or dynamic seals,have become the most widely established. That characteristic means that the risk of failure of each of the individual circuits due to fluid leakage is as low as it is for a single-circuit braking system. In the event of brake-circuit failure due to overheating of one of the brakes, the HI, LL and HH configurations have a critical weakness because the connection of individual brakes to both circuits means that failure of one brake can result in total failure of the braking system as a whole.

In order to satisfy the legal requirements regarding secondary-braking effectiveness, vehicles with a forward weight-distribution bias are fitted with the X configuration. The II configuration is particularly suited to use on vehicles with a rearward weight-distribution bias.

- **II configuration** This layout involves a front-axle/rear-axle split – one circuit operates the rear brakes, the other operates the front brakes.
- **X configuration** This layout involves a diagonal split each circuit operates one front brake and its diagonally opposed rear brake.
- **HI configuration** This layout involves a front/front-and-rear split - one brake circuit operates the front and rear brakes, the other operates only the front brakes.
- **LL configuration** This arrangement involves a two-front/one- rear split. Each circuit operates both front wheels and one rear wheel.
- **HH configuration** The circuits are split front-and-rear/front- and-rear. Each circuit operates all four wheels.

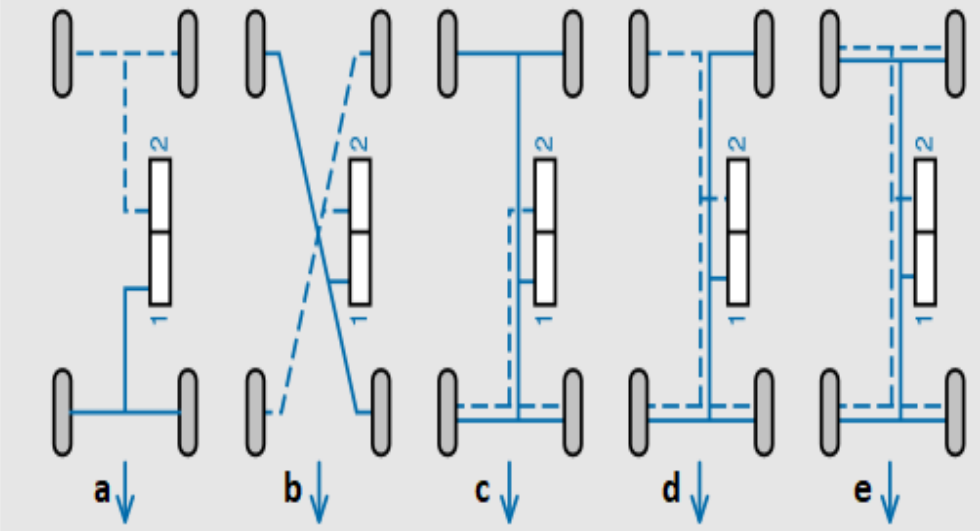

Figure A.1 – Configuration (a-II, b-X, c-HI, d-LL, e-HH), Brake Circuit (1 - 2), Direction of travel (↓) [2].

A.3 Reaction distance and total braking distance

According to ISO 611, the total braking distance is the distance traveled during the total braking time. Thus, the point at which the driver first applies force to the actuation device is a decisive factor in determining the total braking distance. However, as far as the overall braking sequence is concerned, the distance travelled from when the driver first identifies a hazard to when the brakes are first applied is also of significance. This is the driver's reaction time and is different for every driver.

The total distance traveled from identification of a hazard to the point at which the vehicle comes to a halt is thus made up of a number of components consisting of

- the distance traveled during the brake-pressure build-up time at an increasing rate of deceleration,
- the distance travelled under fully developed deceleration at a constant rate of deceleration,
- the distance traveled during the reaction time and the brake-system response time at a constant velocity, υ.

Alternatively, half the period of increasing deceleration can be taken to be under fully developed deceleration at the rate a, and the remaining period taken to be under zero deceleration. This time period is added to the other periods of zero deceleration (reaction time and brake-system response time) to form the dead time, t_{vz}. Thus the distance required for braking is defined by the formula

$$s = \upsilon.t_{vz} + \frac{\upsilon^2}{2a} \tag{A.1}$$

The maximum rate of deceleration is limited by the friction between the tires and the road. Minimum rates of deceleration are defined by law. Assuming a dead time of 1s, the table below shows the combined reaction and total braking distance at various speeds.

	Vehicle speed in km/h prior to braking												
	10	30	50	60	70	80	90	100	120	140	160	180	200
	Distance travelled during dead time of 1s (unbraked) in m												
	2.8	8.3	14	17	19	22	25	28	33	39	44	50	56
Deceleration *a* in m/s²	Reaction and total braking distance in m												
4.4	3.7	16	36	48	62	78	96	115	160	210	270	335	405
5.0	3.5	15	33	44	57	71	87	105	145	190	240	300	365
5.8	3.4	14	30	40	52	65	79	94	130	170	215	265	320
7.0	3.3	13	28	36	46	57	70	83	110	145	185	230	275
8.0	3.3	13	26	34	43	53	64	76	105	135	170	205	250
9.0	3.2	12	25	32	40	50	60	71	95	125	155	190	225

Figure A.2 – Total braking distance to several decelerations [2].

APPENDIX B – Power and Energy

B.1 Power

To electric systems, the product of a voltage $v(t)$ by a current $i(t)$ represents the instantaneous power in a circuit.

- $v(t)$= Voltage between conductors.
- $i(t)$= Current by conductors.

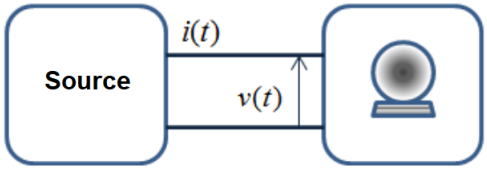

Figure B.1 – Electric circuit.

$$p(t) = v(t).i(t) \tag{B.1}$$

Active power is the average value of the instantaneous power

$$\overline{p(\tau)} = \frac{1}{T}\int_0^T p(\tau)d\tau \tag{B.2}$$

$$\overline{p(\tau)} = \frac{1}{\pi}\int_0^\pi p(\tau)d\tau \tag{B.3}$$

$$\overline{p(\tau)} = \frac{1}{\pi}\int_0^\pi v(\tau).i(\tau)d\tau \tag{B.4}$$

B.2 Energy

Energy (E) is the time integral of the instantaneous power. Considering the curve of Figure B.2 , it is calculated:

$$E = \int_{T_0}^{T_f} p(t)dt \tag{B.5}$$

$$E_{total} = E_A + E_B + E_C \tag{B.6}$$

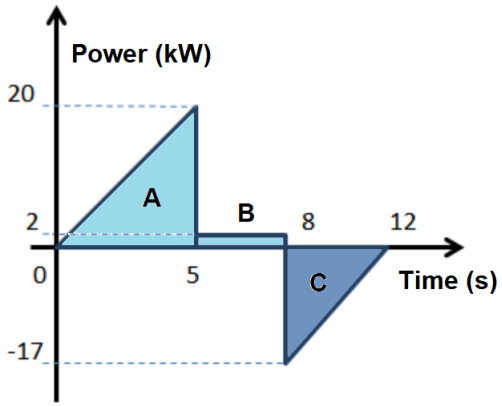

Figure B.2 – Instantaneous power during EV trajectory

Interval A (t = 0s - t = 5s):

$$E_A = \frac{1}{2}.20kW.5s = 50kJ \tag{B.7}$$

Interval B (t = 5s - t = 8s):

$$E_B = 2kW.3s = 6kJ \tag{B.8}$$

Interval C (t = 8s - t = 12s):

$$E_C = \frac{1}{2}.-17kW.4s = -34kJ \tag{B.9}$$

$$E_{total} = 50kJ + 6kJ - 34kJ = 22kJ \tag{B.10}$$

APPENDIX C – Simulation Schematics

This work was simulated on MATLAB 8.9(R2017a)/Simulink. The simulation schematics following of EV system model are divided into five sections:

- V/F Control System (Base)
- V/F Control System with RBS Strategy
- DTC System with RBS Strategy
- DTC on Flat Surface with Variable Friction Coefficient without ABS
- DTC on Flat Surface with Variable Friction Coefficient with ABS

C.1 V/F Control System (Base)

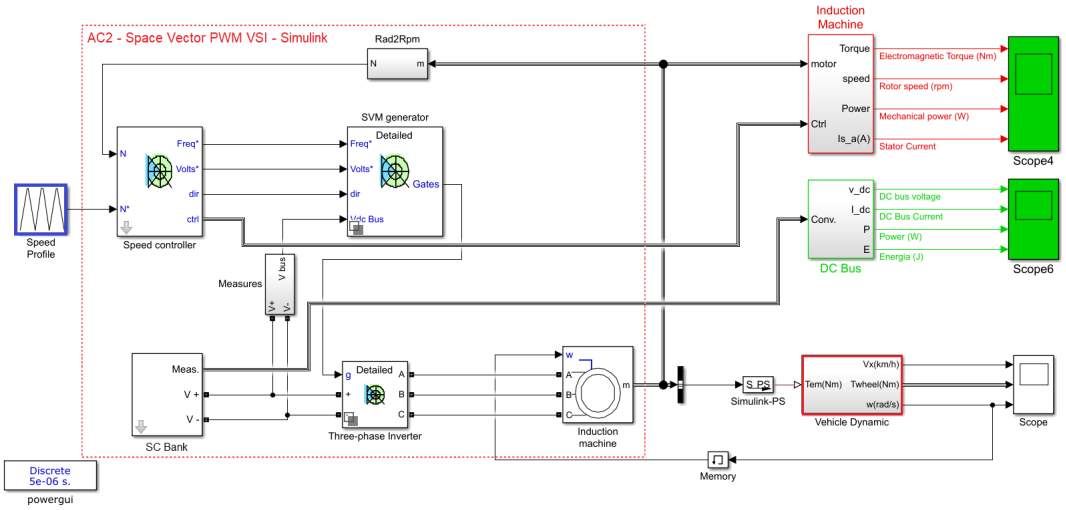

Figure C.1 – EV System Model with Base Scalar Control for driving cycles studies.

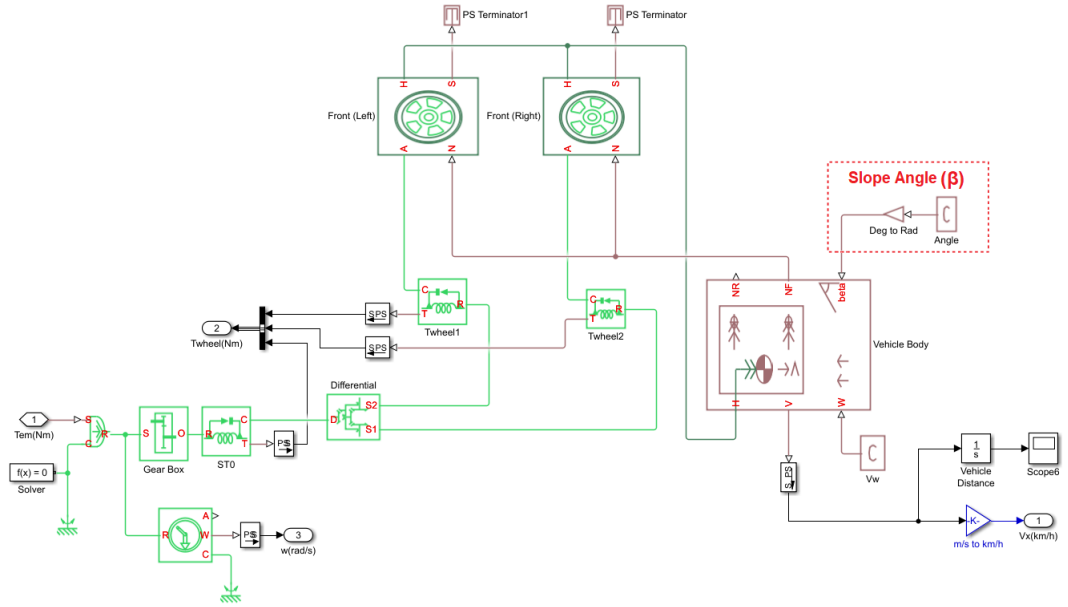

Figure C.2 – "Vehicle Dynamic" Block into EV System Model.

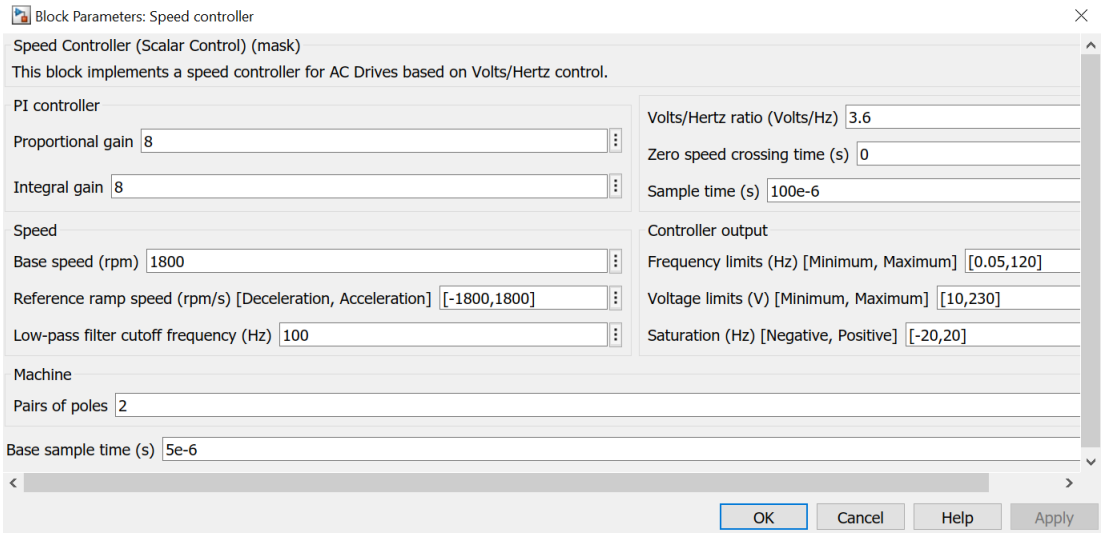

Figure C.3 – Speed Controller Parameters into EV System Model.

C.2 V/F Control System with RBS Strategy

The EV system model includes a PI torque controller, a mechanical torque and a braking strategy.

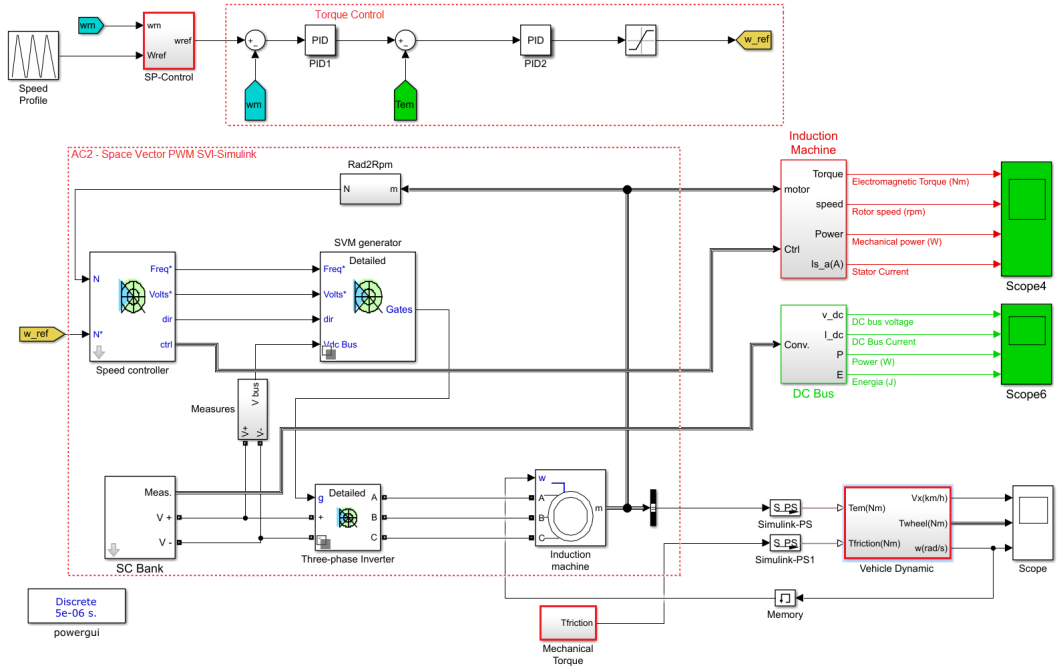

Figure C.4 – EV Model System with Scalar Control with RBS Strategy.

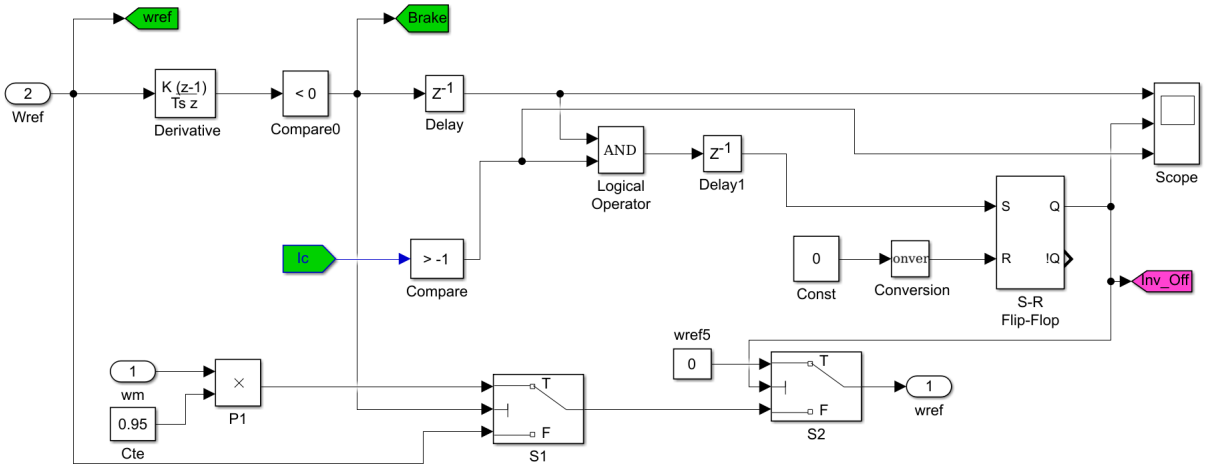

Figure C.5 – "SP-Control" Block into EV System Model with RBS Strategy.

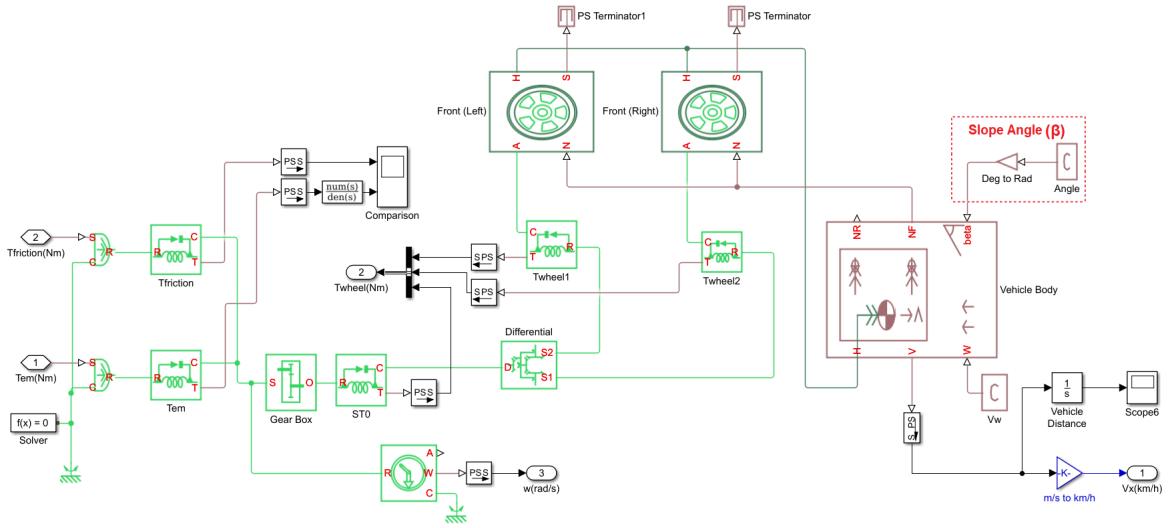

Figure C.6 – "Vehicle Dynamic" Block into EV System Model with RBS Strategy.

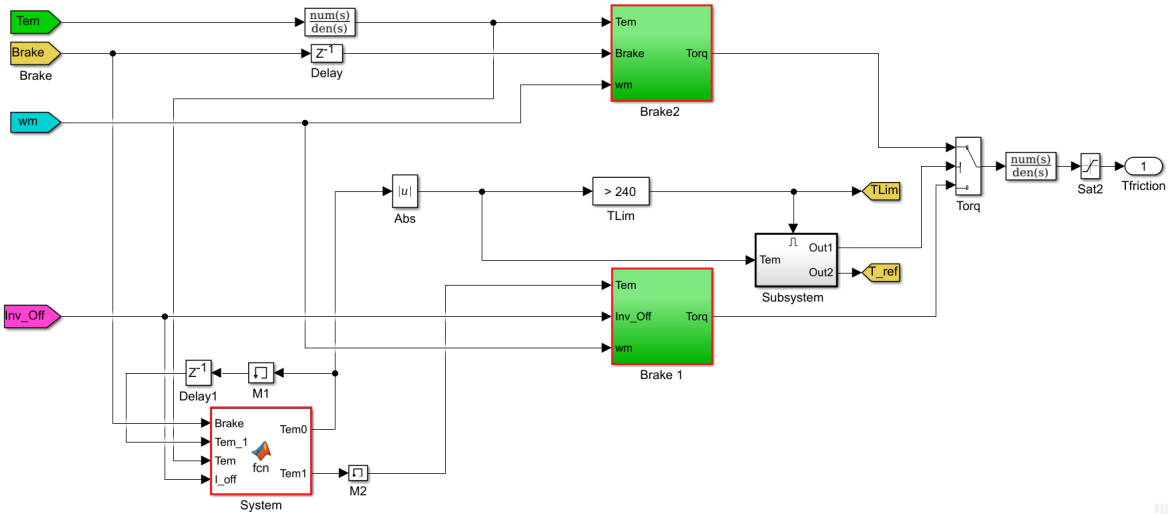

Figure C.7 – "Mechanical Torque" Block into EV System Model with RBS Strategy.

C.2.1 Mechanical Torque Block

The "Mechanical Torque" block contains the regenerative braking strategies in accordance with the flow diagram Figure 33.

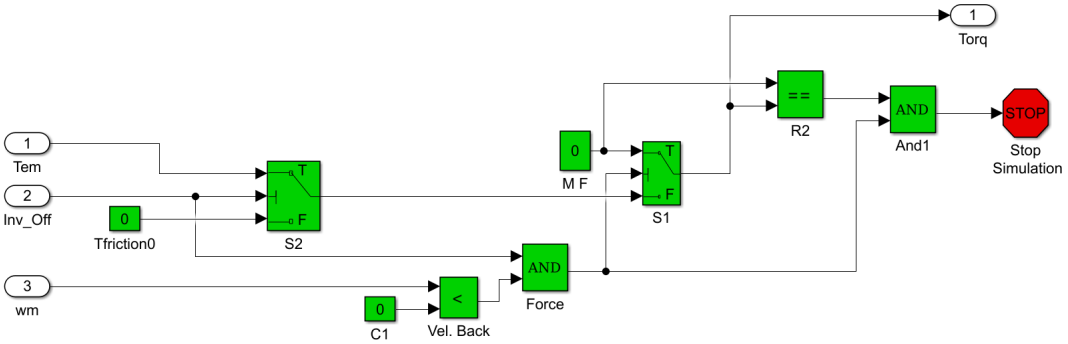

Figure C.8 – "Brake1" Block.

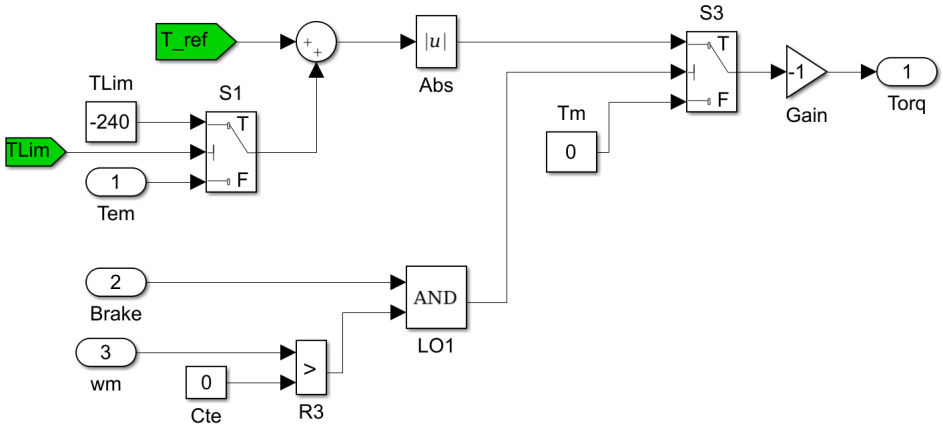

Figure C.9 – "Brake2" Block.

```
function [Tem0,Tem1] = fcn(Brake,Tem_1,Tem,I_off)
Tem1=0;
if Brake==0
Tem0 = 0;
else
Tem0=Tem;
    if I_off==1
    Tem0=Tem_1;
    end

Tem1=Tem_1;
end
```

Figure C.10 – Code programming of "System" Block.

C.3 DTC systems with RBS Strategy

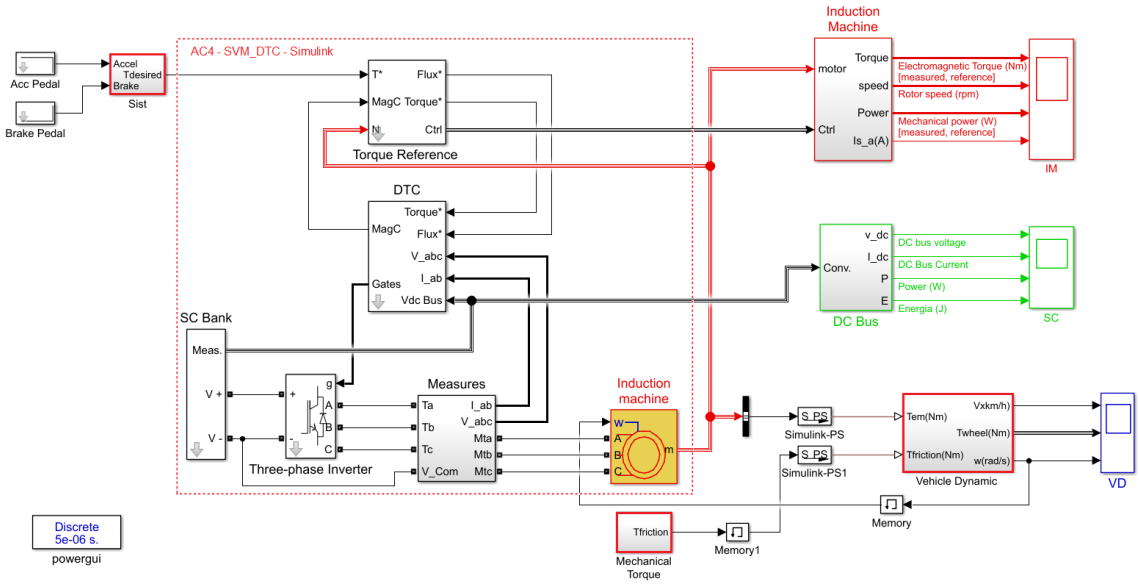

Figure C.11 – EV Model System with DTC Control for driving cycles studies.

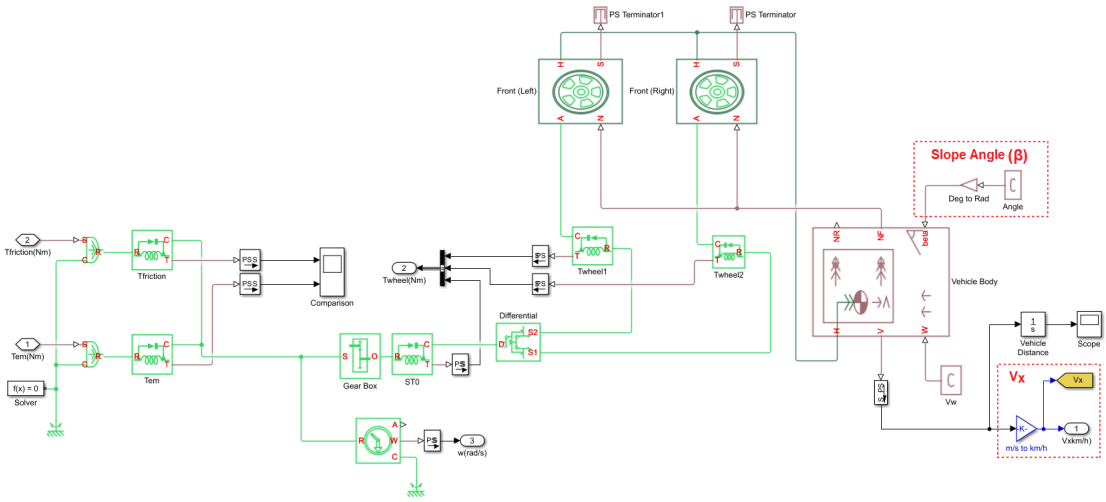

Figure C.12 – "Vehicle Dynamic" Block into EV System Model with RBS Strategy.

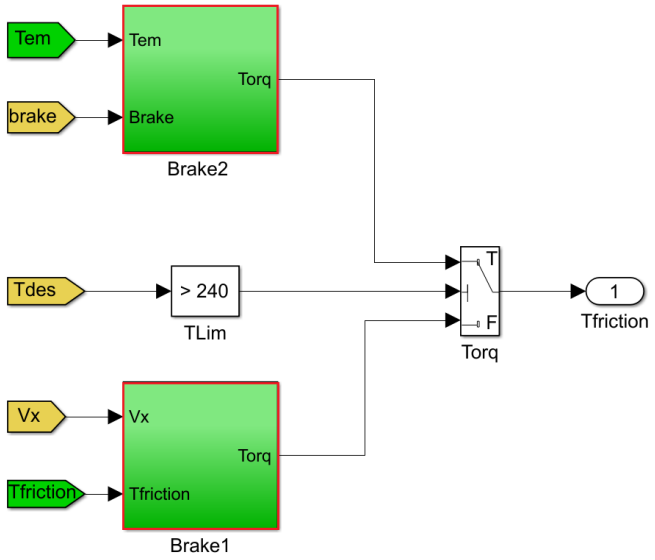

Figure C.13 – "Mechanical Torque" Block into EV System Model with RBS Strategy.

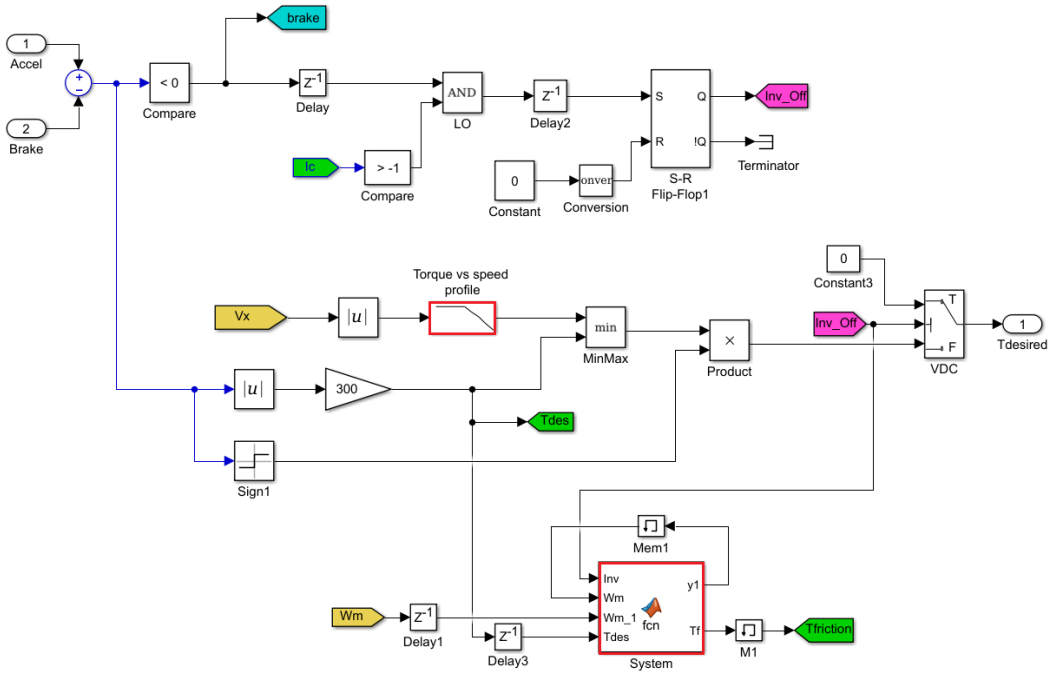

Figure C.14 – "Sist" Block into EV System Model with RBS Strategy.

C.3.1 Mechanical Torque Block

The "Mechanical Torque" block contains the regenerative braking strategies.

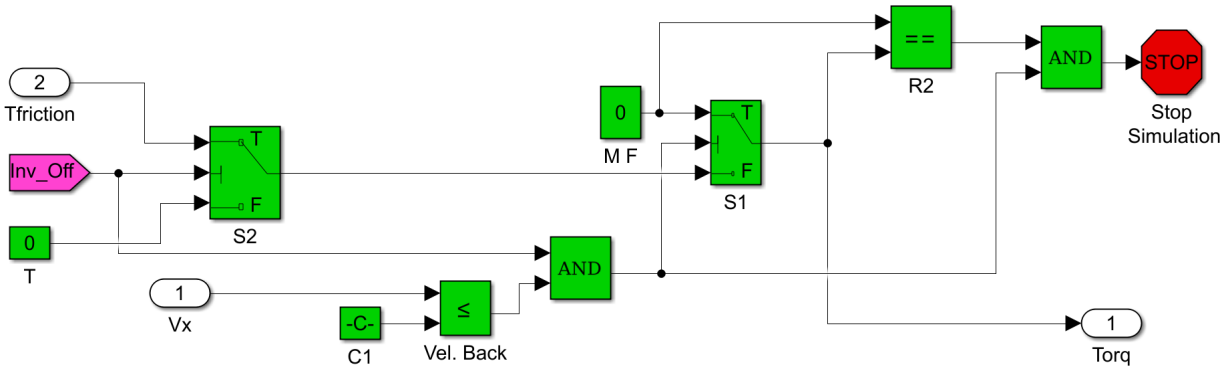

Figure C.15 – "Brake1" Block.

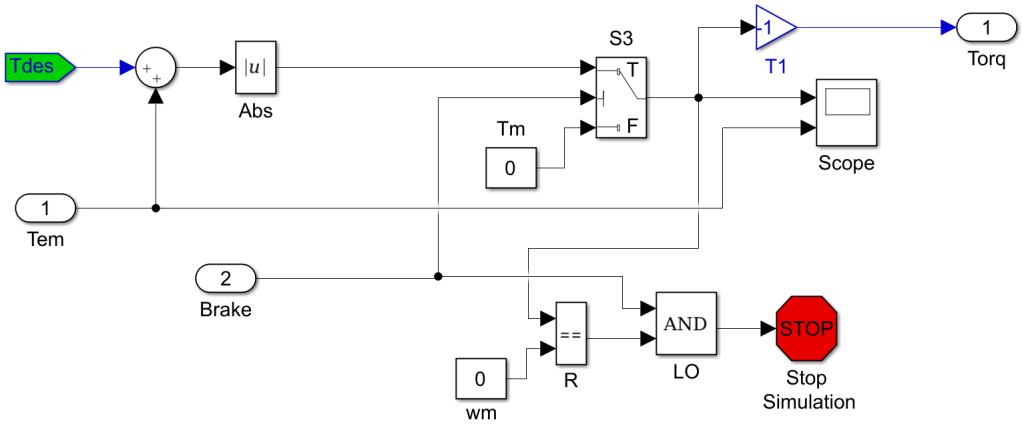

Figure C.16 – "Brake2" Block.

C.3.2 Sist Block

Define parameters (torque desired and friction torque) to RBS with Direct Torque Control

```
function [y1,Tf] = fcn(Inv,Wm,Wm_1,Tdes)
PN=37000;
TN=200;
Tf=0;
y1=0;

if Inv==0
    y1 = Wm*2*pi/60;
else
    y1=Wm_1*2*pi/60;
end

Pdes=Tdes*y1;

if Pdes>PN
    Tf=-(Tdes-240);
else
    Tf=-Tdes;
end
```

Figure C.17 – Code programming of "System" Block.

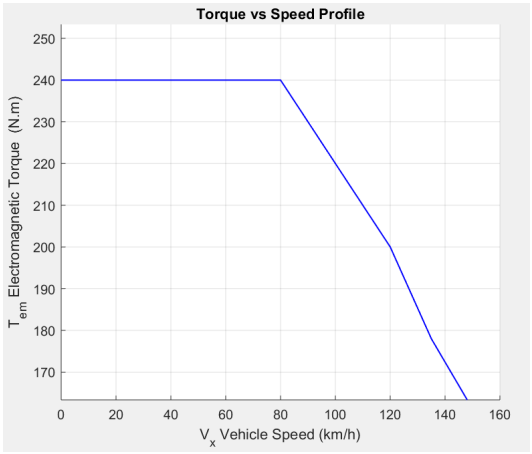

Figure C.18 – Torque- Speed Profile.

C.4 DTC on Flat surface with Variable Friction Coefficient without ABS

The simulations use the same EV model system with DTC with modifications in some blocks as the "sist" block to Inverter turn-off before VFC and Inverter turn-off after VFC. The blocks inside of "Sist" block maintains the same block as shown in Figure C.14

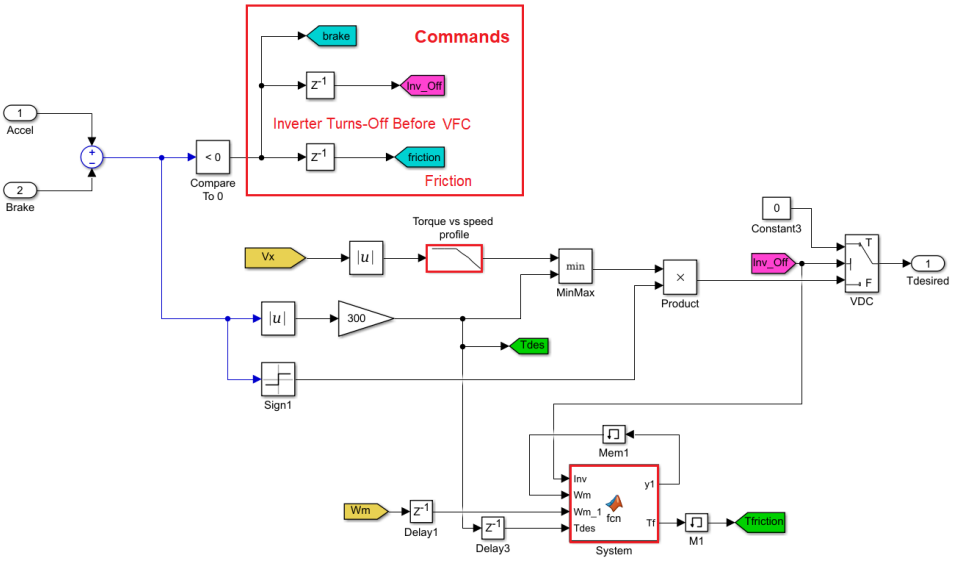

Figure C.19 – "sist" block to Inverter Turns-off before VFC.

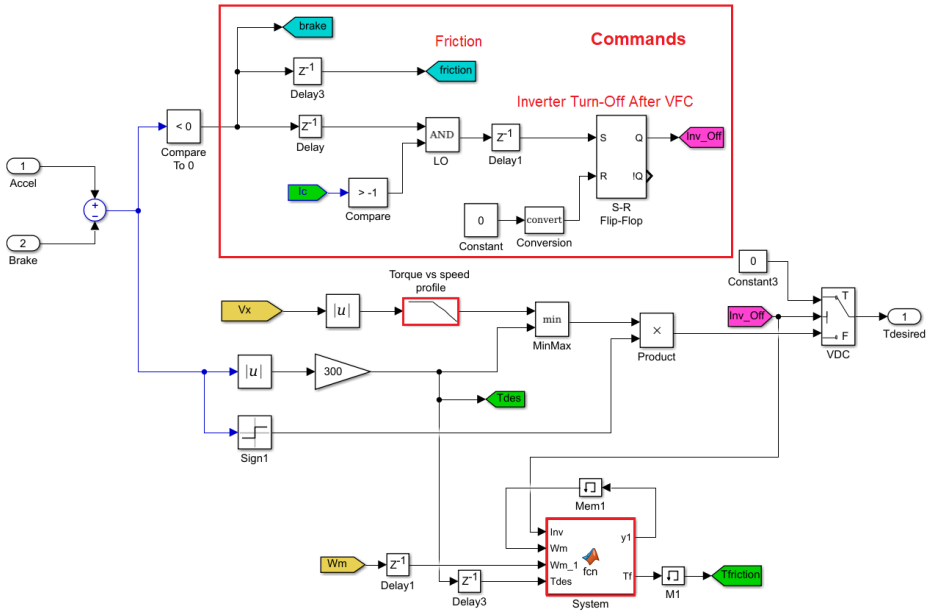

Figure C.20 – "sist" block to Inverter Turns-off after VFC.

The "Vehicle Dynamic" block adds "VFC" block, what contains the variable friction coefficients to the tire model.

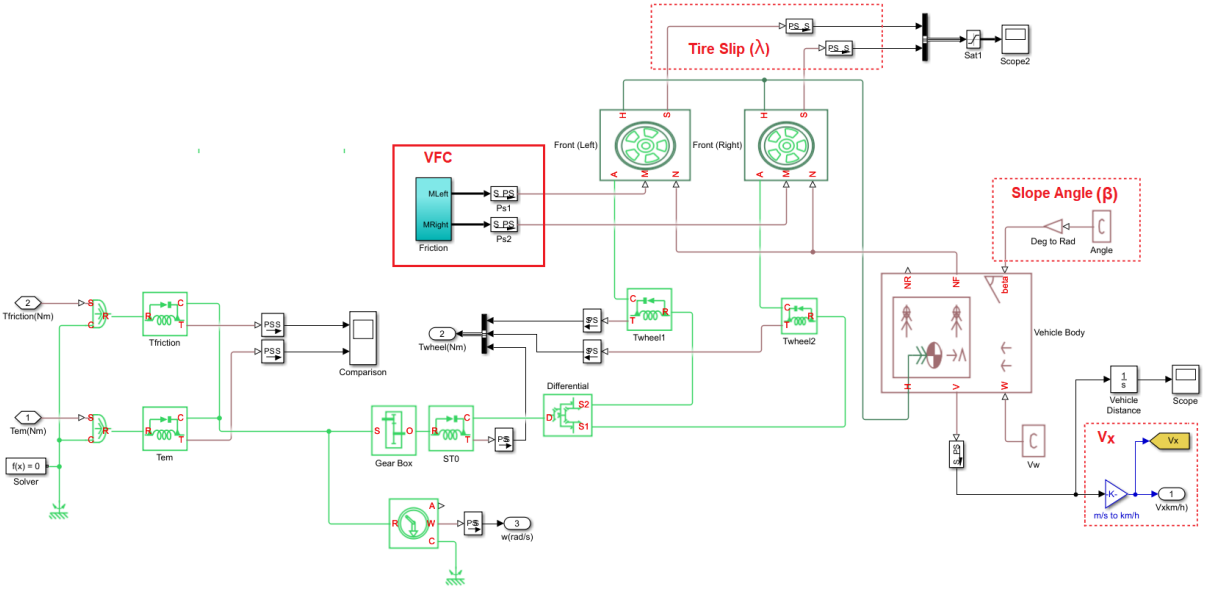

Figure C.21 – "Vehicle Dynamic" block.

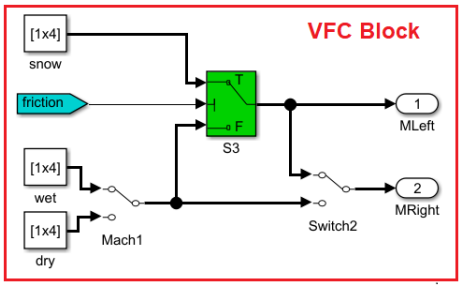

Figure C.22 – "VFC" block into "Vehicle Dynamic" block.

C.5 DTC on Flat surface with Variable Friction Coefficient with ABS

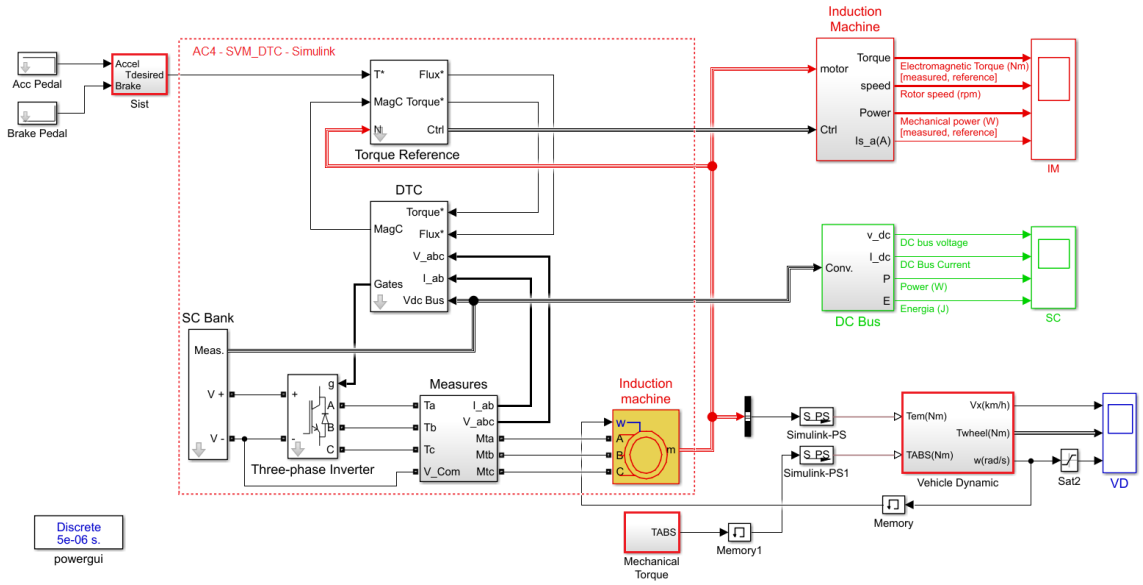

Figure C.23 – EV Model System with ABS.

C.5.1 Flat surface with ABS Mechanical(Bang-Bang Controller)

The "sist" block uses the same block as shown in Figure C.19.

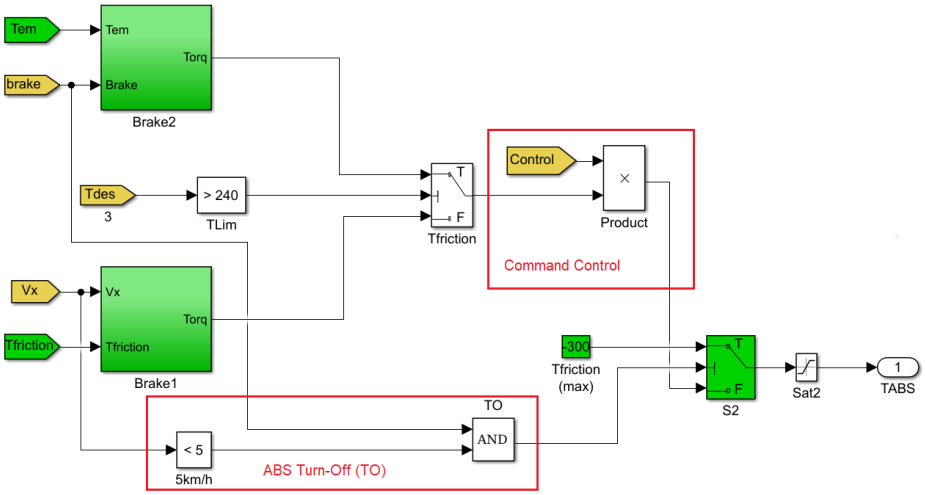

Figure C.24 – "Mechanical Torque" Block with Command Control.

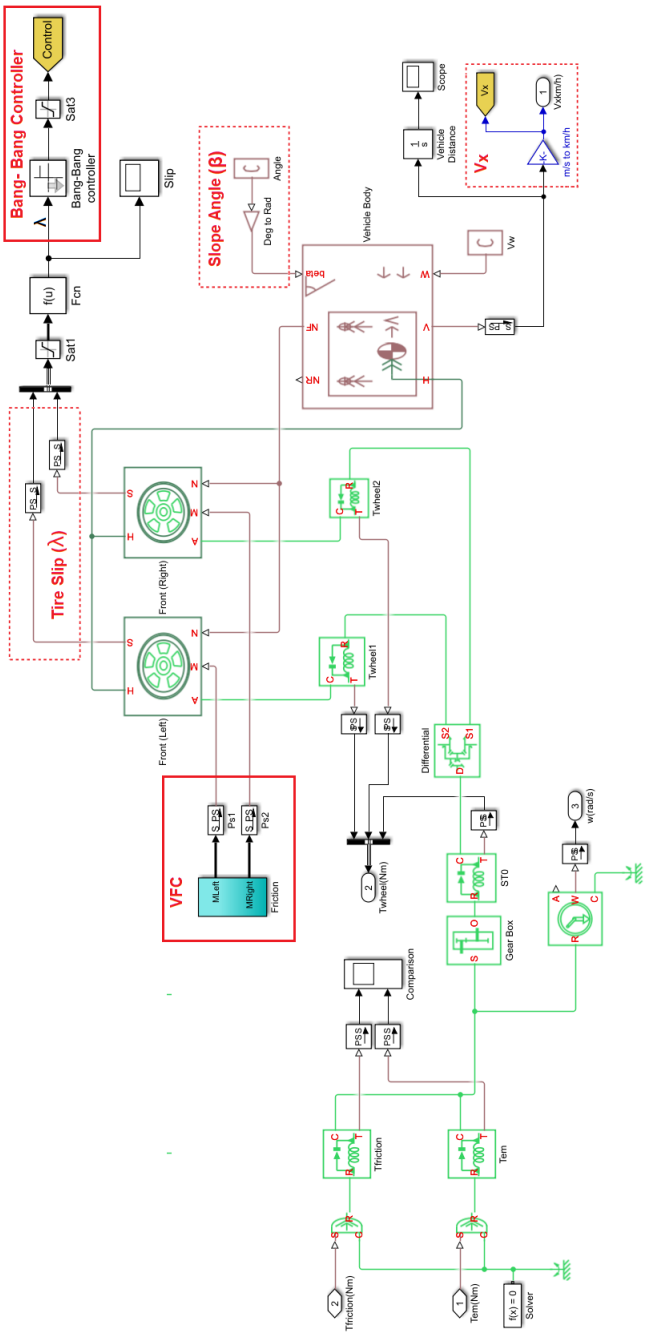

Figure C.25 – "Vehicle Dynamic" Block with Bang-Bang Controller.

C.5.2 Flat surface with ABS Mechanical(PI Controller)

The blocks of the EV system model remain with the same characteristic, the one difference is the type of controller.

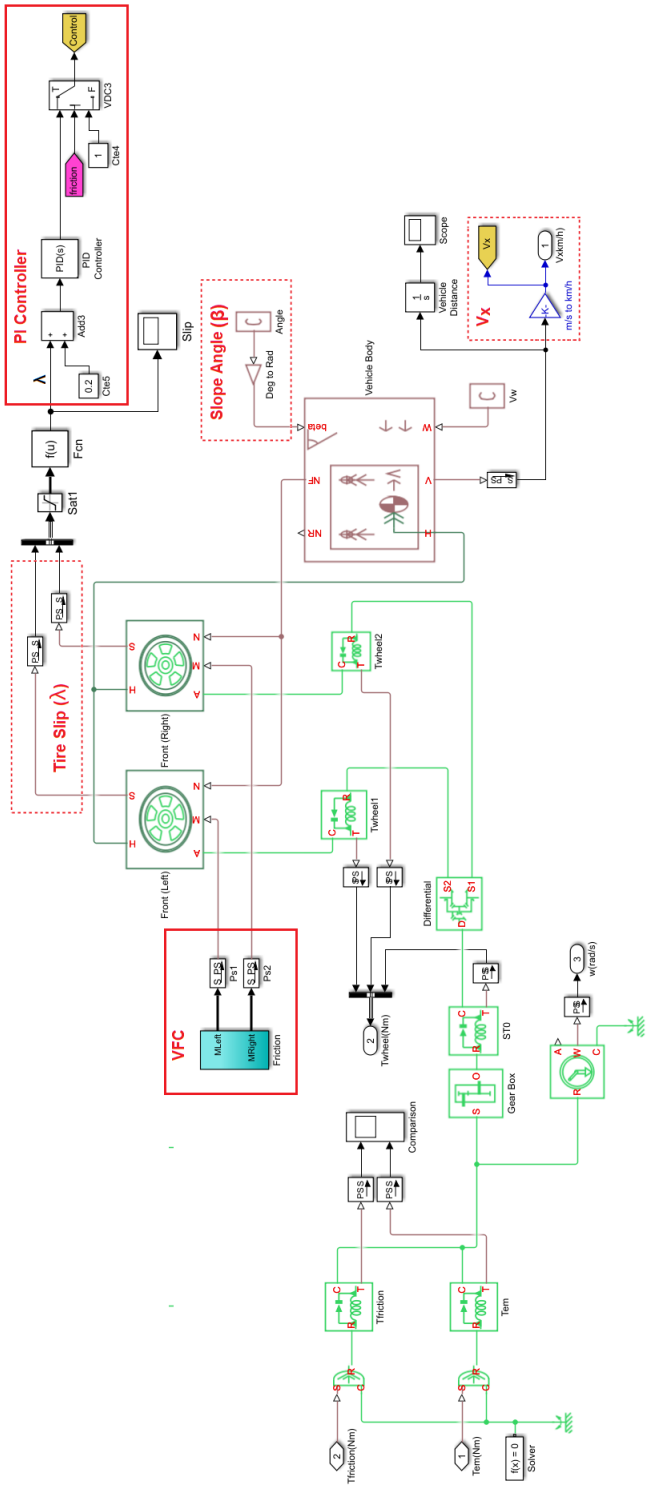

Figure C.26 – Braking torque definition with PI Controller.

C.5.3 Flat surface with ABS Mode (Bang-Bang - PI Controller)

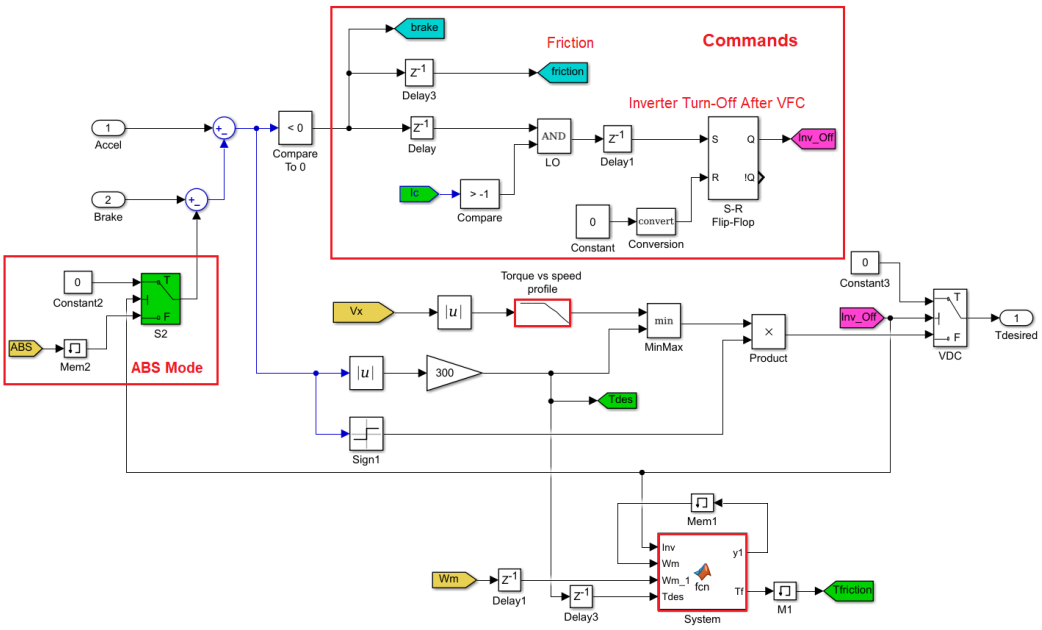

Figure C.27 – "sist" Block.

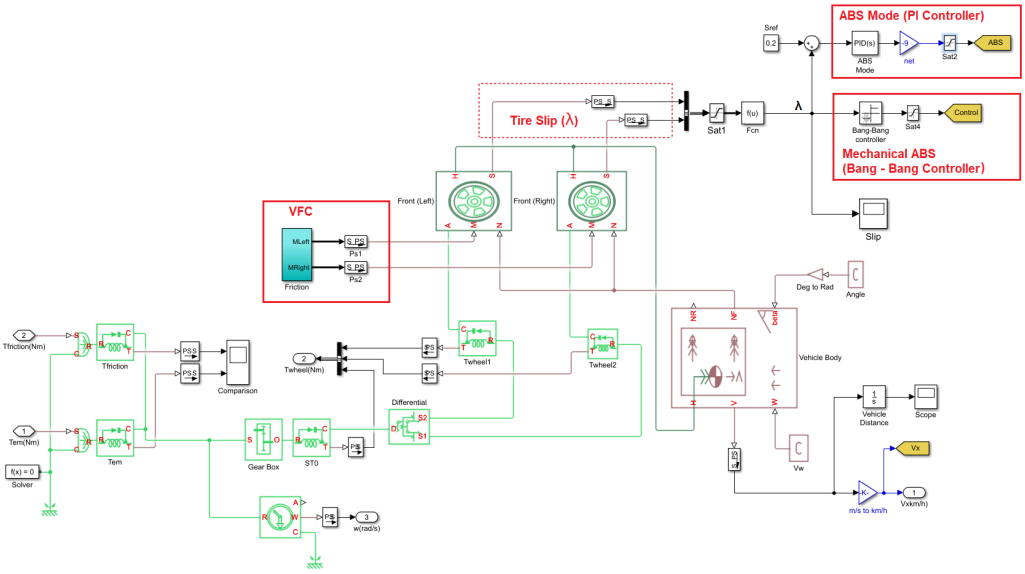

Figure C.28 – Block diagram for RBS with ABS Mode.

C.5.4 Flat surface with ABS Mode (PI - PI Controller)

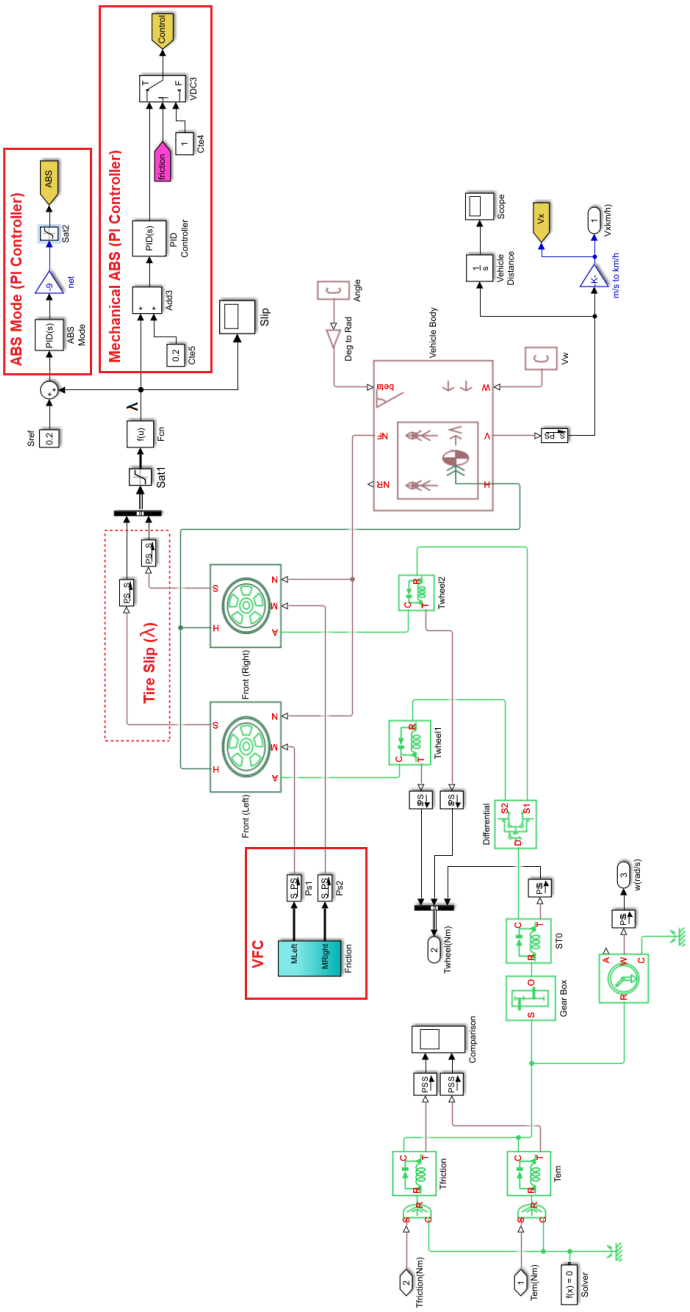

Figure C.29 – Block diagram for ABS Mode with PI Controller.

C.5.5 Complex Drive Cycle

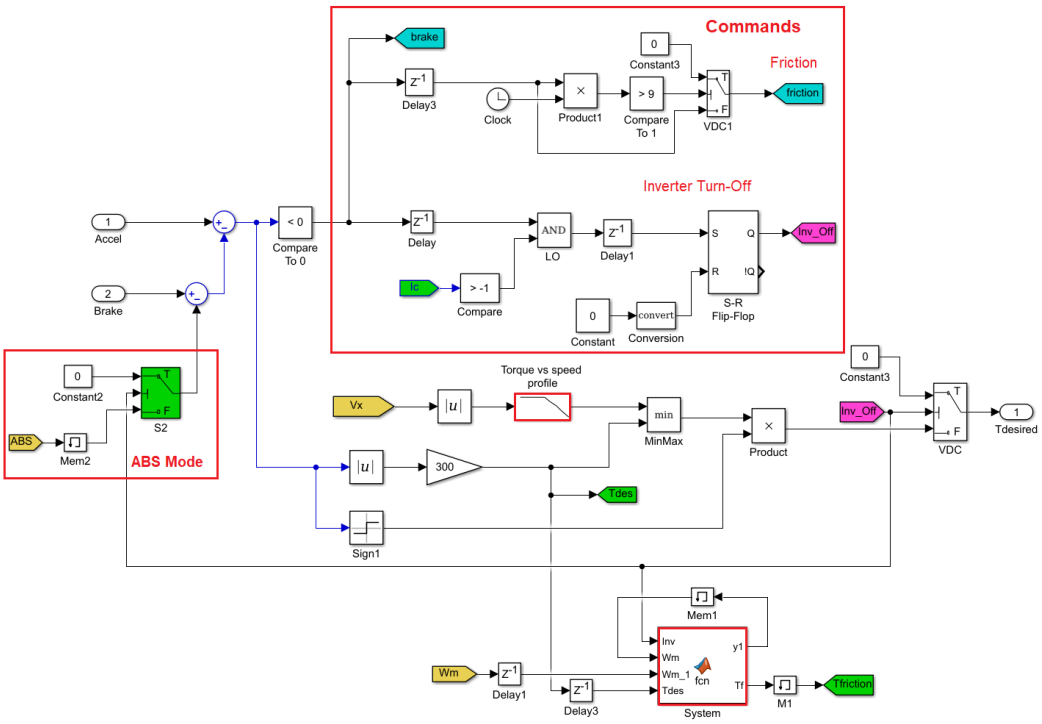

Figure C.30 – "sist" block for a friction's command between t= 7-9s